Adsorptive removal of pharmaceuticals from aqueous solution using end-of life magnetic tyre pyrochars: Experimental investigations and numerical modelling

Farzaneh Feizi

A thesis submitted in fulfilment of the requirements for the degree of

Doctor of Philosophy in Civil and Environmental Engineering,

The University of Auckland, 2021.

Abstract

In recent decades, occurrence of pharmaceutical pollutants in aquatic environment has become a growing concern due to their low biodegradability, high persistence, and facile bioaccumulation. Different carbonaceous materials such as activated carbon, biochar and pyrochar are widely utilised for removal of pharmaceuticals from water or wastewater. This thesis presents a challenge-based innovation of End of Life Tyres (ELTs) pyrolysis for magnetic pyrochar production and synthesis with evidence of its use as low-cost, novel adsorbent for pharmaceuticals removal from aqueous solutions. Magnetic tyre pyrochar (MTC) derived from ELTs at Technology Readiness Level 3-7 (TRL3- 7), was tested for the removal of ciprofloxacin (CIP), propranolol (PRO) and clomipramine (CLO), from water. The morphological and chemical properties of the adsorbents were assessed using Brunauer Emmett Teller (BET) surface area, Vibrating Sample Magnetometer (VSM), Fourier Transform Infrared (FTIR), Scanning Electron Microscope coupled with Energy Dispersive X-ray (SEM-EDS), elemental analysis and zeta potential measurements. Batch adsorption experiments revealed MTC's excellent adsorption efficiency of 85%, 90% and 92% for CIP, PRO and CLO respectively, higher than that of the non-magnetic tyre pyrochar (TC), due to the larger surface area, and porosity and lower polarity. Adsorption of the compounds onto MTC was highly pH dependent, and favourable at lower ionic strength. The experimental data were well described by pseudo-second order kinetic and Freundlich isotherm models. Based on FTIR and zeta potential analysis, the interaction mechanisms were explained by cation-π,

π-π electron donor acceptor (EDA), cation exchange, electrostatic repulsion and hydrophobic effect.

In fixed-bed column experiments, MTC, activated tyre char (ATC) and commercial activated carbon (CAC) were used as packing materials in lab-scale column study for the adsorption of the three pharmaceuticals from aqueous solution. The obtained breakthrough curves (BTCs) suggest that, lower flow rate, greater bed height, higher pH and nano particle size led to increased adsorption of PRO. The lowest adsorption capacity was observed for CIP either from single or ternary solution while it was significantly higher for CLO. Surface area of ATC increased nearly twelve-fold (38.17 to 453.81 m^2/g), after thermal and chemical activation and its adsorption capacity was comparable to commercial activated carbon. The suitability of Hydrus-1D model incorporating chemical non-equilibrium process to simulate the pharmaceutical transport and fit experimental BTCs was demonstrated ($0.97 < R^2 < 0.99$) in comparison to other common models (Adams–Bohart, Thomas and Yoon–Nelson). The modelling suggests the existence of non-equilibrium conditions and rate-limited sorption sites and the effect of dispersion and mass transfer mechanisms in the solute transport under dynamic conditions.

The competitive effects of different fractions of wastewater treatment plant effluent organic matter (EfOM) on adsorption of PRO were investigated in a fixed-bed column packed with MTC. Based on results, presence of EfOM inhibited adsorption of PRO in real wastewater and decreased the PRO adsorption capacity from 5.86 to 2.03 mg/g due to competitive effects and pore blockage by smaller EfOM fractions. Characterization of EfOM using size exclusion chromatography (LC-OCD) showed that the principal factor controlling EfOM adsorption was pore size distribution. Low molecular weight neutral fraction of EfOM had the highest adsorption onto MTC while humic substances were the least interfering fraction. Effect of important parameters (contact time, linear velocity and bed height/diameter ratio) on MTC

performance in large-lab scale columns revealed that linear velocity and contact time were effective in increasing adsorption capacity and delaying breakthrough time. Increase in linear velocity from 0.64 cm/min to 1.29 cm/min increased mass transfer and dispersion, resulting in considerable rise of adsorbed amount (5.86 mg/g to 22.58 mg/g) and increase in breakthrough time (15.8 to 62.7 hours). Efficiency of non-equilibrium Hydrus model considering dispersion and mass transfer mechanism was shown for real wastewater and scale-up purposes. Based on the modelling results, non-equilibrium Hydrus model could describe the experimental data well ($R^2 > 0.98$). Ball milling was used for degradation of adsorbed PRO and regeneration of MTC. The adsorbed PRO onto MTC was degraded more than 79% after 5 hours milling at 550 rpm and the addition of quartz sand increased the efficiency to 92%. In the context of the circular economy, this ELTs based low-cost magnetic adsorbent (estimated at 299 US$/tonne) can be potentially used at full-scale industrial wastewater treatment for the removal of pharmaceutical drugs from aqueous solution, offering sustainable environmental remediation. The cost analysis showed that unit cost for treatment of wastewater using fixed-bed columns of tyre char was calculated to be 1.57 US$/m^3 which can be deemed as commercially feasible.

Acknowledgements

Firstly, I would like to express my sincere gratitude to Assoc. Prof. Ajit K Sarmah for his motivation, patience, continuous support and guidance throughout the course of this PhD work. Thank you for sharing your immense knowledge and helping me in all the time of research and writing of this thesis. Special thanks to my co-supervisor, Dr. Ropru Rangsivek, for providing support, sharing knowledge and reviewing my work.

I am also grateful to Prof. Anastasia Zabaniotou and Dr. Nikos Antoniou from Aristotle University of Thessaloniki and Dr. Febelyn Reguyal from the University of Auckland for sharing their expertise and knowledge in this project.

I would also like to pay gratitude to all the technical staff members who helped and assisted me in my research. Thank you Dr. Yantao Song, Dr. Meet Mistry, Dr. Jishan Liu from the department of Environmental Engineering and Ray Hoffmann from the department of Chemical and Material Engineering. I would like to say a special thank you to Dr. Patricia Cabedo Sanz for her knowledge and guidance and also her precious support for providing the flexibility of conducting my experimental work during the COVID pandemic.

Special thanks to The University of Auckland for providing me with an International Doctoral Research Scholarship.

I would also like to thank my colleagues and friends at the University of Auckland for their help, kindness and sharing such a great working environment. Special thanks and regards goes to Savitri, Nana, Sai, Hasan, Adnan, Tahereh, Swadhina, Maryani, Gohar, Zahras, Mahyar,

Najam, Rowena, Ken, Lamis, Suma and Sundra. Without you my PhD journey would not be enjoyable.

Finally, I would like to thank my parents, my brothers, my sister and my best friend Narges for supporting me spiritually and for always being there for me even though we are a thousand miles apart. Thank you for the words of encouragement and all your kindness.

Last but not least, I would like to pay my deep sense of gratitude to my husband Shahin Torabi who has accompanied me during this PhD journey. You always have been my source of strength and motivation.

Table of Contents

List of Figures

List of Tables

List of Abbreviations and Symbols

NH$_3$	ammonia
ATC	activated tyre char
BET	Brunauer–Emmett–Teller
BJH	Barrett–Joyner–Halenda
BTCs	breakthrough curves
CAC	commercial activated carbon
CO$_2$	carbon dioxide
CIP	ciprofloxacin
CLO	clomipramine
CT	contact time
DI	deionized water
EBCT	empty bed contact time
EDA	Electron Donor Acceptor
EDX	Energy Dispersive X-ray
EfOM	effluent organic matter
ELTs	End of Life Tyres

EU	European Union
FQ	Fluoroquinolone
FTIR	Fourier transform infrared spectrophotometer
HCL	Hydrochloric acid
H$_2$O$_2$	Hydrogen Peroxide
IC	ion chromatography
K$_{ow}$	octanol-water partition coefficient
KOH	Potassium hydroxide
LC-MS/MS	liquid chromatography tandem mass spectrometer
LC-OCD	liquid chromatography with organic carbon detector
LMW	low molecular weight
MTC	magnetic tyre pyrochar
MTZ	mass transfer zone
NaOH	Sodium hydroxide
OMP	organic micro pollutant
pH$_{pzc}$	point of zero charge pH
PPCPs	pharmaceuticals and personal care products
PPMS	Physical Property Measurement System
PRO	propranolol
RMSE	root-mean-square error

SEM-EDS   Scanning Electron Microscope-Energy Dispersive X-ray

SMPs   soluble microbial products

TC   non-magnetic tyre pyrochar

TCA   Tricyclic antidepressants

TRL   Technology Readiness Level

USEPA   Environmental Protection Agency

VSM   Vibrating Sample Magnetometer

WWTP   wastewater treatment plant

CHAPTER 1: Introduction

1.1. Background

Pharmaceuticals, as a class of emerging contaminants, are one of the most important environmentally relevant chemicals due to their ubiquity in the aquatic environment and potential toxic effects on wildlife and human (Ahmed & Hameed, 2018; Grover et al., 2011; Zhou et al., 2009). Antibiotics, used for human and animal therapy, are considered as pseudo-persistent pharmaceuticals due to their permanent presence in the environment and their frequent use causes development of antibiotic resistance to microorganisms (Sarmah et al., 2006; Li, 2014b). Ciprofloxacin (CIP) is a widely used and frequently detected antibiotic in aquatic ecosystems that pose major threats to the ecosystems and human health (Li et al., 2014a). Beta-blockers, another group of pharmaceuticals, are used for the treatment of high blood pressure and are ubiquitous in different environmental compartments. One of the most commonly used beta-blockers with high acute and chronic toxicity is propranolol (PRO) (Giltrowa et al., 2010; Maszkowska et al., 2014b). Antidepressant pharmaceutical such as clomipramine (CLO) has been widely prescribed for the treatment of mood disorders and CLO has been detected in various water matrices at trace levels. CLO has been also found to exert a direct effect on neuro-endocrine signalling and can be potentially harmful to aquatic organisms (Yuan et al., 2013). Discharged effluent from hospital, drug factories and households are major potential sources of range of pharmaceuticals to the aquatic environment (Li, 2014b). Conventional primary and secondary water treatment technologies are not efficient enough to remove or degrade these emerging contaminants. Therefore, to safeguard environmental and public health, development of suitable technologies for satisfactory removal of pharmaceuticals from aqueous solutions is much warranted.

Advanced water treatment techniques such as photodegradation, membrane filtration, oxidation and ozonation have been used for removal of pharmaceuticals from aqueous

solutions (Estrada-Arriaga et al., 2016; Lu et al., 2019; Nassar et al., 2017; Radjenović et al., 2009). However, most of these treatment systems are not techno-economically feasible or they have some disadvantages such as generation of toxic byproduct and complicated procedure (Sophia A. & Lima, 2018). For example, metabolites produced through oxidation process may risk public health (Gwenzi & Chaukura, 2018), while the cost of water treatment using these technologies can range from 10–450 US\$/m^3 (Ali et al., 2012). Amongst all available developed treatment methods, adsorption is considered to be as a promising method for pharmaceuticals removal from water bodies due to its high efficiency, ease of operation, simple design and low energy demand. Activated carbon is the most commonly used adsorbent for water and wastewater treatment; however, its high cost has restricted its widespread use (De Gisi et al., 2016). It is therefore of great importance to develop low-cost adsorbents for large-scale applications in water remediation.

Biochar or pyrochar, a low-cost and renewable adsorbent, is produced via pyrolysis of feedstock in the absence of or under limited oxygen conditions. This emerging adsorbent is a stable carbon dominant material and can be obtained from different types of abundant and low-cost feedstock, mainly agricultural biomass and solid waste (Gwenzi et al., 2017; Tan et al., 2015). Biochar has been found to be highly effective in pharmaceuticals removal from aqueous solutions (Jing et al., 2014; Kong et al., 2017; Li et al., 2018a; Li et al., 2018c; Liu et al., 2017; Shang et al., 2016) . For example, Li et al. (2018a) pyrolyzed used tea leaves at different temperatures to prepare tea-leaf biochar for removal of high concentrations of CIP from aqueous solutions. The biochar obtained at 450 °C showed excellent capacity for adsorption of CIP at pH 6 and 40 °C. Based on the results, hydrogen bonding, electrostatic attraction and π-π interactions were postulated to be the main adsorption mechanisms. In another study, rice husk biochar and methanol modified rice husk biochar were used for adsorption of tetracycline in water (Jing et al., 2014). The adsorption capacity of rice husk biochar for tetracycline

increased considerably after simple methanol modification (95.6 mg/g). This increase could be attributed to the changes in the oxygen containing functional groups in the modified biochar which affected π-π interactions between the adsorbent and adsorbate.

End of life tyres (ELTs), including passenger cars, trucks, airplanes and motorcycle tyres, constitute a big proportion of hazardous solid waste. About 1.5 billion tyres are produced and discarded every year throughout the world. Due to infusible, insoluble, durable and resistant nature of tyres, their disposal has currently become one of the serious environmental problems (Iraola-Arreguis et al., 2018). Moreover, disposing of waste tyres onto landfills is banned in many countries due to the waste management legislation and recycling is now considered as an alternative mode of managing the waste tyres (European Environment Agency, 2009; Iraola-Arregui et al., 2018; Labaki & Jeguirim, 2017). Therefore, pyrolysing waste tyres and converting them into tyre pyrochar and using it as adsorbent for contaminants removal has gained growing attention (Hakimi Mohd Shaid et al., 2019; Manirajah et al., 2019; Mashile et al., 2018; Mui et al., 2010). Biochar is produced through thermal conversion of biomass to black carbon; however, tyre is not a lignocellulosic material or biomass. As a generally accepted terminology between biochar, activated carbon, pyrochar and char is lacking, in this thesis, these terms have been used interchangeably in order to have simplicity to interpret the results and discussion.

In recent years, magnetic adsorbents have been widely used to remove contaminants from water bodies. This technology has eased the separation of powdered biochar from aqueous solution by an external magnetic field which avoids the use of inefficient and costly filtration techniques (Li et al., 2020; Rocha et al., 2020). Magnetisation can also increase the surface area of the adsorbent and its removal capacity for a variety of contaminants (Devi & Saroha, 2014; Zhu et al., 2014), however, reduction in surface area has also been reported (Reguyal et

al. 2017). Magnetic biochar is produced via pyrolysis activation, chemical co-precipitation, calcination and mechanical milling synthesis routes (Li et al., 2020; Rocha et al., 2020).

Most of the studies on the pharmaceuticals adsorption in aqueous solutions have been carried out under batch operation in stirred reactors (Calisto et al., 2014; Liu et al., 2017; Shang et al., 2016; vom Eyser et al., 2015; Wu et al., 2017; Zeng et al., 2018); however, application of continuous fixed-bed adsorption has been considered only in a smaller number of studies (Darweesh & Ahmed, 2017a; Mansouri et al., 2015; Nazari et al., 2016). Compared to batch adsorption, dynamic adsorption has some advantages such as high adsorption performance, flexibility and easy scale-up (Ahmed & Hameed, 2018). Moreover, fixed-bed column studies are more realistic and can be very helpful to simulate the transport of contaminants, using appropriate models. Studies have shown that the models that consider physical and/or chemical non-equilibrium processes, diffusion, dispersion and mass transfer mechanisms are more successful in predicting the solute transport (Jellali et al., 2016; Liao et al., 2013; Vilardi et al., 2019). In dynamic adsorption, breakthrough time and adsorption capacity can be changed regardless of the adsorbent used by altering flow rate, adsorbent bed height, initial concentration of adsorbate, particle size of adsorbent, solution pH and presence of effluent organic matter (EfOM) in water matrix.

Natural organic matter present in WWTP effluents is considered as EfOM and its presence in secondary effluents can pose serious problems for environmental safety and promote irreversible fouling (González et al., 2013). Carbon-based adsorbents have been shown to have high effectiveness in adsorption of EfOM in water solutions (Nguyen et al., 2013; Shanmuganathan et al., 2015). As EfOM consists of hydrophobic and hydrophilic fractions with different molecular sizes, it has been found to strongly deteriorate adsorption of organic micro pollutants (OMPs) such as pharmaceuticals onto adsorbents due to competitive effects (Zietzschmann et al., 2015). After adsorption, spent adsorbents are considered as hazardous

waste and should be regenerated for more use or disposed properly (Muranaka et al., 2010). Regeneration of exhausted adsorbents can reduce the need for new adsorbents and can be beneficial both economically and environmentally (Radhika et al., 2018). There are different methods for reutilization of saturated adsorbents such as chemical regeneration (Zhang, 2002), thermal regeneration (Álvarez et al., 2004), steam regeneration (Xin-hui et al., 2012), oxidative regeneration (Muranaka et al., 2010) and mechanochemical regeneration such as ball milling (Shan et al., 2016). Ball milling is an emerging technique which has been successfully used for destruction of persistent organic compounds and degradation of chemical species. Ball-milling is a low-cost and environmentally friendly technology as it does not require any solvents and consumes relatively low energy during milling process (Cagnetta et al., 2017; Lyu et al., 2018b).

1.2. Rationale for the research

The occurrence of CIP, PRO and CLO emissions to the aquatic environment has been reported to be harmful to human health as well as ecosystem even at trace concentrations (ng/L - µg/L) (Li et al., 2014a; Maszkowska et al., 2014b; Minguez et al., 2016; Yuan et al., 2013). The main source of these OMPs residues in the environment is WWTPs. Therefore, different advanced wastewater treatment technologies such as photodegradation, membrane filtration, oxidation, ozonation and adsorption have been utilized for removing OMPs from WWTP effluent (Kong et al., 2017; Lu et al., 2019; Nassar et al., 2017; Radjenović et al., 2009). Although some studies have investigated removal of CIP and PRO using adsorption technology (Darweesh & Ahmed, 2017a; Deng et al., 2019), CLO adsorption onto carbon-based adsorbents in aqueous solutions has been studied just in one study (Zhao et al., 2018). End-of Life Tyres (ELTs), as non-biodegradable materials, pose serious environmental risks. Production of carbon-based

adsorbents from waste tyres has both advantages of water treatment and waste management. Previous investigations have examined pharmaceuticals adsorption onto different carbon-based adsorbents, however, to-date, tyre char application for pharmaceuticals adsorption has been investigated in only a few studies (Acosta et al., 2016; Azman et al., 2019; Styszko et al., 2017). Moreover, despite many studies on using different magnetic adsorbents for adsorption of pharmaceuticals application of magnetic tyre char for removal of pharmaceuticals from aqueous solutions has been hitherto neglected.

Although continuous adsorption process has the advantages of high adsorption performance, flexibility and easy scale-up, fewer studies have been conducted on the fixed-bed adsorption of pharmaceuticals compared to batch studies (Nazari et al., 2016; Yanyan et al., 2018). Furthermore, column experiments evaluating the transport of pharmaceuticals through the tyre char has not been performed yet. Traditional numerical models which do not consider mass transfer and dispersion mechanism have been used to simulate contaminants transport in continuous columns in many studies in the past. However, there have been only limited number of studies which investigated the effect of mass transfer, dispersion and diffusion mechanisms (Jellali et al., 2016; Liao et al., 2013; Vilardi et al., 2019). Hydrus model considering non-equilibrium process, mass transfer, diffusion and dispersion mechanisms has not been used for the prediction of pharmaceuticals transport in fixed-bed columns packed with carbon-based adsorbents.

EfOM which is contained in WWTP effluents deteriorates OMPs removals. Although adsorption of composite EfOM onto adsorbents has been studied in most published research (Dittmar et al., 2018; Erdem et al., 2020; Yu et al., 2012); adsorption of its individual fractions has been investigated in fewer studies (Filloux et al., 2012; Zietzschmann et al., 2014). There is a lack of knowledge regarding the effect of EfOM fractions on the removal of pharmaceuticals in column-mode experiments in municipal wastewater and their adsorption

mechanisms onto carbon-based adsorbent. Moreover, there is a dearth of information in the literature about scale-up studies in fixed bed column treatment systems and evaluating numerical models for contaminants transport prediction in larger scale column packed with adsorbent (Fernández-González et al., 2019; Vilardi et al., 2019). Techno-economic assessment of tyre char as an adsorbent for contaminants removal from aqueous matrix is also lacking. Moreover, despite simplicity and versatility of ball milling technology for degradation and destruction of organic compounds, the technology is still in its infancy. To-date, there has been only one study on ball-milling application on regeneration of exhausted adsorbent (Shan et al., 2016).

The results obtained in this thesis could be utilised as baseline information to use tyre char as a low cost and environmental friendly adsorbent for removal of contaminants from real wastewater systems. In addition, the results can provide useful information to investigate tyre char production and application at large scale systems.

1.3. Research objectives

The overarching aim of this thesis was to synthesise a low-cost and environmentally friendly adsorbent derived from End of Life Tyres (ELTs) for removal of pharmaceuticals with different physiochemical properties from aqueous solutions.

The specific objectives of this study were to:

1. synthesise and characterize a magnetic pyrochar derived from ELTs for adsorption of CIP, PRO, and CLO selected as model adsorbates in aqueous solution;

2. study the adsorption of the selected pharmaceuticals onto magnetic tyre char (MTC) under batch conditions and elucidate the adsorption mechanisms involved by specifically focusing on the effect of pH and ionic strength of the solution;

3. conduct column experiments packed with MTC, chemically activated tyre (ATC) char and commercial activated carbon (CAC) for pharmaceutical adsorption and simulate the transport of contaminants using Hyrdus-1D model;

4. analyse the effects of operation parameters (flow rate, initial concentrations, bed heights, pH), presence of competitive adsorbates and the particle size of adsorbents on the breakthrough time and adsorption capacity;

5. investigate the effects of water matrix constituents on the PRO removal using MTC and identify EfOM fractions contributing most to adsorption inhibition on the adsorbent;

6. study the applicability of laboratory data as the basis for designing a pilot-scale adsorption column and investigate the effect of important design parameters such as contact time, linear velocity and bed height/diameter ratio on breakthrough curves; and

7. determine the feasibility of MTC regeneration using ball milling and investigate the destruction efficiency for PRO, the influence of milling time, milling speed and different additives on PRO degradation during ball-milling and its final by-products and intermediates, and also.

8. assess the techno-economic feasibility of tyre char as an adsorbent and compare its cost and sustainability with commercial activated carbon.

1.4. Thesis structure

In chapter 1, background, rationale behind the study, overarching aim and specific research objectives and the thesis structure are presented.

Chapter 2 presents the literature review, which includes sources and occurrence of pharmaceuticals in water bodies and discusses properties and ecotoxicity of CIP, PRO and CLO in environment. The chapter also introduces current methods on pharmaceutical removal in aqueous solution and highlights the importance of adsorption technology, low-cost carbon-based adsorbents, magnetic adsorbents and tyre char as an efficient and cost-effective strategy for mitigation option of pharmaceuticals in contaminated waters. Different methods for modification of adsorbents are also discussed in this chapter. Moreover, this chapter introduces methods for regeneration and reuse of exhausted adsorbents. The literature review builds upon the knowledge gaps and the objectives of the whole study.

Chapter 3 explains how tyre char is synthesised and magnetized at Technology Readiness Level 3-7 (TRL3-7). In this chapter, characterization of magnetic tyre char and its application for adsorption of CIP, PRO and CLO in aqueous solution in batch mode are also presented. Moreover, this chapter investigates the adsorption mechanisms of the selected pharmaceuticals onto MTC and the effect of pH and ionic strength on their adsorption. Finally, a techno-economic feasibility assessment of tyre char as an adsorbent for water remediation is presented in this chapter.

Chapter 4 presents the findings of adsorption of the selected pharmaceuticals in a fixed-bed column packed by magnetic tyre char, activated tyre char and commercial activated carbon. In addition, the effect of different parameters, such as flow rate, initial concentration of adsorbate, bed height of adsorbent, solution pH, particle size of adsorbent and the presence of competing compounds (CIP and CLO) on adsorption of PRO under dynamic condition is discussed.

Application of Hydrus-1D model considering equilibrium and non-equilibrium processes to predict transport of contaminants in columns is also proposed in this chapter and compared with other commonly used and traditional models used for adsorption studies on a fixed-column.

Recognizing the importance of EfOM on wastewater treatment, Chapter 5 is devoted to the discussion of the results related to the EfOM present in real wastewater on adsorption of PRO under the fixed-bed column experiments. A particular aspect in this chapter was to determine how different fractions of EfOM could potentially compete for adsorption sites. Moreover, the application of larger scale columns on adsorption of PRO onto MTC and suitability of Hyrdus-1D model for scale-up purposes are discussed. Regeneration of spent adsorbents using ball milling as a green technology is also presented in this chapter.

Finally, chapter 6 discusses and ties up the key findings of the research reported in each of the chapters in this study and provides some recommendations and knowledge gaps for future research.

CHAPTER 2: Literature review

2.1. Occurrence of pharmaceuticals in the environment

In recent decades, the presence of pharmaceutical compounds in surface water, groundwater and wastewater across different parts of the world has been considered as an emerging global concern. These emerging contaminants may pose a significant risk to human health and the environment, even at extremely low concentration levels due to their persistent and potential non-wanted biological effects (Kasprzyk-Hordern et al., 2008; Manaia et al., 2012). Pharmaceuticals are largely excreted unchanged or as metabolites via faeces and urine and subsequently reach the wastewater treatment plant (WWTP) through the reticulated sewers system. Effluents from drug manufacturers, hospitals, and households are considered as the main contributors towards pharmaceutical contamination in wastewater (El-Shafey et al., 2012). The pathways of pharmaceuticals pollution to different receptors are shown in Figure 2.1.

Pharmaceuticals consist of different therapeutic classes, such as antibiotics, β-blockers, and antidepressants. Pharmaceutical antibiotics have been produced in large quantities and extensively used in medical and veterinary practices for several decades. A variety of potential adverse and toxic effects on human health as well as environment were induced due to antibiotics residues released from treated wastewater and agricultural runoff (Zeng et al., 2018). CIP, one of the most widely used antibiotics, belongs to the third generation of the fluoroquinolone (FQs) family and is used to treat infectious diseases in both human and animals (Carabineiro et al., 2011). CIP concentrations have been detected ranging from ng/L to μg/L in surface and ground water (Karthikeyan & Meyer, 2006; Kolpin et al., 2002). Higher concentrations of CIP have been found in the wastewaters of hospitals (3–87 μg/L) and drug factories (31 mg/L) (Carmosini & Lee, 2009). Discharged CIP in aqueous solution can lead to

antibiotic resistant development, even at low concentrations, which is harmful to human health and environment (Sun et al., 2014).

Beta-blockers, which are extensively utilized to treat cardiovascular diseases including hypertension and cardiac arrhythmias also fall in one of the most frequently detected groups of pharmaceuticals in water treatment plants, receiving river waters and groundwater (Wick et al., 2009). Beta-blockers are known as endocrine disrupting chemicals and can cause toxicological effects on non-target organisms (Godoy et al., 2015). PRO, a crucial nonselective beta-blocker, was shown to have the highest acute and chronic toxicity among beta-blockers (Giltrowa et al., 2010).

Human antidepressants, such as CLO, are another group of widely prescribed and commonly detected pharmaceuticals in various environmental compartments and justify the growing public concerns due to their harmful effects on the environment and human health. (Fong & Ford, 2014; Yuan et al., 2013). These psychiatric pharmaceuticals directly affect central nervous system and interrupt neuro-endocrine signalling (Yuan et al., 2013).
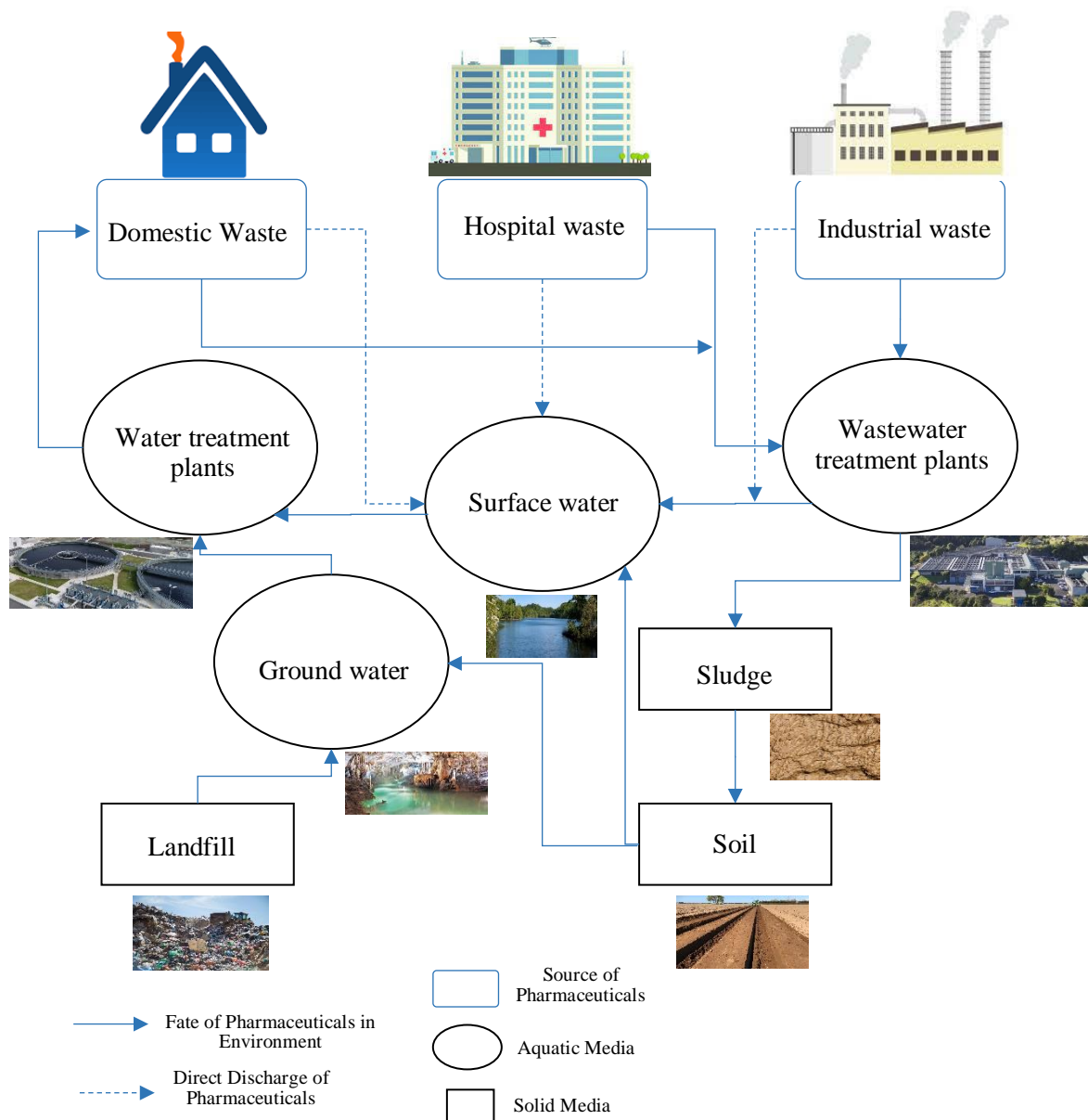
Figure 2. 1. Sources and pathways of pharmaceuticals pollution in the environment.

2.2. Properties and ecotoxicity of selected pharmaceuticals in environment

2.2.1. Ciprofloxacin

CIP, a broad-spectrum antibiotic, is the most active pharmaceutical in FQs group (Załeska-Radziwiłł et al., 2014). The risk posed by the impact of CIP on microorganisms has been assessed in some studies. CIP showed extreme toxicity and high toxicity to nine species and had toxicity to three bacteria species according to the European Union (EU) criteria. For example, as shown in Table 2.1, in a 24-h bioluminescence test, CIP was extremely toxic to Vibrio fischeri and luminescence and the bacteria was inhibited in 50% at the concentration of 0.0137 µg/L. Ecotoxicological assessments for CIP have been conducted in surface waters and a significant risk to microorganisms was demonstrated (Załeska-Radziwiłł et al., 2014). Nałecz-Jawecki et al. (2014) analysed microbial assay for risk assessment (MARA) test on various antibiotics and observed growth inhibition of sensitive microbial strain at concentrations 12–75 µg/L of CIP. Also, adverse effects of CIP on aquatic organisms including the *cynobacterium; Microcystis aeruginosa,* duckweed; Lemna minor, the green alga; *Pseudokirchneriella subcapitata*, the crustacean; *Daphnia magna* and fathead minnow; *Pimephales promelas* have been reported in some studies (Ebele et al., 2017; Obinson et al., 2005). Ecotoxicological risk assessments for CIP, PRO and CLO in various organisms with different toxicological endpoint tests based on effect concentration (EC50) and lethal concentration (LC50) are summarised in Table 2.1.

Table 2. 1. Ecotoxicity of CIP, PRO, CLO.

Pharmaceutical	Organism	Toxicological endpoint	Ecotoxicity data (µg/L)	Toxicity assessment	Reference
CIP	Comamonas testosteroni	EC50 (18 h)	56.1	Extremely toxic	(Załeska-Radziwiłł, Affek, & Rybak, 2014)
	Delftia acidovorans	EC50 (18 h)	6.2	Extremely toxic	
	Citrobacter freundii	EC50 (18 h)	4.6	Extremely toxic	
	Vibrio fischeri	EC50 (24 h)	0.0137	Extremely toxic	
	Pseudomonas fluorescens	EC50 (16 h)	0.175	Extremely toxic	
PRO	Medaka	LC50	24.3	Acutely toxic	(Huggett et al., 2002)
	Medaka	LC50	0.5	Reduced growth	(Huggett et al., 2002)
	Rainbow trout	LC50	10	Impaired growth	(Owen et al., 2007)
	Zebrafish	LC50	7.002	Altered blood flow	(Ferrari et al., 2004)
CLO	Skeletonema marinoi	EC50	1.7	high risk	(Minguez et al., 2016)

2.2.2. Propranolol
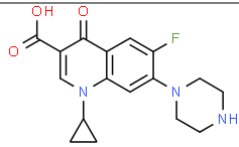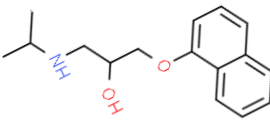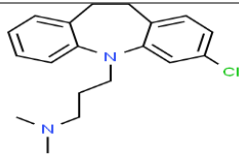
Beta-blockers such as propranolol have been known to be one of the most important therapeutic classes among other pollutants due to their frequent presence and detection at high maximum concentrations in waterbodies. Antihypertensives presence in environment can cause toxicological impacts on non-target organisms (Godoy et al., 2015). According to Maszkowska et al. (2014b), beta-blockers are considered as endocrine-disrupting chemicals because they can disrupt the levels of testosterone in male organisms. Also, in another study, high mobility,

hydrolytic stability and bioavailabllity of beta-blockers were confirmed in the environment which may lead to their accumulation in the water ecosystems (Maszkowska et al., 2014a). One of the most commonly consumed and detected beta-blockers in the environment is PRO which is prescribed to treat high blood pressure (Wick et al., 2009). Based on calculated chronic risk quotients, PRO indicated an ecological risk to both fresh and salt waters (Ferrari et al., 2004). Also, considering ecotoxicological data from the green algae test (*S. vacuolatus*), PRO can be considered to have deleterious effects on aquatic organisms (Maszkowska et al., 2014b).

2.2.3. Clomipramine

Tricyclic antidepressants (TCAs) have been widely used, especially in the developed countries, to treat depression and mood disorders and have been frequently detected in different environmental surface waters. Complete removal or degradation of many TCAs during wastewater treatment process cannot be obtained and their discharge into waterbodies causes potential threats to non-target aquatic organisms (Ziarrusta et al., 2016). Psychiatric drugs are one of the most toxic pharmaceuticals to aquatic life and detrimental effects on aquatic organisms can be revealed by this group because of disturbing homeostasis in vertebrates and invertebrates even at low concentrations (µg/L or even ng/L) (Giebułtowicz & Nałecz-Jawecki, 2014). CLO, a tricyclic antidepressant, is one of the most toxic compounds for *Daphnia magna* (Minguez et al., 2014). Also based on a survey conducted in the Northwest France, CLO was highlighted as high risk pharmaceutical in marine waters at levels of ng/L (Minguez et al., 2016). Therefore, antidepressants deserve attention due to their potential high ecological risk in surface water ecosystems. Table 2.2 shows some physicochemical properties of CIP, PRO and CLO.

Table 2. 2. Some physicochemical properties of CIP, PRO and CLO.

Compound	Water solubility (g/L) at 25℃	Molecular weight (g/mol)	Molecular formula	Structural formula	pKa
CIP	30000	331.35	$C_{17}H_{18}FN_3O_3$		6.18, 8.76
PRO	62	259.34	$C_{16}H_{21}NO_2$		9.42
CLO	0.294	314.85	$C_{19}H_{23}ClN_2$		9.20

2.3. Current methods on pharmaceutical removal in aqueous solution

Mixtures of multiple pharmaceuticals of different physico-chemical properties are present in WWTPs which complicate the removal process and their removal rate depends on the physiochemical characteristics of the pharmaceuticals and treatment technology of plants (Nielsen & Bandosz, 2016). Removal and degradation of CIP, PRO and CLO have been done by different treatment methods such as ozonation (Lu et al., 2019), oxidation by chlorine (Estrada-Arriaga et al., 2016), photo-Fenton process (Perini et al., 2018), photocatalytic degradation (Nassar et al., 2017), membrane bioreactor (Radjenović et al., 2009) and adsorption (Kong et al., 2017). It is worth-mentioning that conventional treatment technologies are not efficient enough to remove pharmaceuticals, and tertiary treatments technologies suffer

from some disadvantages, such as being expensive, complicated treatment process, or producing secondary pollution (Deng et al., 2011; Mondal et al., 2016). Therefore, developing effective, inexpensive and environmentally friendly technologies to remove pharmaceuticals from aqueous solution is of utmost importance and the following section briefly discusses this aspect.

2.4. Adsorption technology and biochar

Among the existing advanced treatments technologies, adsorption has been demonstrated as an effective and simple technique to remove contaminants from water bodies even at very low concentrations. Batch and dynamic conditions are two different operation modes of adsorption experiments involving contaminants. Batch adsorption takes place in stirred reactors while column adsorption is performed in fixed-bed columns. Adsorption in fixed bed is simpler and more effective than batch adsorption. Moreover, continuous adsorption is capable of treating larger volumes of contaminated water and can be easily scaled up for industrial applications (Ahmed & Hameed, 2018). Activated carbon, the most commonly used adsorbent, has been extensively applied to remove pollutants from water (Deng et al., 2011). However, its high cost has limited its application in water and wastewater treatment systems. Therefore, developing effective, low-cost and environmentally friendly adsorbents is imperative.

Biochar is produced through pyrolysis of biomass in the absence or under oxygen-limited environment resulting in a porous and low-density carbon-rich solid material. As a multifunctional product, biochar has been utilised for a variety of applications including clean energy provision, carbon sequestration, greenhouse gas emission mitigation, soil remediation and fertilization, and contaminant remediation (organic and inorganic) in water systems

(Rajapaksha et al., 2016), development of wood plastic biochar composites (Das et al., 2015) and use in construction materials (Akhtar & Sarmah, 2018; Praneeth et al., 2020). There are several advantages of using biochar as an adsorbent for water and wastewater remediation (Figure 2.2). A wide range of feedstock including plant waste, crop residues, agro-processing wastes (e.g., sawdust), wastewater sludge, wood biomass, animal wastes and waste tyres can be utilized to produce different types of biochar (Acosta et al., 2016; Tan et al., 2015). The renewable resource, economic and environmental benefits of biochar make it a promising adsorbent for water contaminants treatment.
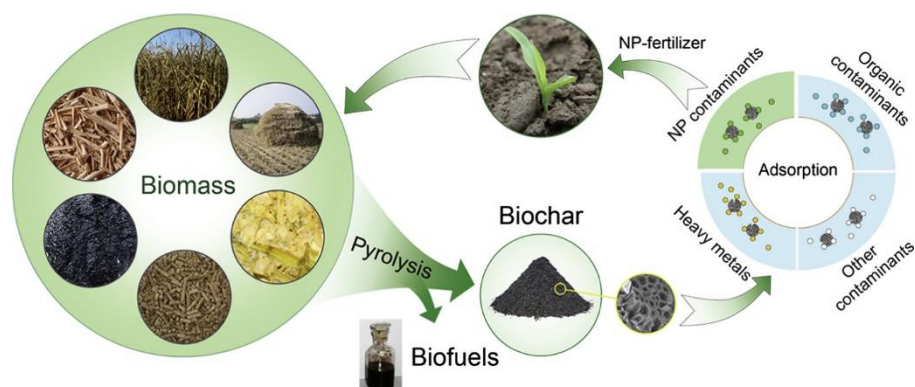
Figure 2. 2. Biochar benefits for wastewater treatment (Source: Tan et al., 2015).

The main processes to produce biochar are conventional carbonization (i.e. slow pyrolysis), intermediate pyrolysis, fast pyrolysis and gasification (Table 2.3) (Ahmad et al., 2014; Manyà, 2012). The physiochemical properties of biochar such as porosity, pore size distribution, surface area, and surface functional groups greatly depend on key determinants such as pyrolysis temperature, heating rate, residence time and feedstock types (Ahmad et al., 2014). For example, at pyrolysis temperature less than 400 °C and between 550 °C to 600 °C, the specific surface area of biochars vary from less than 10 to 400 m^2/g, respectively (Brown, 2012). In general, biochars with more aromatic groups were formed through high-temperature

pyrolysis (600-700 °C), but they contained fewer hydrogen and oxygen-containing surface functional groups because of deoxygenation and dehydration reactions of the biomass. On the other hand, biochar pyrolysed at lower temperatures (300-400 °C) showed more variety of organic charactersistics, and was found to possess more C=O and C-H functional groups (Rajapaksha et al., 2016). Using biochar as an adsorbent can be deemed as a ''win–win'' scenario for both waste management and protecting the environment.

Table 2. 3. Pyrolysis processes for biochar production (Source: (Ahmad et al., 2014)).

Process	Temperature (°C)	Residence time	Products		
			Liquid (bio-oil) (%)	Solid (biochar) (%)	Gas (syngas) (%)
Fast pyrolysis	300–1000	Short (<2 s)	75	12	13
Intermediate pyrolysis	~500	Moderate (10–20 s)	50	25	25
Slow pyrolysis	100–1000	Long (5–30 min)	30	35	35
Gasification	>800	Moderate (10–20 s)	5	10	85

Biochar, a carbon rich by-product, has been recognized as an emerging technology for water remediation. Compared to activated carbon, biochar appears to be renewable, low-cost and sustainable and could potentially replace activated carbon which is considered a universal adsorbent for water treatment (Mohan et al., 2014). There is a growing body of literature that provides evidences pertaining to using biochar for adsorption of organic and inorganic

contaminants in aqueous solutions. Biochar and its activated derivatives have been successfully used for the removal of different organics (Li et al., 2018d; Liang et al., 2019; Mohan et al., 2011; Oladipo & Ifebajo, 2018; Reguyal & Sarmah, 2018) and inorganic (Wang et al., 2014; Wang et al., 2015; Zhang et al., 2015) pollutants from aqueous solutions. Meanwhile, some studies have shown comparable or better adsorption efficiency for biochar than activated carbon (Karakoyun et al., 2011; Xue et al., 2012; Yang et al., 2014). Process parameters such as dosage of adsorbent, initial contaminant concentration, solution pH, competitive compounds, and solution temperature are some of the factors that influence the adsorption capacity of biochar. Moreover, generic properties of biochar, such as high carbon content, porous microstructure, specific surface area and cation exchange capacity play an important role in contaminant remediation in water. Intermolecular transfer of contaminants onto the surface of the adsorbents is involved in adsorption process and adsorption mechanisms are dependent on the composition of adsorbent and chemical nature of adsorbate (De Gisi et al., 2016). Electrostatic interactions, hydrophobic effect, pore-filling, π-π interactions, and hydrogen bonding are accounted as dominant adsorption mechanisms for binding organic contaminants to biochars (Figure. 2.3) (Gwenzi et al., 2017; Tan et al., 2015).
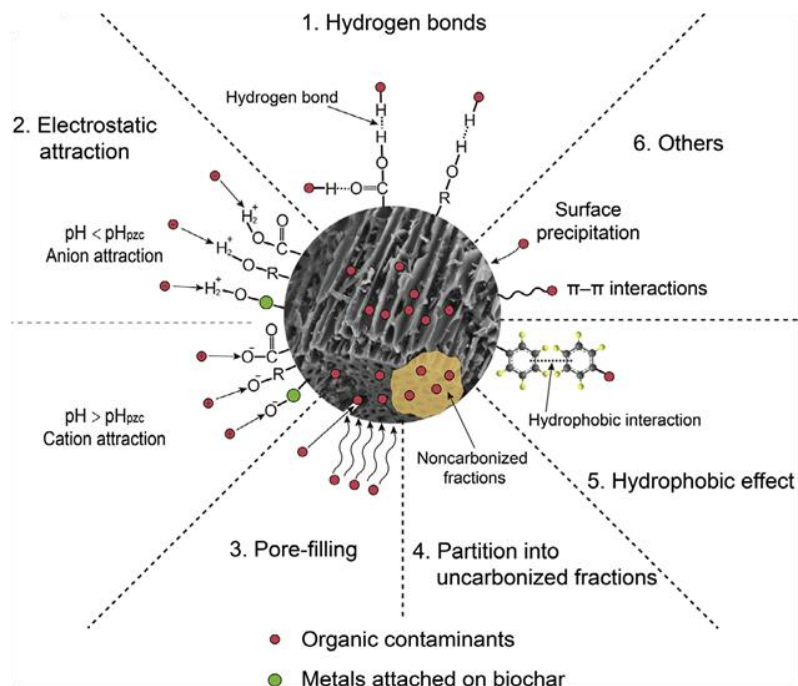
Figure 2. 3. Summary of proposed mechanisms for organic contaminants adsorption on biochars (Source: Tan et al., 2015).

2.5. Biochar Modification

In recent times, much attention has also been placed on biochar modification to enhance its properties such as pore structure, surface area and functionality to increase its removal efficiency for variety of contaminants from water and wastewater (Jung et al., 2013; Sophia A. & Lima, 2018; Zhang et al., 2015). Different modification methods to enhance biochar's sorption capacity have been introduced and applied including chemical modification (such as chemical oxidation and acid/base modification), physical modification (such as steam and gas purging), impregnation with mineral oxides, and magnetic modification (Figure 2.4) (Rajapaksha et al., 2016).

2.5.1. Chemical and physical modifications

Treatments to raw biochar via chemical activation have been shown to have a profound effect on efficiency of biochar (Kasparbauer, 2009). Acidic modification can produce both oxygen and nitrogen containing acidic surface functional groups such as amine and carboxylic groups on biochar. These functional groups play a significant role in increasing biochar's sorption capacity due to cation exchange and surface complexation. Alkaline modification via potassium hydroxide (KOH) and sodium hydroxide (NaOH) leads to an increase in oxygen containing surface functional groups and surface basicity (Fan et al., 2010; Li, 2014a) and also introduces larger surface area and more surface hydroxyl groups (Basta et al., 2009; Oh & Park, 2002). Furthermore, production of positive surface charges via alkali activation contributes to adsorption onto negatively charged biochar sites (Ahmed et al., 2016). In addition, KOH or NaOH modification has been reported to produce additional and abundant sorption sites on increased surface areas for biochar (Chia et al., 2015). Hydrogen peroxide (H_2O_2) has been demonstrated to enhance oxygenated functional groups (particularly carboxyl groups) on biochar surfaces, cation exchange sites, and finally its contaminant sorption ability (Tan et al., 2011; Xue et al., 2012). Compared to chemical modification methods, physical modifications are simpler and less effective. Through steam activation process, new pores and oxygen-containing functional groups (e.g. carboxylic, carbonyl, ether and phenolic hydroxyl groups) on surface of adsorbents are created. Also, it contributes to an increment of pore volume of the biochar due to the removal of the trapped products and surface areas by liberating the additional syngas (Rajapaksha et al., 2016; Ahmed et al., 2016). Xiong et al. (2013) demonstrated that carbon dioxide (CO_2) and ammonia (NH_3) modification increased surface area and pore volume of cotton stalk biochar.

2.5.2. Impregnation with mineral oxides

Impregnation of minerals such as montmorillonite, kaolinite, iron oxides and gibbsite with biochar is considered as a new concept for biochar modification. These minerals have been extensively applied for removal of contaminants because of their cation exchange capacity, composition, surface charge and mineralogical structure (Rajapaksha et al., 2016). Yao et al. (2014) mixed clay minerals (montmorillonite and/or kaolin) with three biomass feedstocks (bamboo, bagasse, and hickory chips) and then pyrolyzed at 600 °C for 1 h in a N_2 environment. The results showed an increase in biochar's functionality and adsorption ability to methylene blue, a model contaminant after impregnation with minerals. In another study, Song et al. (2014) modified corn straw biochar using $KMnO_4$ at 600 °C. Results showed that addition of $KMnO_4$ had a great impact on surface area and pore volumes of biochar, leading to a substantial decrease in surface area (61 to 2.28 m^2/g) and decrease in average pore width (23.7 to 92.2 nm). Moreover, O-containing functional groups increased considerably in the biochar modified with $KMnO_4$ (Song et al., 2014).
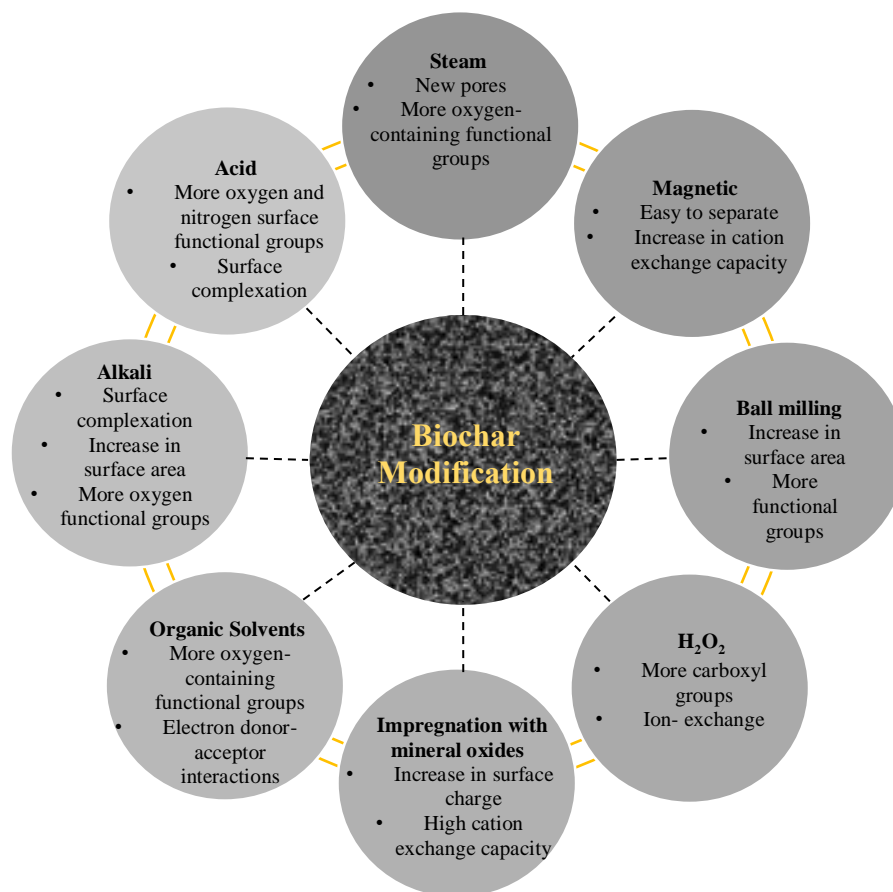
Figure 2. 4. Biochar modification techniques

2.5.3. Magnetic modification

Biochar with multi-functional characteristics has shown to have excellent ability to adsorb different organic and inorganic pollutants in water and wastewater. However, difficulty in separating these powdered adsorbents after treatment from a large volume of water is one of the drawbacks of biochar's use. Magnetic modification of biochar has overcome the referred shortcoming by facilitating separation of adsorbents by application of magnetic field or using a magnet (Chen et al., 2011; Shan et al., 2016). Also, due to negative charge on surfaces of biochar, the adsorption of anionic compounds by biochar is relatively low, and therefore, these engineered biochars have shown enhanced adsorption potential for anionic contaminants

(Beesley & Marmiroli, 2011). In some studies, decreased surface area and/or adsorption efficiency after magnetisation have been reported (Chen et al., 2011; Mohan et al., 2011; Reguyal et al., 2017); however, magnetisation has been also found to lead to increase surface area and adsorption efficiency in other studies (Devi & Saroha, 2014; Shan et al., 2016; Zhu et al., 2014). Magnetic biochar, as a promising method has attracted widespread attention in water treatment field and several studies have been conducted to prepare magnetic adsorbents in order to contribute to easy separation of biochar particles from aqueous solutions after treatment (Danalıoğlu et al., 2017; Hu et al., 2019; Zhang et al., 2013b). There are four kinds of methods that have been reported in the literature for the production of magnetic adsorbents: pyrolysis activation, calcination, chemical co-precipitation and mechanical milling and the following sections briefly discuss them.

2.5.3.1.   Pyrolysis activation

Magnetic adsorbents can be produced in one-step by pyrolysis activation via synthesis of biomass saturation in iron oxides or iron salts followed by pyrolysis. Although pyrolysis activation method is effective, it may reduce surface area and can cause unavailability of some surfaces for adsorption. Also, it may lead to formation of hematite which is less magnetic than magnetite (Shan et al., 2016). For instance, in a study by Chen et al. (2011), three different biochars were produced by pyrolysing a mixture of orange peel and $FeCl_3.6H_2O$ and $FeCl_3$ under different temperatures (250 °C, 400 °C and 700 °C) for 6 hours. The authors reported that that destruction of pores led to smaller surface area after magnetization and iron oxide (Fe_2O_3) was introduced as the magnetic source of the adsorbents. In another study by Wang et al. (2015), pinewood was suspended in solution of hematite mineral for 2 hours and then was dried in a vacuum oven at 80 °C. Following that, the mixture was pyrolysed in a tube furnace at temperature of 600 °C for 1 hour. Based on the results, magnetisation did not block pores of

biochar and the magnetic biochar had high magnetic property and higher adsorption efficiency compared to non-magnetic biochar (Wang et al., 2015).

2.5.3.2. Calcination

Calcination method is a thermal treating process, where carbonaceous precursors are impregnated with iron or other salts and then heated in a pressurized autoclave under certain temperature and period. In this process, H_2O, CO_2, SO_2 and other volatile components are removed and magnetic particles are incorporated into the biochar. This process is relatively simple and is widely applied in the production of magnetic biochar (Rocha et al., 2020; Thines et al., 2017). Saucier et al. (2017) and Sellaoui et al. (2017) used calcination method to magnetise commercial activated carbon. Carboxylic acid and metal salts were mixed to form Fe^{III} and Co^{III} carboxylates, combined with commercial activated carbon followed by calcination at different temperatures (between 260 and 600 °C) (Saucier et al., 2017; Sellaoui et al., 2017). Their results showed that the magnetic adsorbents can be easily separated from solution. Elsewhere in a separate study conducted by Gao et al. (2015), pinecone was employed for the production of magnetic biochar in the presence of $FeCl_3$ in a Teflon-lined high-pressure reaction autoclave. The authors reported the surface area and pore size of the magnetic biochar increased due to combination of calcined porous pinecone (Gao et al., 2015).

2.5.3.3. Co-precipitation

Chemical co-precipitation modification involves pyrolysing raw feedstock and subsequently mixing with magnetic particles in an aqueous solution followed by microwave heating. In this method, as shown in Eq. 1, ferrous (Fe^{2+}) and ferric (Fe^{3+}) salts are mixed in an aqueous medium and magnetite (Fe_3O_4) is precipitated and produced at pH between 8 and 14. Magnetite

is unstable and can be oxidised and transformed into maghemite (Eq. 2) which is less magnetic (Thines et al., 2017). This method is relatively simple, but it may lead to unavailability of some surfaces due to the blockage of the adsorbent pores (Shan et al., 2016).

$$Fe^{2+} + 2Fe^{3+}8OH^- \longrightarrow Fe_3O_4 + 4H_2O \qquad (2.1)$$

$$Fe_3O_4 + 2H^+ \longrightarrow \gamma\text{-}Fe_2O_3 + Fe^{2+}H_2O \qquad (2.2)$$

Some parameters such as pH, temperature, type of iron salts, the ratio of ferrous to ferric and ionic strength can change the particle size and magnetisation of adsorbents (Thines et al., 2017). Many researchers have utilised this method in the synthesis of magnetic biochars. Mohan et al. (2011) synthesised a magnetic adsorbent by suspension of almond shell activated carbon in a solution of $FeCl_3$ and $FeSO_4$, followed by NaOH treatment and the mixture was oven-dried at 50 °C. The surface area of magnetic biochar (527 m^2/g) was found to be lower than non-magnetic biochar (733 m^2/g) which was attributed to blockage of pores by iron oxide particles or smaller proportion of carbon content in the magnetic adsorbent. Similarly, Devi & Saroha (2014) employed paper mill sludge biochar to produce zero-valent iron magnetic biochar through the chemical precipitation in the $FeSO_4$ solution. The authors used $NaBH_4$ as the reducing agent for the reduction of Fe(II) to Fe(0). The findings showed that magnetisation increased surface area (1.5-fold) and micropore volume of biochar. The increase in surface area can be due to immobilization and distribution of the zero-valent iron particles on biochar surface (Devi & Saroha, 2014).

2.5.3.4.   Mechanical milling

An effective and economical technique that can be used to prepare magnetic materials is the high energy ball milling (Shan et al. 2016), which produces ultrafine magnetic powders. In their study, Shan et al. (2016) used different types of biochars and activated carbon, by mixing

with iron or iron oxides, followed by milling in a planetary ball mill at a speed of 550 rpm for different duration of time (1-7 h) to obtain the optimized milling time. The results showed that the adsorbents produced after 2 h milling had higher adsorption efficiency and surface area than non-magnetic adsorbents and could be easily separated from solution (Shan et al., 2016).

2.6. Adsorption of pharmaceuticals onto magnetic biochar

Magnetic biochar has been widely applied for the removal of pollutants from aqueous solution as it overcomes the limitation of biochar in separating from the treated water and also improves the adsorption capacity of adsorbents due to increased surface area. The magnetic biochar can be separated easily from water solution by applying an external magnetic field. Magnetic separation of adsorbents after treatment has been shown as an advantage for effective wastewater treatment and a solution for practical separation and recovery problem of exhausted/spent adsorbents (Rajapaksha et al., 2016).

In a study conducted by Oladipo & Ifebajo (2018), chicken bone biochar was magnetized and used to adsorb rhodamine B dye and tetracycline in aqueous solution. Based on results, the surface area of the adsorbent increased slightly after magnetisation (316 to 328 m^2/g). Freundlich model best described the adsorption isotherm of rhodamine B dye and tetracycline which indicates multilayer sorption mechanism of contaminants on magnetic adsorbent with maximum sorption capacity of 113.31 and 98.89 mg/g, respectively. Based on the comparative performance, the adsorption capacities for both adsorbate are higher than similar adsorbents in previous studies (Oladipo & Ifebajo, 2018). Similarly, in the work of Kong et al. (2017), the BET surface area of herbal biochar increased magnetic modification. The magnetic biochar was used for CIP removal and it was found to be a cost-effective and environmental friendly

adsorbent for adsorption of CIP in the aqueous phase. Results from isotherm modelling showed that the Langmuir model described the adsorption process well (Kong et al., 2017). Elsewhere, Shan et al., (2016) proposed using ball milling to synthesize magnetic biochar/Fe_3O_4 and magnetic activated carbon/Fe_3O_4 for carbamazepine and tetracycline elimination from aqueous solutions. A substantial increase in surface area of biochar was observed after magnetisation (30.9 to 365 m^2/g); however, magnetisation decreased surface area of activated carbon (994 to 486 m^2/g). According to the authors, the kinetic profiles of pharmaceuticals onto magnetic biochar were faster than onto magnetic activated carbon. In addition, the adsorption occurred at the surface of the biochar, however, the contaminants adsorbed preferentially on micrpores of activated carbon. The authors also reported that Langmuir model best described the adsorption of carbamazepine and tetracycline with maximum adsorption capacity of 62.7 and 94.2 mg/g for magnetic biochar and 135.1 and 45.3 mg/g for magnetic activated carbon, respectively. In another study, Reguyal et al. (2017) synthesized magnetic pine saw-dust biochar using oxidative hydrolysis of $FeCl_2$ and formed magnetic iron oxides onto biochar which led to high saturation magnetisation of the adsorbent. The magnetic biochar was used for adsorptive removal of sulfamethoxazole from aqueous solution and the authors reported that sulfamethoxazole adsorption onto modified biochar was efficient at low pH and isotherm was best described by the Redlich-Peterson model. However, the adsorption capacity and surface area of modified biochar decreased after magnetisation. Tang et al. (2018) investigated the effect of different modification methods and pyrolysis temperatures on biochar's properties. They synthesized an alkali-acid modified magnetic biochar derived from municipal sewage sludge to adsorb tetracycline in water solution. Authors reported an increase in surface area (39 to 2020 m^2/g) and optimum adsorption capacity (286.913 mg/g) of the biochar after alkali-acid combined modification. Other studies included Wang et al. (2017a) who prepared magnetic biochars with corn stalks, reed stalks, and willow branches and used for adsorption of

norfloxacin in water. Surface area and pore volume of magnetic biochars were found to be >700 m^2/g and >0.3 cm^3/g, respectively. All the magnetic biochars demonstrated strong adsorption of norfloxacin which could be related to their large surface area and pore volume. Similarly, Hu et al. (2019) fabricated novel magnetic biochars derived from camphor leaf for CIP adsorption from water solution. The results demonstrated a substantial increase in surface area of magnetic biochar from 19 to 915 m^2/g (49 times). Also, the adsorption capacity of the adsorbent increased after magnetization (449.40 mg/g) that can be attributed to the large surface area of modified biochar.

2.7. Adsorption mechanisms of pharmaceuticals onto magnetic biochar

In order to use magnetic adsorbents in water treatment rationally, understanding adsorption mechanisms of pollutants on magnetic biochar is important. Important mechanisms contributing adsorption of pharmaceuticals onto magnetic biochar are electrostatic attraction, π-π interaction, cation exchange and hydrogen bonds. Pharmaceuticals with different physiochemical properties have different functional groups, hydrophobicity and molecular charge. These various properties lead to different affinities towards magnetic adsorbents (Rocha et al., 2020). Solution pH as an important parameter for ionisable pharmaceuticals can affect pharmaceuticals' speciation and consequently change their interaction with the magnetic adsorbent (Reguyal et al., 2017). In addition, Octanol–water partition coefficients (K_{OW}) of pharmaceuticals can play an important role on their adsorption. Pharmaceuticals with higher log K_{OW} (>2) are more hydrophobic and therefore, they have higher affinity to hydrophobic surface of adsorbents. Point of zero charge (pH_{pzc}) of adsorbents can influence their adsorption affinity toward pharmaceuticals. For solution $pH < pH_{pzc}$, the adsorbent is positively charged

and for Solution pH > pH$_{pzc}$, the adsorbent is negatively charged. Electrostatic interactions is highly dependent on the adsorbent's pH$_{pzc}$ and pharmaceuticals' speciation (Rocha et al., 2020).

Investigating the removal of sulfamethoxazole from aqueous solution using magnetic pine sawdust biochar, Reguyal et al. (2017) found that the main adsorption mechanisms might be the hydrophobic interactions as electrostatic interactions cannot occur between the positively charged adsorbent (pH$_{pzc}$ = 9.5) and neutral adsorbent (pKa:1.25 and 5.29) at pH 4. Wan et al. (2014) studied the adsorption mechanism of sulfamethoxazole on magnetic manganese ferrite nanoparticles and reported that that π–π interaction and hydrogen bonds were responsible for sulfamethoxazole adsorption process. Wong et al., (2015) showed higher adsorption capacity of ibuprofen (pKa=4.91) by palm shell waste-based at pH 4 than pH 7. Based on the results obtained, the authors concluded that the governing adsorption mechanism did not occur via electrostatic interactions between positive surface of adsorbent (pH$_{pzc}$=9.1) and the deprotonated form of ibuprofen at pH 7. Instead, the main involved mechanism was due to π-π interactions between the graphitic carbon of adsorbent and aromatic ring of ibuprofen. The study by Hu et al. (2019) showed that the adsorption mechanism of CIP on magnetic camphor leaves biochar was mainly due to π-π interaction, electrostatic interaction and cation exchange.

2.8. Tyre char

2.8.1. Waste tyre as an environmental problem

About 1.4 billion/year of new tyres are produced and sold worldwide and as many are discarded as end-of-life tyres (Figure 2.5) (Martínez et al., 2013). In New Zealand, nearly 5 million tyres reach their end of life each year (Tasalloti et al., 2020). The considerable rise in global tyre production due to ground transportation need and the lack of proper mechanisms for waste

tyres disposal make them a matter of increasing concern as it poses a serious threat to public health and environment. Tyres are produced from synthetic and natural rubber (60-65 wt.%) plus other additives like carbon black (25-35 wt.%) with high carbon content (70–75 wt.%), sulphur and zinc oxide (Martínez et al., 2013; Miguel et al., 1998; Mui et al., 2010).
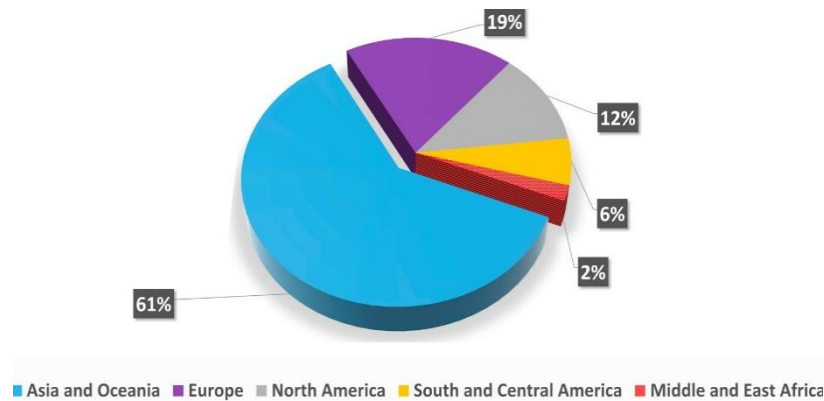
Figure 2. 5. Global production of tyre (2011) (Source: Antoniou et al., 2014).

Waste rubber tyres are extremely durable, non-biodegradable and do not decompose easily, and as a result majority of them are disposed in landfills traditionally (Merchant & Petrich, 1993). The disposal of tyres in landfills occupies large volumes resulting in massive stockpiles that poses a risk of accidental fires with high emissions of dangerous gases such as sulphurous compounds, oxides of carbon and nitrogen and particulates (Norqay, 2004). Leachate from ELTs also contain heavy metals which can infiltrate and contaminate soils, groundwater and surface water (Šandrk Nukic & Milicevic, 2019). Environmental pollution and wasting valuable rubber are the two problems caused by disposal of waste rubber tyre. ELTs have been used for various useful applications, such as a supplementary fuel in cement kilns and power plants, concrete and asphalt manufacturing, or roofing applications (Arabani et al., 2010; Barlaz et al., 1993; Navarro et al., 2010; Siddique & Naik, 2004). Alternatively, characteristics

of value-added pyrolysis products of ELTs such as fuel oil, gas and activated carbons for industrial applications have attracted much attention.

2.8.2. Adsorption of organic contaminants onto tyre char

Considering the environmental problems caused by ELTs and the cost of adsorbents for water treatment as key factors, tyre char, as a low-cost adsorbent, is gaining attention for large-scale applications in water treatment. Many researchers have recently worked on ELTs pyrolysis and tyre char production for water treatment and they have shown the capability of such carbon-based adsorbents for removal of different types of contaminants like heavy metals, dye, pesticides and pharmaceuticals from aqueous media. Production of carbon-based adsorbents from ELTs is shown in Figure 2.6. Different factors such as activating agent (steam or carbon dioxide), the degree of the activation, and pyrolysis temperature can affect characteristics of tyre char. In spite of being similar to activated carbon, the carbonaceous tyre char has much smaller surface area (Saleh & Gupta, 2014b). However, the surface area of untreated tyre char can be greatly improved by physical or chemical modification methods and therefore its adsorption efficiency is enhanced (Acosta et al., 2016; Li et al., 2010a; Styszko et al., 2017).
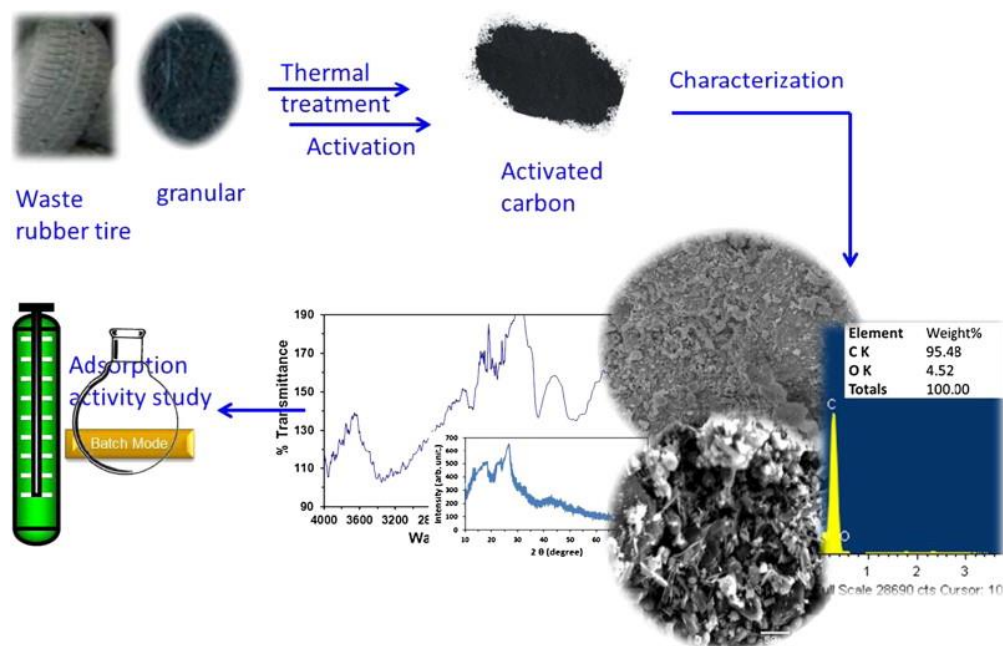
Figure 2. 6. Schematic diagram of the main steps in production of carbon-based adsorbents from ELTs (Source: Saleh & Gupta, 2014b).

Use of tyre char for adsorption of organic contaminants other than pharmaceutical compounds has been reported in some studies; however, to-date, adsorptive removal of pharmaceuticals using tyre char has been studied by just a few authors (Acosta et al., 2016; Azman et al., 2019; Styszko et al., 2017). Table 2.4 depicts literature works regarding the production and utilization on tyre char for the removal of organic contaminants from aqueous solutions. The following information is provided: treatment activation agent, specific surface area, target organic compound, experimental conditions, adsorption kinetics and adsorption equilibrium. For instance, Azman et al. (2019) reported the use of tyre char (pyrolysed at 800 ℃), followed by activation with nitric acid (HNO_3) to study the removal capacity for aspirin in aqueous phase. The best adsorption was reported to be 40.40 mg/g at an adsorbent dosage of 0.02 g at pH 3 with an initial concentration of 100 mg/L (Azman et al., 2019). In the study by Acosta et al. (2016), the application of tyre pyrolysis char activated with KOH was investigated for the removal of tetracycline from aqueous solutions. The surface area of tyre char increased

substantially after KOH activation (60 to 814 m^2/g). The maximum adsorption capacity of tetracycline was obtained 312 mg/g which was higher than commercial activated carbon as mentioned in the literature. In another study, tyre char was activated by CO_2 and impregnated with amines solutions and then was employed for adsorption of selected xenobiotics in aqueous phase. Based on results, a considerable increase in surface area (36 to 128 m^2/g) was observed after activation and high removal efficiencies (up to 99 %) were obtained for adsorption of the pharmaceuticals onto the activated char (Styszko et al., 2017). In all these aforementioned studies, tyre char was shown to be an effective and promising adsorbent for the removal of pharmaceuticals from aqueous solutions.

Tyre char has also been utilised for the adsorption of other organic contaminants from water bodies. In a study by Li et al. (2010a), activated carbon derived from waste scrap tyres applied for cationic dye removal, Rhodamine B, from aqueous solutions. The results showed that the adsorption was highly dependent on solution pH and temperature while ionic strength had little influence on the adsorption process. The maximum adsorption capacity of Rhodamine B onto tyre char was 307.2 mg/g which was higher than other adsorbents reported in the literature. In another report (Ariyadejwanich et al. , 2003), waste tyres were pyrolysed at 500 °C in nitrogen atmosphere and then was activated with steam at 850 °C. High mesopore volumes (1.09 cm^3/g) and surface areas (737 m^2/g) were obtained after activation. Treatment with 1 M HCl at room temperature for 1 day prior to steam activation further increased the mesopore volumes and surface areas of the adsorbents to 1.62 cm^3/g and 1119 m^2/g, respectively. Activated adsorbents were used for adsorption of phenol and Black 5 dye from aqueous solutions and their adsorption capacities were reported to be comparable with commercial activated carbons (Ariyadejwanich et al. , 2003). Table 2.4 shows published works on adsorption of organic compounds in aqueous media using tyre char.

Table 2. 4. Adsorption studies for the removal of organic compounds from aqueous solutions with tyre-based adsorbents

Organic Compound	Modification method	BET (m^2/g)	Adsorption conditions	Adsorption kinetic	Adsorption equilibrium	References
Aspirin	HNO_3	-	•T: 30, 50, 70 °C • pH: 3,7,11 • Dose: 2-20 g/L • Contact time: 30 s–150 min • C_i: 10-100 mg/L	•pH: 7 •T: 30 °C • t_e: 60 min • C_i: 100 mg/L •Dose: 2 g/L	• pH:3 •T: 30 °C • Dose: 2 g/L • q_{max}: 40.40 mg/g	(Azman et al. 2019)
Tetracycline	KOH, HCl	814	•T: 15, 25, 35 °C • pH: 6.5-7.5 • Dose: 1 g/L • Contact time: 30 s–25 h • C_i: 50-300 mg/L	• T: 25 °C • t_e: 15 h • C_i: 100, 300 mg/L • Dose: 0.5 g/L	• T: 25 °C • Dose: 0.5 g/L • q_{max}: 312 mg/g	(Acosta et al. 2016)
Acid Blue 113	H_2O_2, HCl	562	•T: 25 °C • pH: 5 • Dose: 10 g/L • Contact time: 30 s–100 min • C_i: 1–12×10−5 M	• pH: 5, 25 °C • t_e: 40 min • P1O	• T: 25 °C • Langmuir • q_{max}: 9.20 mg/g	(Gupta et al., 2011a)
Methylene blue	Steam or CO_2	1070	•T: 20 °C • pH: 6.8 • Dose: 1 g/L • C_i: 100–1000 mg/ l	-	• T: 20 °C • Langmuir • q_{max}: 360 mg/g	(San Miguel et al., 2003)
Basic Astrazon Yellow and Reactive Rifafix Red	HNO_3	1126	•T : 25 °C • pH: 2,7,12 • Dose : 0.5 g/L • Contact time: 48 h • C_i: 12 - 1000 mg/l	-	• Langmuir • q_{max} for Basic dye (PH 12): 1055 mg/g • q_{max} for Reactive dye (PH 2): 68 mg/g	(Acevedo et al., 2015)
Triton X-100	KOH, HCl	426	•T: 18, 35, and 65 °C • t_e: 7 days • Dose: 2 g/L • C_i: 10–1000 mg/ l	-	•T: 18 °C • Langmuir • q_{max}: 220 mg/g	(Kuśmierek et al., 2020)
phenol and methylene blue	HNO_3	135	•T: 25 °C • pH: 6.6 • Dose: 0.1 g/L • Contact time: 30 s and 2 h • Ci (C_{phenol} : 2, 5, 10, 20, 50, 100mg/L, $C_{methylene\ blue}$: 2, 5, 10, 20, 40, 80, 100 mg/L	• pH: 6.6 • t_e: 60 min • P2O •C_i of 10 mg/L for phenol, C_i of 20 mg/L for methylene blue	• q_{max} phenol (Langmuir): 51.92 mg/g • q_{max} methylene blue (Freundlich): 65.81 mg/g	(Makrigianni et al., 2015)

Microcystin LR	H_2O_2	1111	• T: 25 °C • pH: 3-9 • Dose: 1-5 g/L • Contact time: 5-60 min • C_i: 0.52 to 65 µg/L	• pH:4 • Dose: 3 g/L • t_e: 34 min • P2O • C_i:25 µg/L	• pH:4 • Dose: 3 g/L • Langmuir • q_{max}: 357 µg/g	(Mashile et al., 2018)
Anthracene	H_2O_2, KOH	-	• T: 20–50 °C • pH: 2-12 • Dose: 0.02-0.2 g/L • Contact time: 15–150 min • C_i: 40 mg L^{-1}	• t_e: 80 min • P2O	• Freundlich • q_{max}: 142.24 mg/g	(Gupta, 2018)
Rhodamine B	Steam	720	• T: 25–45 °C • pH: 3-11 • Dose: 0.02-0.2 g/L • Contact time: 0-800 min • C_i: 20–150 mg/L	• T: 25–45 °C • pH: 3-10 • Dose: 0.1-0.5 g/L • C_i: 20–150 mg/L • t_e: 12 hr • P2O	• pH:4 • T: 45 °C • Dose: 0.2 g/L • Langmuir • q_{max}: 307.2 mg/g	(Li et al., 2010a)
Cylindrosper mopsin	-	-	• pH: 3-9 • Dose: 2-10 g/L • Contact time: 5-60 min • C_i: 5-65 µg/L	• pH: 3 • Dose: 5 g/L • t_e: 60 min • P2O (Ci of 25 µg/L)	• pH:3 • Dose: 5 g/L • Langmuir • q_{max}: 110 µg/g	(Mashile et al., 2019)
Methyl orange	HCl, H_2O_2	465	• T: 40,55,70 °C • pH: 3-7 • Dose: 0.02-1 g/L • Contact time: 5-50 min • C_i:1×10^{-6} to 1×10^{-4} M	-	-	(Saleh & Gupta, 2014a)
2-Chlorophenol	H_2O_2, KOH, HCl	208	• T : 25 °C • pH: 3, 5, 7, and 10 • Dose: 1-10 g/L • Contact time: 0 s and 30 min • C_i: 10-100 mg/l	• pH: 5 • Dose : 2 g/L • t_e : 10 min	-	(Manirajah et al., 2019)
Methylene blue, phenol	HNO_3	352	• T: 30-50 °C • pH: 2-12 • Dose: 1 g/L • Contact time: 0 s and 72 h • C_i: 5-200 mg/l	• t_e: 72 hr • P2O • Ci of 5 and 20 mg/L	• q_{max} phenol: 34.8 mg/g • q_{max} methylene blue: 108 mg/g	(Hakimi Mohd Shaid et al., 2019)
Methylene blue	Steam	602	• T: 30, 40 and 50 °C • Dose: 4-20 g/L • C_i: 5-600 mg/l	-	• T: 50 °C • Langmuir • q_{max}: 250 mg/g	(Lin & Teng, 2002)
Methoxychlor, atrazine and methyl parathion	KOH, HCl	981	• T: 25 °C • pH: 2-11 • Dose: 0.02 to 0.10 g/L	• T: 25 °C • pH: 2 • Dose: 0.1 g/L	• pH: 2 • Langmuir • q_{max} methoxychlor: 112.0 mg/g	(Gupta et al., 2011b)

			• Contact time: 0-150 min • C_i: 2 mg/L to 12 mg/L	• C_i: 12 mg/L • t_e: 60 min • P1O	• q_{max} atrazine: 104.9 mg/g • q_{max} methyl parathion: 88.9 mg/g	
p-cresol and phenol	KOH, HCl	1802	•T: 25–45 °C • pH: 2-11 • Dose: 0.6 g/L • Contact time: 5–210 min • C_i: 3–300 ppm	•T: 45 °C • pH: 7 • Dose: 0.6 g/L • C_i: 12 mg/L • t_e: 90 min • P1O	•T: 25 °C • pH: 7 • Langmuir • q_{max} p-cresol: 250mg/g • q_{max} phenol: 100 mg/g	(Gupta et al., 2014)
Dichloromethane, chloroform, carbon tetrachloride	HNO$_3$ and H$_2$O$_2$	62.35	•T: 25 °C • pH: 6.6 • Dose: 0.2-10 g/L • Contact time: 30 s and 100 min • C_i: 3-12 mg/l	• Dose: 5 g/L • t_e : 60 min • P2O (Ci of 0.5, 1, 2 mg/L)	• Dose: 5 g/L • Freundlich	(Abdelbassit et al., 2020)

Abbreviations: initial concentration of Compounds (C_i); maximum adsorption capacity (q_{max}); pseudo first order kinetic model (P1O); pseudo second order kinetic model (P2O); equilibrium time (t_e).

2.9. Adsorption of pharmaceuticals onto biochar in fixed-bed columns

The batch adsorption studies do not provide accurate equilibrium and kinetic data for optimization and proper design of fixed-bed columns. Moreover, laboratory experiments under dynamic conditions using columns are easy to scale up for industrial applications (Jaria et al., 2019; Ahmed & Hameed, 2018). Therefore, in order to have practical information for scale-up applications, studying fixed-bed columns and associated breakthrough curves determination are of paramount importance as the information obtained from such studies under dynamic conditions provide realistic parameters for pilot scale study. Design parameters and the best operating conditions can be identified and determined by analysing data obtained from continuous experiments (Mondal et al., 2016). Simple operation mode, high removal efficiency and easy scale-up are accounted as advantages of fixed-bed adsorption (de Franco et al., 2017). Compared to batch studies, a smaller number of column studies have been carried out on

adsorptive removal of organic compounds from water. Nazari et al. (2016) used walnut shell activated carbon for adsorption of cephalexin, a beta-lactam antibiotic, from aqueous solution in a fixed-bed column. The authors reported that the highest adsorption capacity (211.78 mg/g) was obtained under inlet concentration of 100 mg/L, bed height of 2 cm and flow rate of 4.5 mL/min flow rate. High flow rates resulting in rapid breakthrough could be attributed to the insufficient contact time between cephalexin and adsorbent. Mondal et al. (2016) tested the influence of inlet concentration, bed depths and flow rates on the shape of the breakthrough for adsorption of ranitidine onto activated mung bean husk biochar. The results suggested that breakthrough time decreased with rise in initial concentration and flow rate. At higher bed heights, ranitidine molecules obtained a sufficient time to diffuse into the SMBB. Thus, drug uptake was elevated, and breakthrough time was prolonged.

Darweesh & Ahmed (2017a) illustrated the adsorption dynamics of CIP and norfloxacin on date-stone carbon and the influence of flow rate, bed height, and initial concentration on the behaviour of breakthrough of CIP and norfloxacin curves was investigated. Results demonstrated that the adsorption capacity of both drugs and their breakthrough and saturation time decreased at higher flow rates that can be related to the high rate of mass transfer. In another study, Yaghmaeian et al. (2014) explored the trend of the breakthrough curves for the adsorption of amoxicillin onto NH_4Cl-activated carbon (NAC) and standard activated carbon (SAC) in the fixed-bed columns. Adsorption capacity of NAC was shown to be much higher than SAC at different empty bed contact times. Elsewhere, Liao et al. (2013) studied the continuous adsorption of tetracycline and chloramphenicol on a bamboo charcoal. Higher adsorption capacities of tetracycline and chloramphenicol on the charcoal were observed at higher flow rate, lower bed height, and lower initial concentration.

2.10. Modeling the transport of contaminants in fixed-bed columns

To represent and correlate the experimental breakthrough curves, numerical or mathematical models are required which provide some useful information such as adsorption capacity, regeneration time, breakthrough time and mechanism of the adsorption process (Patel, 2019). Numerical models can also facilitate the scale-up and industrial design. Estimation of concentration profile for a given adsorbate in the liquid phase within the fixed-bed column can be determined using verified mathematical models (Ahmed & Hameed, 2018; Lin et al., 2017). Several adsorption phenomena such as dispersion, mass transfer and intraparticle diffusion occur simultaneously during the adsorption of contaminants onto adsorbents packed in columns (Vilardi et al., 2019). The models that consider these adsorption mechanisms can successfully predict transport of contaminants in fixed-bed column (Jellali et al., 2016; Liao et al., 2013). Therefore, to obtain a more accurate estimation of adsorption parameters for scale-up applications and real industrial plants, suitable theoretical models should be used as they can successfully simulate breakthrough curves and accomplish evaluation of adsorption processes in fixed-bed columns.

Adams–Bohart, Thomas, and Yoon–Nelson are commonly used models for analysing breakthrough curves obtained in fixed-bed column studies. However, these models consider insignificant and/or no axial dispersion and mass transfer in modelling breakthrough curves (Ahmed & Hameed, 2018; Chu, 2010; Patel, 2019). In contrast, non-equilibrium adsorption and mass transfer, dispersion and diffusion are taken into account in some models such as Hydrus (Jellali et al., 2016; Šimůnek & van Genuchten, 2008). Based on previous studies (Hanna et al., 2010; Jellali et al., 2016, Suárez et al., 2007), models that consider physical and/or chemical non-equilibrium processes, mass transfer and dispersion mechanisms have been found to successfully predict the transport of contaminants in porous media.

Nazari et al. (2016) analysed the data for adsorption of cephalexin onto walnut shell biochar using Adams–Bohart, Thomas and Yoon–Nelson models. Thomas and Yoon–Nelson models (R^2 of 0.54–0.95) described the measured data better than Adams–Bohart model (R^2 of 0.29–0.84) under various conditions. Mondal et al. (2016) reported the simulation of ranitidine adsorption data for an activated mung bean husk biochar packed in a fixed-bed column. All the three common models were tested for modelling the data and Yoon–Nelson model was shown to simulate the breakthrough curve of the adsorbate better than other models. In another study (Darweesh & Ahmed, 2017a), a poor correlation was reported by the Adams–Bohart model for adsorption of CIP (0.750–0.84) and norfloxacin (0.767–0.854) on date-stone activated carbon. However, Thomas and Yoon–Nelson models could predict the data well for both adsorbates. Based on the results, Langmuir type isotherm, second-order kinetics, and decreasing adsorption rate were related to the to the adsorption of CIP and norfloxacin in the fixed-bed column (Darweesh & Ahmed, 2017a). Yaghmaeian et al. (2014) used the Thomas and Yoon–Nelson models to predict the breakthrough data for amoxicillin adsorption on permanganate activated carbon. Both Thomas and Yoon–Nelson models described the experimental data well with R^2 values of 0.95–0.97 and 0.93–0.97, respectively. Liao et al. (2013) developed a mass transfer model considering surface and intraparticle diffusion to investigate adsorption process of tetracycline and chloramphenicol. Based on their findings, the developed model predicted the experimental data well and the surface diffusion was shown to be the rate-limiting step for adsorption of both contaminants.

Hydrus model has been used for predicting the transport of organic and inorganic contaminants in porous media in last two decades (Jellali et al., 2010; Martínez-Hernández et al., 2017; Suárez et al., 2007); however its application for modelling contaminants transport in carbon-based adsorbents in fixed-bed columns was tested in only one recent study (Jellali et al., 2016). Jellali et al. (2016) used Hydrus model for prediction of transport parameters of lead adsorption

in fixed-bed columns packed with raw sawdust and magnesium pretreated biochar. The results showed that non-equilibrium Hydrus model described the experimental data well (R^2 of 0.97-0.99) for both adsorbents and provided valuable data for scale-up purposes. To date, application of Hydrus model for modelling the fate and transport of pharmaceuticals in fixed-bed columns packed with carbon-based adsorbents has not yet been studied.

2.11. Regeneration of spent adsorbent using ball milling

Regeneration of spent adsorbents can make adsorption technology more economical and feasible. Moreover, disposal of the exhausted biochar represents serious environmental problems as they are loaded with toxic pollutants. Some techniques such as microbiological, chemical, thermal, microwave, and electrochemical can be utilized in regeneration of spent adsorbents (Ahmed et al., 2016). Solvents such as HCl, NaOH, ethanol, methanol, acetone, acetic acid, EDTA and NaCl are extensively used in desorption cycles (Ahmed et al., 2016; Reguyal et al., 2017). In order to investigate the reusability of spent adsorbents, some studies have been conducted on desorption of adsorbed contaminant and regeneration of used adsorbents (Parshetti et al., 2014; Reguyal et al., 2017; Zhang et al., 2013a). However, desorption of adsorbed contaminants and reintroducing them back into the environment may not be a logical and appropriate way to solve the issue. Moreover, these methods are usually sophisticated and need high energy input and toxic and costly reagents.

Ball-milling technology has recently been receiving increasing interest as a cheap, effective and green technique for mechanochemical degradation of contaminants such as pharmaceuticals and production of nanoparticles (Naghdi et al., 2017; Samara et al., 2016). Mechanochemical degradation process is a chemical reaction driven by the application of force

by milling, grinding or compression. Mechanical forces may cleave the particles and increase their surface area (Samara et al., 2016). Important parameters affecting the degradation of chemicals are shown in Figure. 2.7. Ball milling technology is still in its infancy and only a few studies have been done on degradation of pharmaceuticals using ball milling (Shan et al., 2016, Samara et al. 2016). For example, Shan et al., (2016) used ball milling to degrade the adsorbed contaminants (carbamazepine and tetracycline) onto the adsorbent. The results demonstrated that about 90% of adsorbed carbamazepine and tetracycline onto biochar were easily degraded by mechanochemical ball milling. The degradation of carbamazepine was improved after adding quartz to the adsorbent. In another study conducted by Samara et al. (2016), ball milling degraded 94% of applied carbamazepine after milling for 30 min. Yan et al. (2017) reported that ball milling could greatly degrade Hexabromocyclododecane after 2 hours milling and with addition of sodium hydroxide and sodium persulfate as co-milling reagents. Gao et al. (2021) reported the successful degradation of high concentrations of dichlorodiphenyltrichloroethane (DDT) in contaminated soil using ball milling. Removal rate of DDT after ball milling for two hours with ball diameters of 19.6 mm was around 95%.
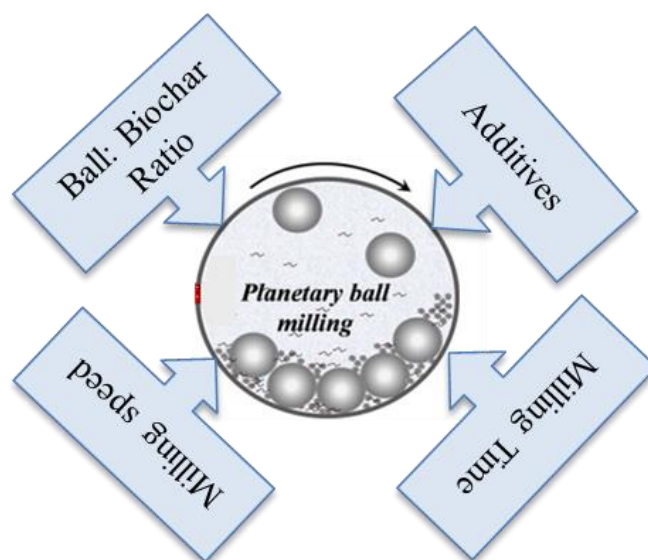
Figure 2. 7. Schematic diagram of the main factors affecting degradation.

2.12. Scale-up and techno-economic feasibility of tyre char as an adsorbent

Scarcity of data in techno-economic feasibility of engineered biochars and design and scale-up of biochar-based treatment systems has constrained application of biochar technology in industry-scale applications for water and wastewater treatment. Therefore, to determine the economic standing of biochar-based adsorbents, future studies should focus on the cost analysis of engineered biochars produced from different feedstocks. Also, design and optimization of biochar-based water treatment systems could be a focus in future research.

Techno-economic assessment of biochar production derived from different feedstocks has been investigated in a few studies (Choy et al., 2005; Lai & Ngu, 2020; León et al., 2020; Toles et al., 2000). Similarly, cost analysis of pyrolysis of waste tyre has been also reported by a few authors (Islam et al., 2011; Ko et al., 2004; Li et al., 2010b; Zabaniotou et al., 2014). For example, in the study by Islam et al. (2011), techno-economic feasibility of pyrolysis process for converting ELTs into pyrolysis oils, solid char and gases was carried out in three different plant sizes. The authors reported that the medium commercial-scale plant gave the lowest unit production cost for the production of pyrolysis oil (136 US$/tonne). By considering the revenue from solid char and gas, the total production cost for oil was reduced to 62 US$/tonne. An example of the conceptual design for pyrolysis plant used by Islam et al. (2011) is presented in Figure. 2.8. In another study, pyrolysis was shown as the most eco-effective treatment technology for ELTs, where Li et al., (2010b) found that pyrolysis of tyre char had higher economic benefit and lower environmental impacts compared to dynamic devulcanization and ambient grinding treatment technologies. It was found that the cost of carbon black obtained from pyrolysis was estimated to be 450 US$/tonne. Much earlier, Ko et al. (2004) demonstrated the feasibility of converting waste tyres and coal to activated carbons and the results from economic analysis revealed that using waste tyres as precursor for production of activated

47

carbon has higher return of investment (27.4%) and lower operating costs compared to using coal as precursor.

Other studies include an economic evaluation of activated carbons production derived from almond shell and activated through different activation/oxidation conditions (Toles et al. 2000). The authors compared their findings against commercial activated carbon and reported that based on the estimated production costs, the unoxidized almond shell adsorbent activated through steam activation was found to have the lowest production costs (1540 US$/tonne). Also, the estimated costs for all other activated carbons derived from almond shell were lower than commercial activated carbon (3300 US$/tonne). Elsewhere, cost estimation of activated carbon derived from waste nutshells using pyrolysis and steam activation was studied by León et al. (2020). Based on the production rate of 6.6 tonne/day in a 10-year project, the production cost of the activated carbon was calculated 2150 US$/tonne.
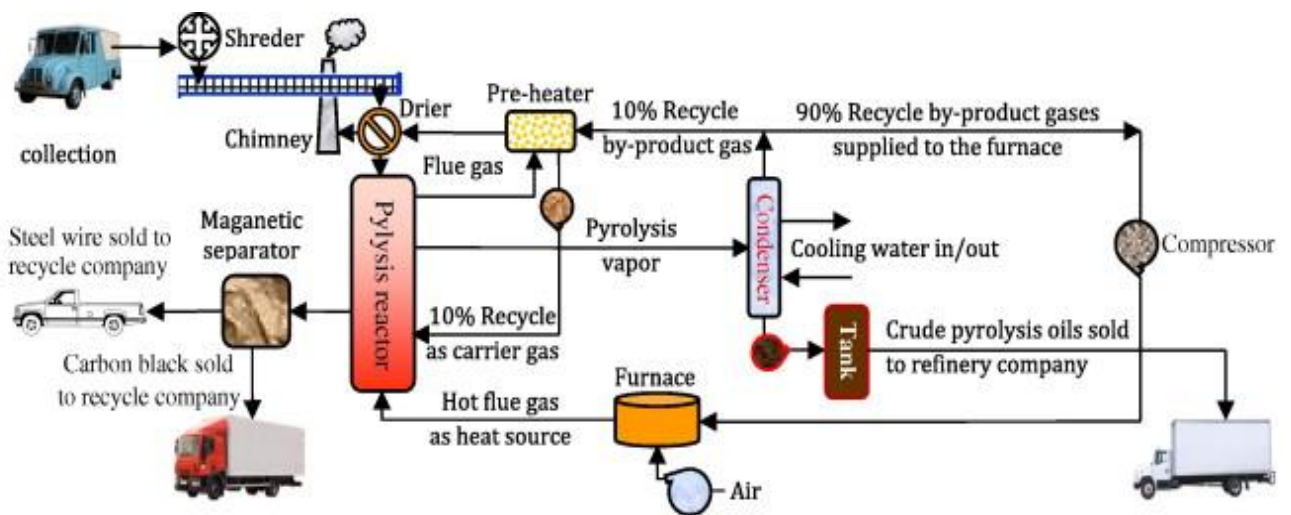
Figure 2. 8. An example of conceptual design for pyrolysis plant (Source: Islam et al., 2011).

2.13. Summary and knowledge gaps

Pharmaceuticals are emerging contaminants of growing concern that are ubiquitously found in the aquatic environment with a potential risk for human health and ecosystem. CIP, PRO and CLO as widely prescribed pharmaceuticals have been frequently detected in the aquatic environment. These pharmaceuticals could cause harmful effects on human and aquatic life and have been found to be toxic in different organisms even at small concentrations (ng/L to µg/L) (Maszkowska et al., 2014b; Minguez et al., 2014; Załeska-Radziwiłł et al., 2014). In response to this, special attention to their environmental fate is required.

Based on available studies in literature, various treatment methods such as ozonation, oxidation, photo-Fenton process, photocatalytic degradation and membrane bioreactor have been applied for removing these pharmaceuticals from aqueous solutions (Estrada-Arriaga et al., 2016; Lu et al., 2019; Nassar et al., 2017; Nielsen & Bandosz, 2016; Perini et al., 2018; Radjenović et al., 2009). These methods, however, have some disadvantages such high cost, complicated treatment process, or producing toxic by-products. Adsorption technology has been recognized as a promising method for removal of emerging contaminants due to its low-cost, ease of operation and high efficiency. However, difficulty in separation of adsorbents from aqueous solution after treatment is one of the drawbacks of the adsorption technology. This difficulty can be overcome by magnetisation of adsorbents using various metallic ions and then separation of the powdered magnetic adsorbent by application of the external magnetic field. In some studies, magnetic adsorbents have demonstrated higher surface area and significant morphology after magnetisation that could increase their capacity for adsorption of contaminants (Devi & Saroha, 2014; Shan et al., 2016; Zhu et al., 2014).

Different carbon materials are extensively used as adsorbents for adsorption of contaminant from water bodies. However, low-cost activated carbons derived from ELTs are more

promising for real applications as they have co-benefits including provision of clean water and minimisation if solid waste. Although removal of pharmaceuticals using different adsorbents have been investigated in many studies, there is very few information available on adsorption of pharmaceuticals on tyre char (Acosta et al., 2016; Azman et al., 2019; Styszko et al., 2017). Therefore, removal of pharmaceuticals from aqueous solutions using tyre char and studying adsorption mechanisms warrant investigation. Moreover, adsorption of pharmaceuticals onto magnetic tyre char has not been investigated yet.

Many studies have demonstrated the high capacity of biochar for adsorption of contaminants from water bodies (Li et al., 2018d; Liang et al., 2019; Mohan et al., 2011; Oladipo & Ifebajo, 2018; Reguyal & Sarmah, 2018). However, the bulk of existing research is on batch adsorption of pollutants and limited studies have been conducted on the fixed-bed adsorption of contaminants. Therefore, to date there has been no attempts for development of column pilot and industrial scale of biochar-based water treatments systems. Moreover, information obtained from column studies is critical and helpful for predicting contaminants transport in column, validating existing models and propagation of data in industrial scale especially using appropriate mathematical models. Based on recent studies, the models that consider non-equilibrium processes, dispersion, mass transfer and diffusion mechanisms can successfully predict the transport of contaminants in fixed-bed columns (Jellali et al., 2016; Liao et al., 2013). There are limited studies on the modelling the transport of pharmaceuticals in fixed-bed column using appropriate models (Liao et al., 2013) and most studies have used traditional models such as Adams–Bohart, Thomas, and Yoon–Nelson which do not consider all adsorption mechanisms in column studies (Darweesh & Ahmed, 2017b; Mondal et al., 2016; Nazari et al., 2016).

Biochars obtained from feedstocks or waste materials are considered as low-cost and renewable technology for water and wastewater treatment; however, there is limited literature on reliable

techno-economic assessment of carbon-based adsorbents (Choy et al., 2005; Islam et al., 2011;

Ko et al., 2004; Lai & Ngu, 2020; León et al., 2020; Toles et al., 2000).

CHAPTER 3: Environmental remediation in circular economy: End of life tyre magnetic pyrochars for adsorptive removal of pharmaceuticals from aqueous solution

Introduction

Antibiotic residues released from treated wastewater and agricultural runoff can lead to the development of antibiotic resistance in human health and wildlife (Sun et al., 2014; Zeng et al., 2018). CIP, a broad-spectrum antibiotic, is marketed and used globally for the treatment of infectious diseases in humans and animals (Carabineiro et al., 2011). Beta-blockers are known as endocrine disrupting chemicals and have toxicological effects on non-target organisms in the environment. PRO is one of the beta-blockers which is prescribed for heart disease and commonly detected in water bodies (Wick et al., 2009). Another group of widely prescribed pharmaceuticals are antidepressants, such as CLO, which have a direct effect on central nervous system and can interrupt neuroendocrine signalling (Yuan et al., 2013).

In WWTP, mixtures of multiple pharmaceuticals with diverse chemical structures exist simultaneously, and their removal rates are different based on the physiochemical properties of the pharmaceuticals (Nielsen & Bandosz, 2016). It is well recognized that conventional treatment technologies are not capable enough to eliminate these pollutants, even with tertiary treatment. Therefore, developing effective technologies to eliminate pharmaceuticals from the environment is continuously in demand and imperative.

Biochar or pyrochar, a carbon-rich porous solid material derived from thermochemical conversion of biomass, has been demonstrated as a promising adsorbent for the removal of various pollutants from waterbodies because of its high efficiency, low-cost and low environmental risk (Kong et al., 2017). Recent studies have shown biochar as an effective adsorbent for pharmaceuticals and personal care products (PPCPs) removal (Yao et al., 2012; Zhu et al., 2014). However, one of the drawbacks of using biochar is the difficulty in separating from aqueous solution after treatment. Hence, magnetic biochar, as an emerging method, has attracted considerable interests in water treatment as it can be easily collected after adsorption

by application of external magnetic field or using a permanent magnet instead of filtration and centrifugation (Wang et al., 2014).

Magnetic adsorbents, because of its ease of recovery and regeneration properties are potentially applicable at full-scale industrial wastewater treatment and batch adsorption tests for several times. Magnetic medium (such as maghemite) and carbonaceous adsorbents are typically combined by chemical co-precipitation or pyrolysis activation (Rajapaksha et al., 2016; Reguyal et al., 2017; Reguyal & Sarmah, 2018). The introduction of magnetic particles to the carbon-based adsorbent has led to reduction in surface area and adsorption capacity in comparison to pristine adsorbents (Reguyal et al., 2017); however, opposite trend of increased surface area and adsorption efficiency after magnetisation has also been reported (Chen et al., 2011; Devi & Saroha, 2014; Mohan et al., 2014; Shan et al., 2016; Zhu et al., 2014).

While pyrochar can be produced from a range of waste biomass (rice-husk, coconut shell, pine sawdust, sewage sludge, orange peel etc.) via pyrolysis, the end of life tyres (ELTs) can be a feasible raw material due to its high carbon content. Globally, over one billion waste automotive tyres are being generated every year causing serious environmental problems associated with their improper disposal, non-biodegradable nature and pollution emissions (de Toledo et al., 2018; Loloie et al., 2017). The disposal of tyres in landfills occupies large volumes resulting in massive stockpiles that poses a risk of accidental fires with high emissions of dangerous gases such as sulphurous compounds, oxides of carbon and nitrogen and particulates (Norqay, 2004). Leachate from ELTs also contain heavy metals which can infiltrate and contaminate soils, groundwater and surface water (Šandrk Nukic & Milicevic, 2019). Environmental pollution and wasting valuable rubber are two problems caused by disposal of waste rubber tire. Adsorbents produced from ELTs have been successfully used for the adsorption of different inorganic (Quek & Balasubramanian, 2009; Quek & Balasubramanian, 2011) and organic contaminants (Rozada et al., 2005a; Rozada et al., 2005b;

Rozada et al., 2007). However, until now only a few studies have been conducted on the use of ELTs based adsorbents to remove pharmaceuticals from aqueous solution (Acosta et al., 2016; Azman et al., 2019; Styszko et al., 2017). For instance, Azman et al. (2019) evaluated aspirin removal using tyre waste adsorbent synthesized with chemical and thermal treatment and concluded the highest adsorption performance of aspirin at pH 3 and temperature of 30 °C. Similarly, tyre pyrochar activated with CO_2 and impregnated with amines was utilized for the elimination of selected pharmaceuticals in aqueous phase (Styszko et al., 2017). In the study conducted by Acosta et al. (2016), tyre pyrolysis pyrochar, tyre pyrolysis pyrochar activated by KOH and a commercial activated carbon were used to investigate Tetracycline removal from aqueous solution. Although the application of tyre pyrochar to treat drug pollutants has been studied, adsorption mechanisms of pharmaceuticals onto tyre adsorbents has not been explained well.

Despite a large number of research studies on the development of char as adsorbents for water treatment, transposing the process from small-scale studies to large-scale systems in order to demonstrate feasibility and performance remains a significant barrier. TRL assessment is carried out to identify the challenges and describe the maturity of a new technology based on technology concepts and requirements. TRL are based on a scale from 1 to 9 assigned to lab-scale development (levels 1–4), pilot-scale development (levels 5–7) and industrial-scale development (levels 8, 9) (Buchner et al., 2019).

Therefore, the overarching aim of this Chapter was to produce low-cost and environmentally friendly adsorbent achieving two targets with environmental, market and societal outcomes: a) a new low-cost product for environmental remediation and b) sustainable management of ELTs. Specific objective was to produce and synthesise magnetic tyre pyrochar at TRL3-7 and investigate the adsorptive removal of CIP, PRO, and CLO selected as model adsorbates in aqueous solution. Effects of pH and ionic strength on the adsorption of the contaminants onto

magnetic tyre pyrochar were studied to gain information on the behaviour of the compounds. A secondary objective was to conduct a preliminary assessment on the techno-economic feasibility of tyre pyrochar's usage as an adsorbent by comparing the proposed innovative process and product with the activated carbon in terms of production cost, effectiveness and sustainability.

3.2.   Materials and methods

ELTs samples, mixtures of car tyres and truck tyres, to a mass ratio (90/10) were used as pyrolysis feedstocks to produce the pyrochars. All chemicals (CIP, PRO, CLO, $FeCl_3 \cdot 6H_2O$, $FeSO_4 \cdot 7H_2O$) and methanol (LCMS grade, 99.9% purity) were purchased from Sigma-Aldrich, New Zealand. Other chemicals including KOH, formic acid (CH_2O_2), NaOH, NaCl and HCl used in this study were of analytical grade and commercially available.

3.2.1. Pyrolysis of ELTs at TRL7

Pyrolysis of the ELTs was carried out in a prototype designed in Greece and constructed by the Irish PGE company in collaboration with the University College of Cork, in the context of an EU Life + project, the LIFE10 ENV/IE/000695 (Antoniou & Zabaniotou, 2018). The TRL of Pyrolysis was 7. The continuous-operation pilot plant, is based on a rotary kiln reactor and is consisted of the following sections: feeding system, rotary kiln reactor, vessel for solids collection, liquid cooling, condensing and collection system, gas furnace and control systems (Figure 3.1). The prototype plant can process up to 100 kg/h of pre-treated, steel-free tyre granulates with a mass flow rate of 20 kg/h. The pyrolysis experiments were carried out at the optimised conditions: Temperature = 550 °C, heating rate = 20 °C min^{-1} and particle size 20 mm, under oxygen-free and atmospheric pressure. Nitrogen (N_2) was initially used to purge the whole system, thus assuring oxygen-free conditions for pyrolysis.
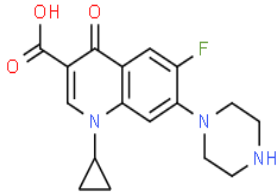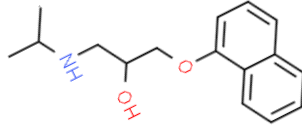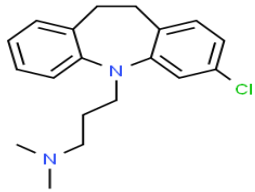
For replicability reasons, five consecutive samplings were performed under the same feeding rate. Sampling of non-condensable gas, liquid and solid products took place when the steady state was reached, approximately after 30 min from pyrolysis start-up. Every 30 min, gas, liquid and solid samples were taken so that the continuation, replicability and reproducibility of the process could be verified.

The gas, liquid, and solid product yields in percent weight (wt. %) were $14.5 \pm 2\%$, $37.5 \pm 1\%$ and $48.0 \pm 2\%$, respectively. The results showed high reproducibility and stability. The standard deviation and the absolute error were considered as very low, considering the complexity involved in pilot plants of this size and the associated experimental error, related to solid residues handling.

Char was collected in a vessel for solids recovery, during pilot-scale pyrolysis. Char composition depends on both pyrolysis conditions and ELTs composition. ELTs pyrolysis char, known also as pyrochar or recovered carbon black, consisted of the initial carbon black (used during tyre manufacturing), ashes and tarry compounds produced during pyrolysis.

Table 3. 1. Physicochemical properties of CIP, PRO and CLO.

Parameter	Ciprofloxacin	Propranolol	Clomipramine
Molecular formulae	$C_{17}H_{18}FN_3O_3$	$C_{16}H_{21}NO_2$	$C_{19}H_{23}ClN_2$
CAS number	85721-33-1	525-66-6	303-49-1
Molecular weight	331.35 g/mol	259.34 g/mol	314.85 g/mol
Log K_{ow}	0.28	2.90	5.19
pK_a	6.18, 8.76	9.42	9.20

Water solubility (25℃)	30,000 mg/L	62 mg/L	0.294 mg/L
Chemical Structure			

3.2.2. Synthesis of magnetic tyre pyrochar (MTC) at TRL 3

MTC in this study was prepared using a modified method developed earlier by Wang et al. (2014). Briefly, sieved pyrochar (10 g) was added into a solution containing 1.5 g of $FeCl_3 \cdot 6H_2O$, 3.5 g of $FeSO_4 \cdot 7H_2O$ and 200 mL of deionized (DI) water with continuous stirring (900 rpm) for 1 h at 60 °C. The pH of the mixture was increased to 9–11 with dropwise addition of KOH solution (3.0 M) and the reaction was undertaken for another hour. After being stirred for 60 min, the magnetic pyrochar was separated from the solution via centrifugation at 4000 rpm. Finally, the obtained pyrochar was rinsed with deionized water for five times, dried in a vacuum oven at 50 °C for 48 h and sieved to a uniform size (75–300 μm) before performing adsorption experiments. Figure 3.2 shows the schematic representation of the sample pyrolysis and magnetisation at TRL 7 and TRL 3, respectively. Table 3.1 presents the physicochemical properties of CIP, PRO and CLO.
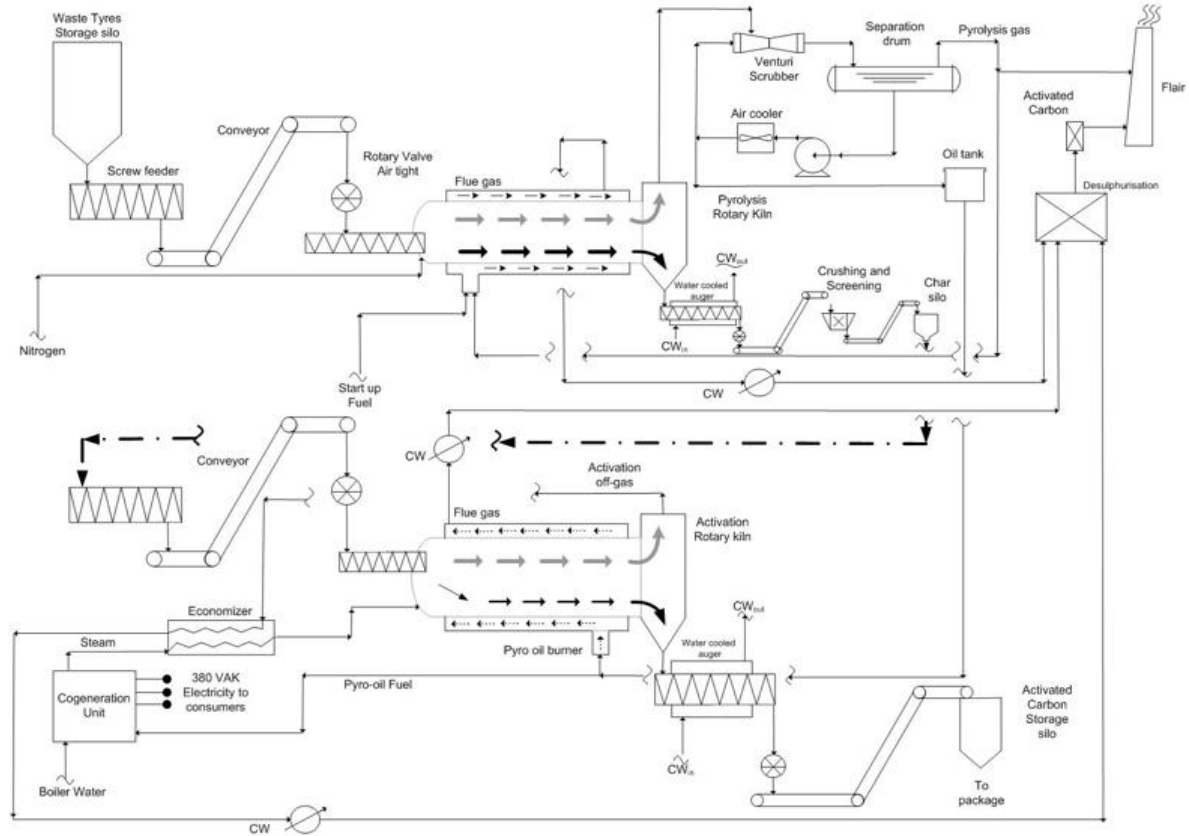
Figure 3. 1. Flow sheet and photos of the pyrolysis prototype (Source: Antoniou & Zabaniotou, 2018)

3.2.3. Characterisation of adsorbents

Brunauer–Emmett–Teller (BET) specific surface areas and Barrett– Joyner–Halenda (BJH) cumulative pore volumes of pyrochars were obtained from the N_2 adsorption isotherm data under liquid nitrogen at −196 °C by Micromeritics Tristar 3000 instrument. Samples were first

degassed for 12 hours at 60 ± 1 °C under N_2 gas. The elemental composition (C, H and N) of the pyrochar was determined using an elemental analyser at Mass Spectrometry Centre, The University of Auckland, New Zealand. The magnetic strength was assessed at external magnetic fields by Physical Property Measurement System (PPMS) under Vibrating Sample Magnetometer (VSM) option at room temperature. Fourier transform infrared (FTIR) spectroscopy (Varian 7000) analyses of pyrochar samples were carried out to detect the functional groups. Surface morphologies of the adsorbents and distribution of iron on the surface were observed by using Hitachi SU-70 FE-SEM equipped with Energy Dispersive X-ray (EDX) facility at 1 kV and 5 kV acceleration voltages. MTC zeta potential was tested by a Zetasizer analyser (Nano ZS90, Malvern, UK).
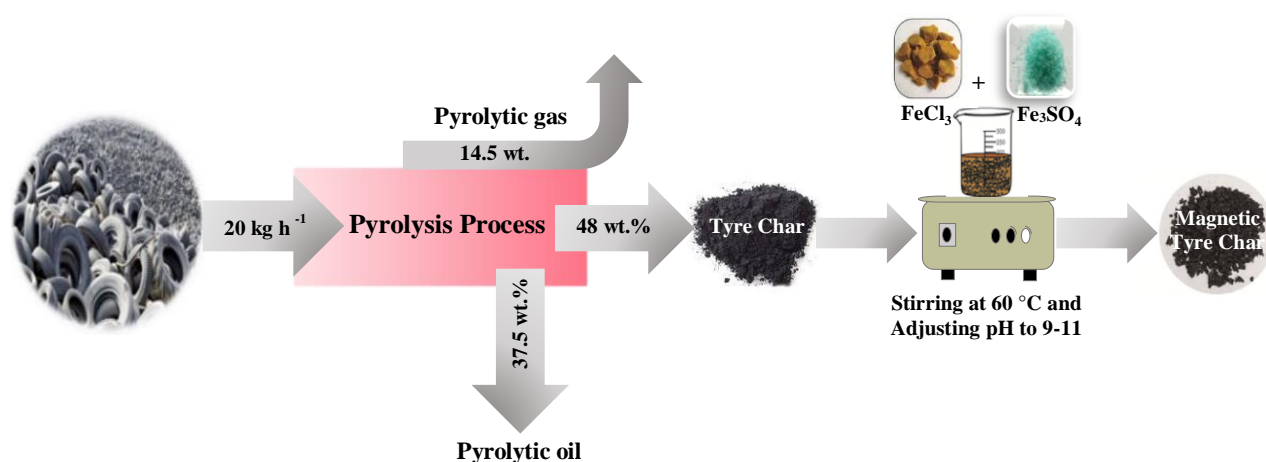
Figure 3. 2. Schematic representation of sample pyrolysis and magnetisation.

3.2.4. Batch adsorption studies

Batch adsorption studies were conducted in a 50 mL glass Kimax centrifuge tube with Teflon-lined screw caps. A volume of 25 mL of pharmaceuticals solution (CIP, PRO, CLO) and 50

mg MTC was used. The centrifuge tubes were then shaken in an end-over-end shaker in the dark at 50 rpm at room temperature (22 °C ± 2) for 24 hours. The effect of different parameters including contact time, pyrochar dosage, solution pH, ionic strength, sorption kinetics and sorption isotherm were examined. Based on preliminary studies, equilibrium time for all three compounds were obtained in <15 h. The influence of adsorbent dosage of 25, 50 and 100 mg in 25 mL (which corresponded to 0.8–4 g/L) of solution was studied at two concentrations: of 0.2 and 1 μg/mL. In order to identify optimum initial pH, the pH of solution at concentration 0.2 and 1 μg/mL was adjusted between 3 and 10 using dropwise solution of 0.1 mol/L of HCl or NaOH. The concentration of NaCl (0–1 mol/L) was varied to investigate the effect of ionic strength on the sorption of selected pharmaceuticals onto magnetic pyrochar.

In addition, kinetic studies were performed at two concentrations of 0.5 and 5 μg/mL with different contact times ranging from 30 s to 15 hours, at pH ~ 6 for CIP and 9 for PRO and CLO, and ionic strength of 0.01M NaCl for CLO. For the isotherm studies, initial equilibrium concentrations were used in the range of 0.2 to 10 μg/mL for both TC and MTC. All the experiments were performed in duplicates.

The amounts of CIP, PRO and CLO adsorbed, q_e, were determined as follows:

$$q_e = (C_i - C_e) \times \frac{V}{m} \tag{3.1}$$

where, C_i and C_e are the initial and equilibrium concentrations of CIP, PRO and CLO (μg/mL), m is the mass of the pyrochar (g), V is the volume of solution (mL) and q_e is the amount of compound sorbed (μg/g).

3.2.5. Analytical quantification of pharmaceuticals

Following centrifugation, all samples were filtered through 0.20 μm cellulose acetate membrane filters. The concentrations of CIP, PRO and CLO were measured directly with a liquid chromatography tandem mass spectrometer (LC-MS/MS) using an Eclipse plus C18 column (100 × 2.1 mm, particle size 3.5 μm). The mobile phase consisted 0.1% formic acid in water (A) and 100% methanol (B) and were used at a flow rate of 0.2 mL/min and a column temperature of 40 °C. All three compounds were determined in the positive mode electrospray ionization (ESI). Sample injection volume was set at 1 μL and the run time was 14 min with retention times 6.12, 7.19 and 7.89 min for CIP, PRO and CLO, respectively. The detection limit for all three compounds is 2 ppb.

3.2.6. Data analysis and modelling

In order to investigate the mechanism of the adsorption onto pyrochars, measured kinetic datasets were fitted to two kinetic models: the pseudo-first order and pseudo-second order models as shown in Eqs. (3.2) and (3.3), respectively below.

$$q_t = q_e(1 - e^{-k_1 t}) \tag{3.2}$$

$$q_t = \frac{q_e^2 k_2 t}{1 + q_e k_2 t} \tag{3.3}$$

where t is the adsorption time, q_e and q_t (μg/g) are the amount of CIP, PRO and CLO adsorbed onto pyrochars at equilibrium and at time t, respectively. k_1 (1/min) and k_2 (g/μg min) are rate constants of pseudo-first and pseudo-second, respectively.

To have a better description and deepen the understanding of the adsorption process, experimental data of the pharmaceuticals sorption onto the adsorbents were fitted to four

typical isotherm models: Langmuir (Eq. (3.4)), Freundlich (Eq. (3.5)), Temkin (Eq. (3.6)) and

Dubinin- Radushkevich (Eq. (3.7)) models as below.

$$q_e = \frac{q_m k_L c_e}{1 + k_L c_e} \tag{3.4}$$

$$q_e = K_f C_e^n \tag{3.5}$$

$$q_e = B_1 \ln(AC_e) \tag{3.6}$$

$$q_e = q_t \exp(B\varepsilon^2) \quad where \quad \varepsilon = RT\ln\left(1 + \frac{1}{C_e}\right) \tag{3.7}$$

In the above equations, C_e is the equilibrium concentration (μg/mL), q_e is the amount of CIP

adsorbed per gram of pyrochar (μg/g), K_L is the Langmuir constant (mL/μg), q_m is the

maximum adsorption capacity (μg/g), K_f is the Freundlich isotherm coefficient (μg/g)(mL/μg)^n,

n is a measure of adsorption linearity. A (mL/μg), R (8.314 J/mol K), and T (K) are Temkin

isotherm equilibrium binding constant, gas constant and absolute temperature, respectively.

The parameter b is Temkin isotherm constant, $B_1 = RT/b$, B is a constant related to the mean

free energy of adsorption (mol^2/KJ^2), q_t is the theoretical isotherm saturation capacity (μg/g),

and ε is Dubinin-Radushkevich isotherm constant.

3.3. Results and discussion

3.3.1. Pyrochar characteristics

Selected physical and chemical properties of non-magnetic tyre pyrochar (TC) and magnetic

tyre pyrochar (MTC) are summarised in Table 3.2.

Surface characteristics of TC and MTC are shown in SEM images (Figure 3.3a and b). The

surface morphologies of pyrochars indicate a porous texture of the material that can provide

active sites for the sorption. It can be observed from SEM images that the surface of the MTC

was covered with iron nanoparticles after magnetic activation. Based on the elemental composition of pyrochars, the lower C content for magnetic pyrochar versus non-magnetic pyrochar could be attributed to the introduction of iron particle onto the magnetic pyrochar. Also, O and H content decreased after magnetisation. Elemental molar ratios for the sorbents were calculated to estimate their aromaticity (H/C) and polarity (O/C), which were 0.252 and 0.127, respectively for MTC, suggesting its lower aromaticity and polarity as compared to the raw pyrochar. The EDS spectra of MTC showed the presence of iron in particles on the surface of the adsorbent which is 27.45% Fe (Figure 3.3c).

Table 3. 2. Chemical and physical properties for pyrochars.

Properties	TC	MTC
C (%)	79.93	59.45
H (%)	1.39	1.25
N (%)	<0.3	<0.3
S (%)	1.74	1.42
O^* (%)	16.64	10.13
H/C	0.208	0.252
O/C	0.156	0.127
Fe (%)	n.d.	27.45
BET surface area (m^2/g)	38.17	49.23
BJH cumulative pore volume (cm^3/g)	0.37	2.66
BJH average pore diameter (nm)	35.38	19.65

*Oxygen content was determined by difference.

The BET surface area of TC and MTC are 38.17 m^2/g to 49.23 m^2/g, respectively. This increase in S_{BET} could be attributed to the activation processes resulting in more porous MTC compared to TC. Magnetic composites with larger surface area compared to raw material have been reported in several of the past studies (Devi & Saroha, 2014; Kong et al., 2017; Shan et al., 2016; Zhu et al., 2014). Also, it is noteworthy that the cumulative pore volume of magnetic pyrochar was higher than the pristine pyrochar which could be due to the result of crushing of iron particles into the pyrochar and creating more pores. However, the average pore size of pyrochar decreased from 35.38 nm to 19.65 nm after magnetisation. The low BET surface area of TC is consistent with previous studies (61 m^2/g (Acosta et al., 2016), 22 m^2/g (Gupta et al., 2011b), 32 m^2/g (Hadi et al., 2016) and 61.09 m^2/g (Kim et al., 2018)). The differences in surface areas might be due to different brands and rubber components in tyres as feedstock that can lead to the different properties of pyrochar (Lah et al., 2013). Also, original carbon black compounds and more abundant elements and additives which are presented in raw tyre tread from waste tyre might be ascribed to higher surface area of char products (Wang et al., 2019).

Magnetic hysteresis curves of MTC represent the saturation magnetisation of 10.8 emu/g which is magnetic strength of the pyrochar (Figure 3.4a). In addition, the magnetic separation power of MTC was tested by application of an external magnet as shown in Figure 3.4b.

The FTIR spectra of pyrochars, magnetic and non-magnetic, measured in the 4000–500 1/cm region and are shown in Figure 3.5. The broad band observed at approximately 3550 1/cm can be assigned to the hydroxyl groups (–OH) and the peak at around 2700 1/cm can be ascribed to aromatic C–H. The bands at about 2150 and 2200 1/cm correspond to C≡C and C≡N, respectively. The band at 1194 and 1650 1/cm can be assigned to C–O and C=C. These relative peaks show that original organic residues are present on the surface of pyrochars and may contribute to adsorption process as discussed later. Based on the FTIR spectra results,

magnetisation did not change surface functional groups of pyrochars, but decreased the intensity of peaks.
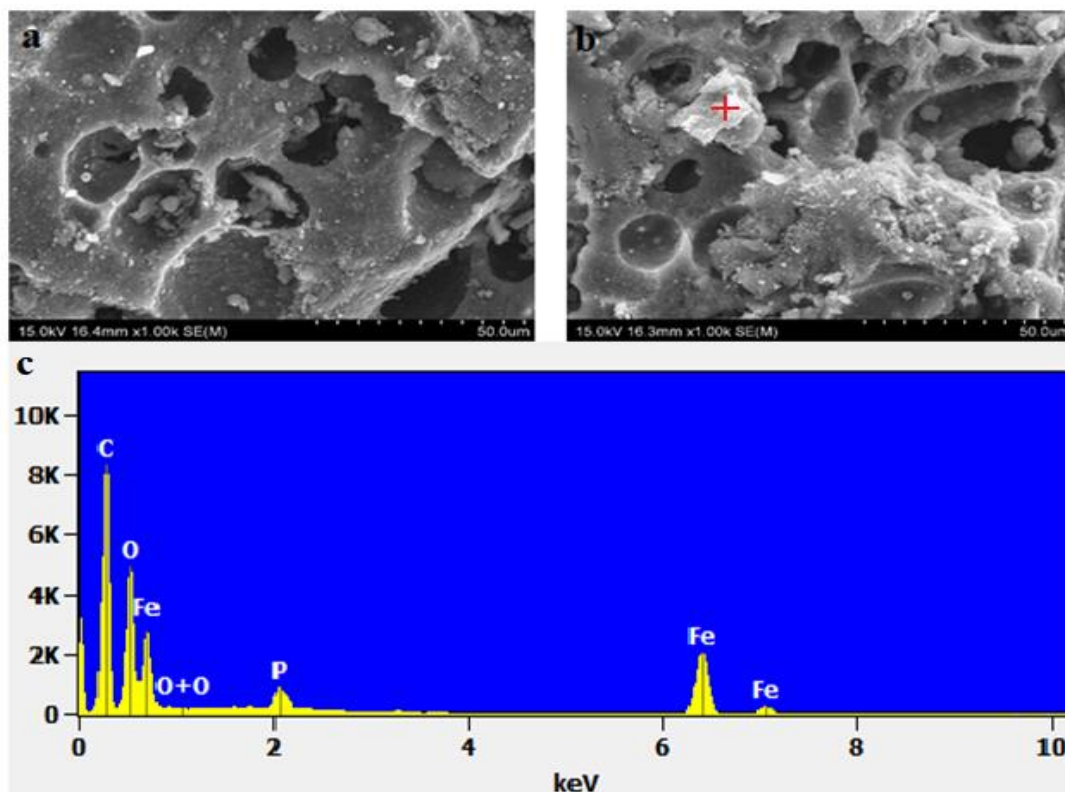
Figure 3. 3. SEM/EDS elemental mapping analysis for TC and MTC (SEM images of TC (a) SEM images of MTC (b) and EDX result of selected area of MTC (c)).
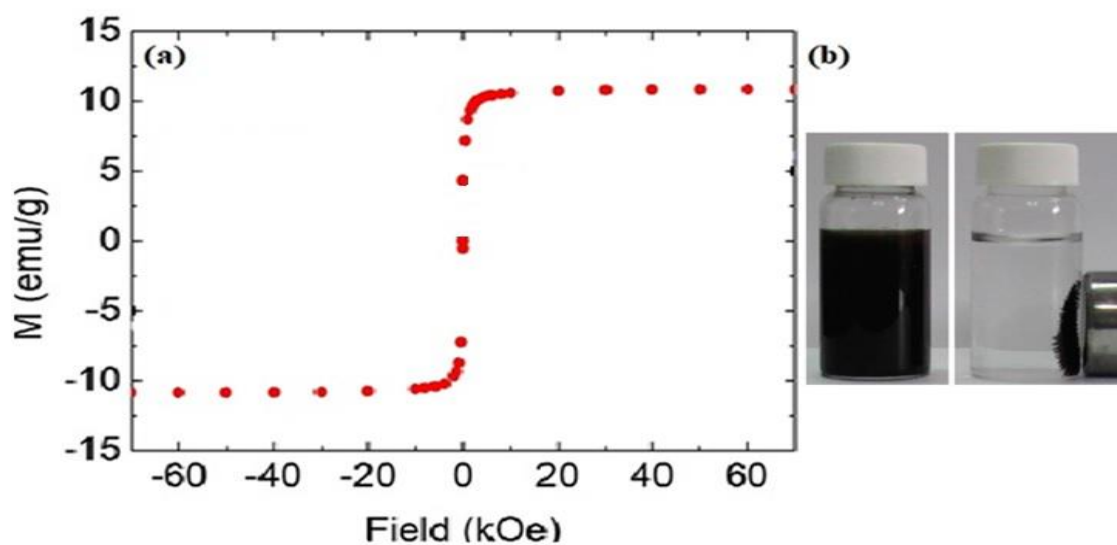
Figure 3. 4. Magnetic hysteresis cycles of MTC (a) and Magnetic separation of MTC after adsorption (b).
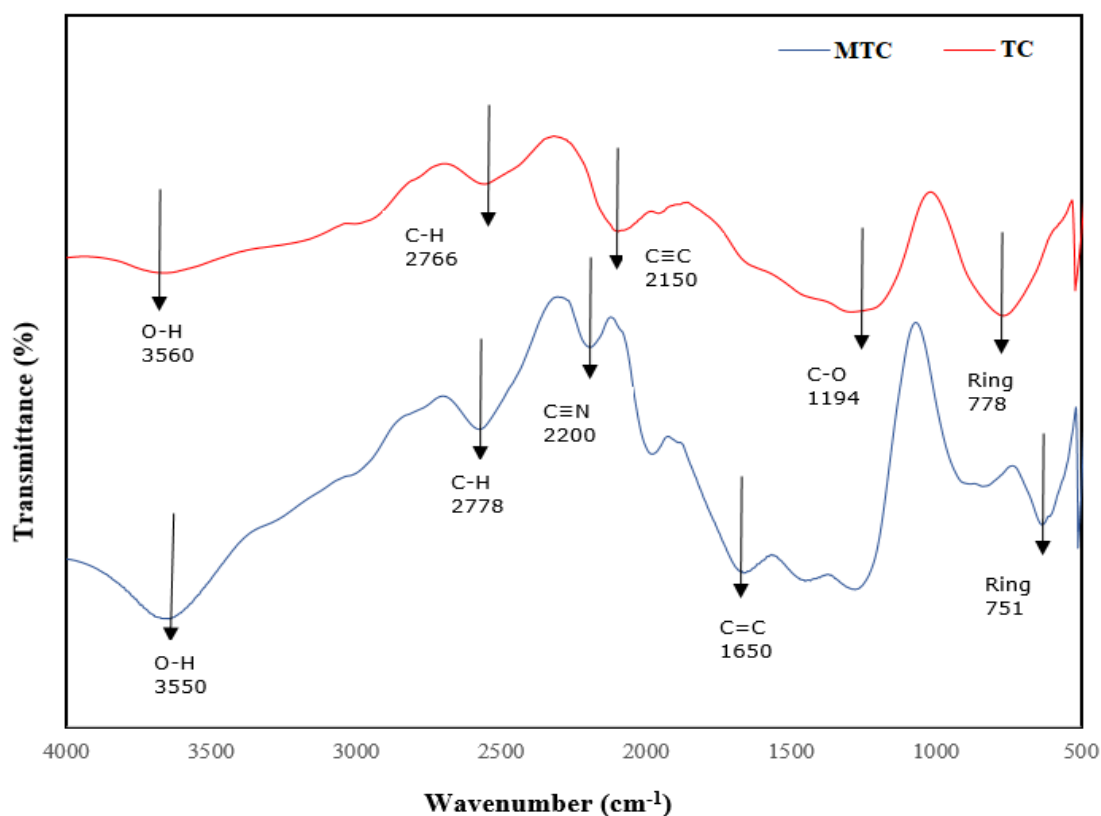
Figure 3. 5. FTIR spectra of TC and MTC.

3.3.2. Effect of pH on the adsorption of CIP, PRO and CLO onto MTC

One of the most important parameters in adsorption process is the pH of the solution as it affects the surface charge of the adsorbent and the degree of ionization and the speciation of the adsorbates (Kołodyńska et al., 2012). To identify the optimum pH for the adsorption of the pharmaceuticals onto MTC, the impact of solution pH on the adsorption of CIP, PRO and CLO was investigated at different initial pH values (3–10) at two initial concentrations of 0.2 and 1 µg/mL (Figure 3.6). Given these pharmaceuticals have different physiochemical properties and all being ionisable compounds, the trend in their adsorption capacity is dependent on the pH which varied from 3 to 10. As CIP molecules contain amine and carboxylic acid groups, it can behave as cation (CIP^+), anion (CIP^-), uncharged molecule (CIP^0) and zwitterion ($CIP^\pm$) in

solution at different pH levels (CIP: $pK_{a1} = 6.18$ and $pK_{a2} = 8.76$). In the present study, an increase in the solution pH resulted in higher removal rate of CIP using MTC. The trend can only be observed from pH 3 to 6, however, at pH > 6, the CIP removal rate decreased. Similar findings were also observed in earlier published studies (Kong et al., 2017; Rakshit et al., 2013). The effect of solution pH on the removal behaviour of CIP can be ascribed to a combination of pH-dependent speciation of CIP and surface charge characteristics of the adsorbent.
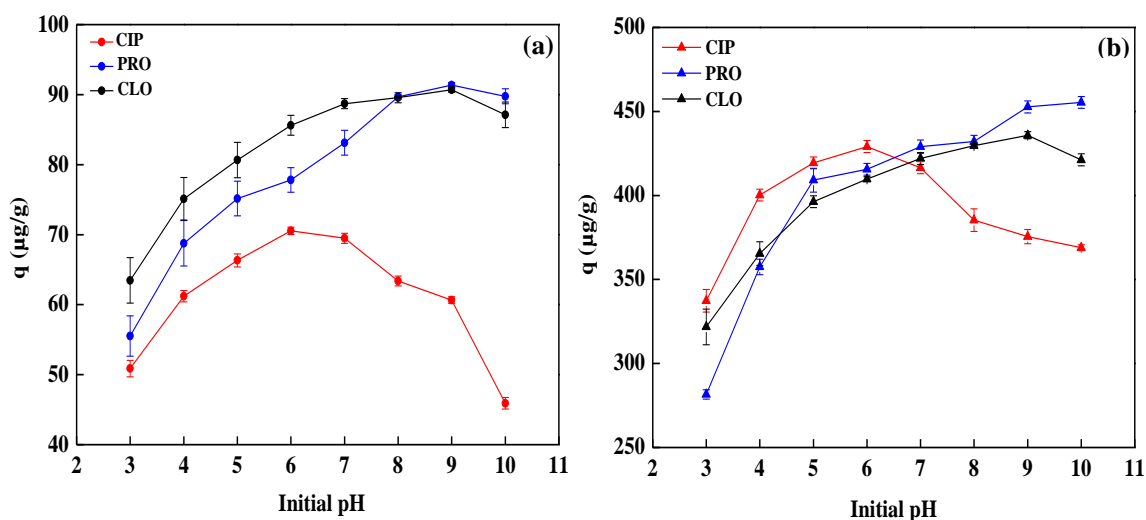
Figure 3. 6. Effect of solution pH on magnetic pyrochar adsorption capacity of MTC at initial concentrations of 0.2 μg/mL (a) and 1 μg/mL (b).

PRO has pKa > 9 and exists in the cationic form at pH < 9. The adsorption capacity of MTC increased between pH 3 and 9 and reached the highest value at pH 9, which is close to the pKa of PRO. At pH > 9, the adsorption capacity of MTC pyrochar slightly decreased which was also observed in a recent study (Wang et al., 2016). Similar results were obtained for the removal of CLO, with adsorption increased at pH range from 3 to around 9 (CLO: pKa = 9.2), and then decreased with the change in pH from pH 9 to 10.

Raw wastewater generally has a pH near neutral, and it may, however range between 6 and 8. The average pH of raw wastewater in NewZealand is 7.5 (Ray, 2002). In general, MTC can maintain a high adsorption rate in a large pH range (4–9), indicating that the material can be applied for the removal of the pharmaceuticals in different pH water bodies.

3.3.3. Effect of ionic strength on the adsorption of CIP, PRO and CLO onto MTC

Most wastewater contains a certain amount of salt, which may affect the removal of pharmaceuticals. Thus, the effect of ionic strength on the adsorption of selected pharmaceuticals onto MTC was carried out via a series of experimental studies by adjusting the additive amount of NaCl in the range of 0.001, 0.01, 0.1, 0.5 and 1M and the results are presented in Figure 3.7. Theoretically, when the adsorbate ions have attractive electrostatic forces on the adsorbent surface, increasing ionic strength leads to a decreasing removal rate (Al-Degs et al., 2008). For example, CIP removal capacity decreased with increasing NaCl concentration, which could be ascribed to electrostatic attraction. Explanations for this observation could be also attributed to the fact that high salt concentration fills the pores of adsorbent resulting in a decline in adsorption capacity (Afzal et al., 2018). For PRO, there was a decrease in the rate of adsorption when the NaCl concentration was < 0.5 M. A plausible explanation for this could be the competition between Na^+ cations and PRO molecules for occupying the adsorption sites of the adsorbent (Deng et al., 2019). The adsorption capacity of PRO increased when the NaCl concentration was > 0.5 M. This increase in PRO uptake can be due to the 'salting-out' effect which improves the activity coefficient of hydrophobic organic compounds and decreases their solubility in salt solution and has been observed in several studies (Li et al., 2018a; Reguyal & Sarmah, 2018). Furthermore, it can be observed that CLO

is insensitive toward ionic strength and its adsorption capacity remained almost constant indicating the high stability of interaction between CLO and MTC in a certain range of salt concentration. At very low concentrations of NaCl i.e., 0.001 M, the removal rate of CLO was found to be the highest (Figure 3.7).
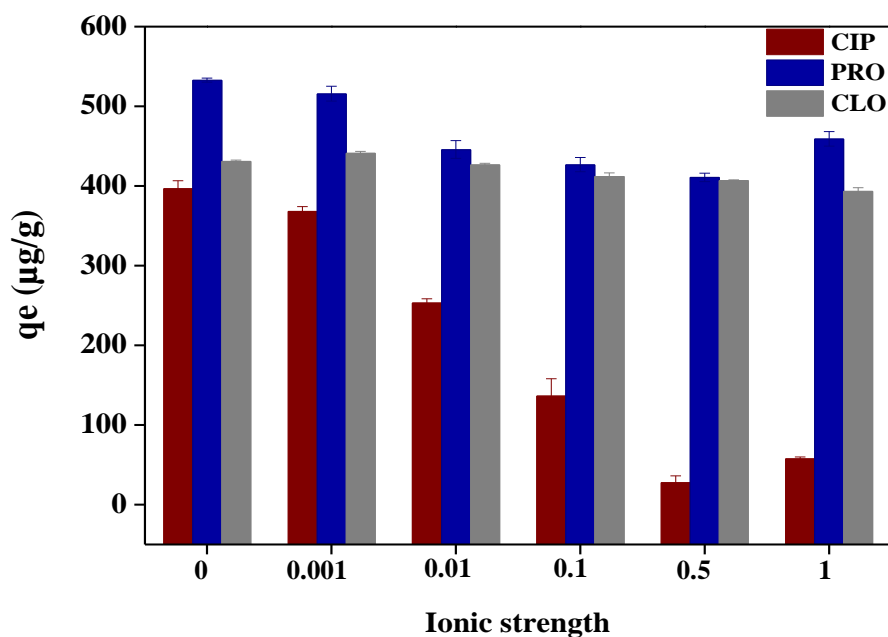
Figure 3. 7. Effect of ionic strength on CIP, PRO and CLO (~1 μg/mL) sorption onto MTC.

3.3.4. Adsorption kinetics

To better understand the adsorption process and mechanisms associated with their kinetics onto MTC, kinetic studies were carried out using two different initial concentrations. The adsorption kinetics of CIP, PRO and CLO onto the MTC are shown in Figure 3.8a to c. For all three compounds, the adsorption capacity increased rapidly during the first 2 hours, followed by a gradual rise, and then the adsorption equilibrium was achieved within 15 hours. The initial fast adsorption could be attributed to the high number of available adsorption sites.

The pseudo-first order and pseudo-second order models were utilized to evaluate the adsorption kinetics parameters. The kinetic parameters for the adsorption of CIP, CLO and PRO onto MTC are summarised in Table 3.3. For all the compounds, pseudo-second order model best described the experimental data (R^2=0.95–0.99) at both concentrations, 0.5 and 5 μg/mL. The pseudo-second order model was based on the assumption that the rate-determining step may be controlled by chemisorption and chemical bonding between adsorbate molecules and functional groups on the surface of adsorbent might be involved (Tan et al., 2015). A similar behaviour of adsorption kinetics was also observed during the CIP and PRO adsorption by other carbon-based adsorbent (Afzal et al., 2018; Avcı et al., 2019; Deng et al., 2011; Kong et al., 2017; Li et al., 2018b; Zhou et al., 2019). However, in the absence of data specific to CLO adsorption by char-like materials; a direct comparison of the past studies with the obtained results in this research is not possible. The plots for pseudo-first order kinetics were less comprehensive with poorer R^2 values (0.79–0.95) and plots were provided in Appendix A (Figure A.1). Meanwhile, as can be observed in Table 3.3, there was a good agreement between experimental q_e values and the adsorbed amount calculated by the best fit equation.
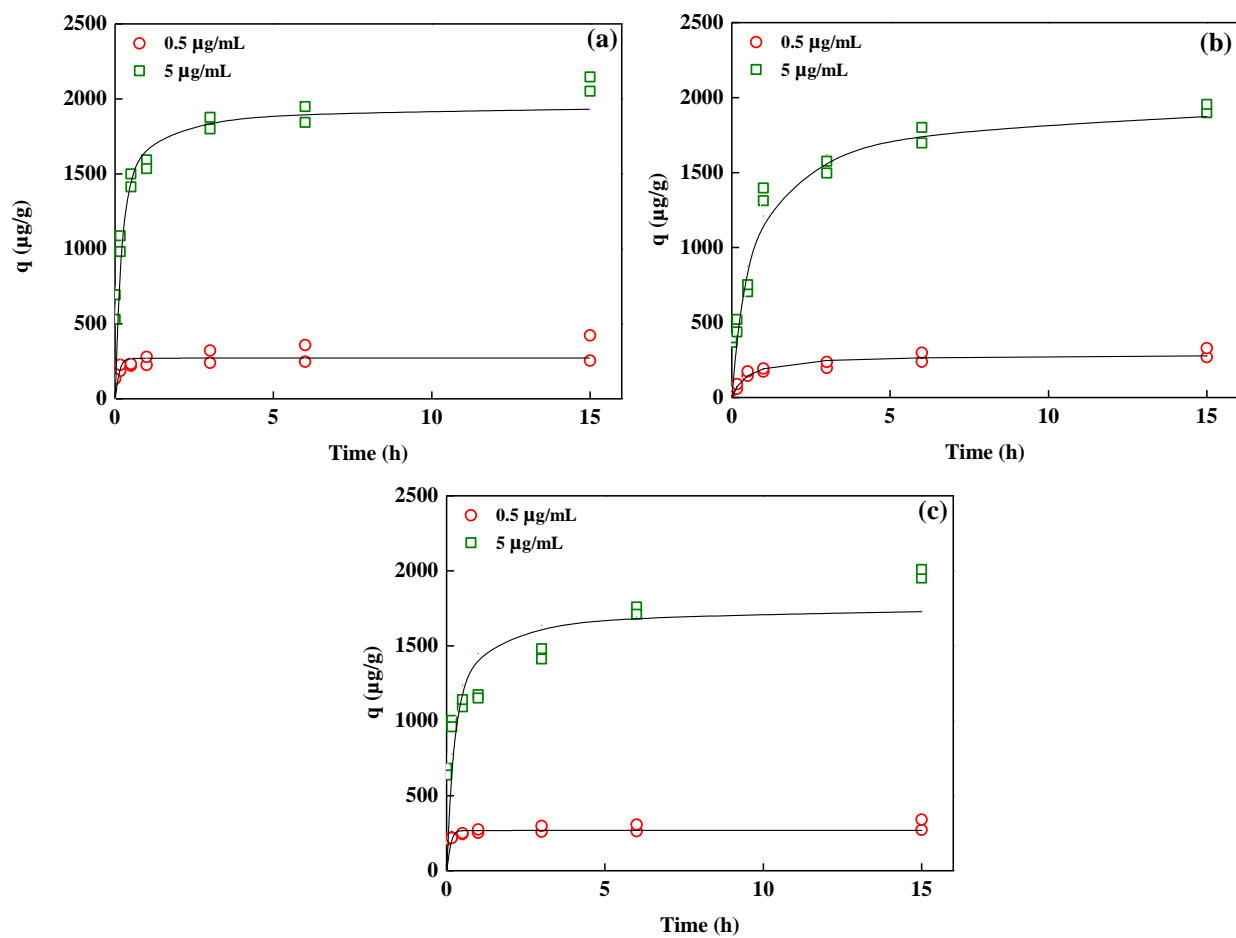
Figure 3. 8. Adsorption kinetics of CIP (a), PRO (b) and CLO (c) onto MTC. Symbols represent measured data and solid lines are Pseudo-second order kinetic model fit.

Table 3. 3. Kinetic parameters for pseudo-first order and pseudo-second order of CIP, PRO and CLO onto MTC.

Compound	C_0 ($\mu g/mL$)	$q_{e,exp}$ ($\mu g/g$)	Pseudo-first-order kinetics			Pseudo-second-order kinetics		
			$q_{e,cal}$ ($\mu g/g$)	k_1 (1/min)	R^2	$q_{e,cal}$ ($\mu g/g$)	k_2 ($g/\mu g$ min)	R^2
CIP	0.5	253.89	55.34	0.0028	0.88	248.65	1.1671	0.99
	5	2048.74	926.40	0.0029	0.89	1978.23	0.0553	0.99
PRO	0.5	270.16	167.03	0.002	0.87	239.77	0.2300	0.99
	5	1896.83	1307.37	0.0032	0.95	1903.31	0.0195	0.98
CLO	0.5	271.28	39.11	0.0024	0.80	265.36	1.8980	0.99
	5	1974.99	1248.53	0.0029	0.91	1865.67	0.0238	0.96

3.3.5. Adsorption isotherm

Important information on the adsorption behaviour of adsorbent and adsorbate can be derived from the adsorption isotherm data. In this study, four well-known isotherm models, Langmuir, Freundlich, Dubinin-Radushkevich and Temkin were utilized to derive the isotherm parameters for CIP, PRO and CLO onto MTC at initial concentrations ranging from 0.2 to 10 µg/mL (Figures 3.9 and A2), with parameters being summarised in Table 3.4. Among the isotherm models, sorption of the pharmaceuticals onto synthesized pyrochars was best described by Freundlich model having the highest correlation coefficients (R^2), which is based on the assumption that the adsorption occurs at a heterogeneous surface without formation of a monolayer (Jiang et al., 2017). Isotherms as described by other three models (Langmuir, Temkin, Dubinin-Radushkevich) considerably resulted in poor fits as shown in Appendix A (Figure A.2). An examination of the data presented in Figure 3.9a to c and Table 3.4 revealed that MTC exhibited high adsorption capacity for all three pharmaceuticals than TC, which

might be ascribed to the lower polarity and larger surface area of MTC. Elimination of organic contaminants might have been inhibited by polar sites via formation of larger and denser water clusters (Ahmad et al., 2012).

As defined by McKay (1982), the essential features of the Langmuir equation can be described according to the constant separation factor (R_L):

$$R_L = \frac{1}{1 + K_L C_0} \tag{3.8}$$

Langmuir constant. The value of R_L indicates whether the type of the isotherm is irreversible ($R_L = 0$), favourable ($0 < R_L < 1$), linear ($R_L = 1$) or unfavourable ($R_L > 1$). The calculated values of R_L, which range between 0.13 and 0.21, indicate that the adsorption behaviour of the pharmaceuticals onto pyrochars are favourable. Moreover, this consequence could be confirmed by the n values in the Freundlich model, which are < 1 and represent a beneficial adsorption condition. Also, E_a, the average free energy of adsorption from Dubinin-Radushkevich model has been found to be useful in determining the adsorption mechanism. For $E_a < 8$ kJ/mol, physical adsorption is dominant in the adsorption process and chemical adsorption such as ion exchange exists at $8 < E_a < 16$ kJ/ mol, while value of E_a 20–40 kJ/mol shows chemisorption (Tahir & Rauf, 2006). In the present study, as the values of E_a are over 17 kJ/ mol, it is conceivable that the CIP, PRO and CLO adsorption process on both adsorbents is likely to be mainly chemisorption.

For CIP, PRO and CLO, the maximum adsorption capacities were 6.94, 6.6 and 10.55 mg/g, respectively. Recently, Avcı et al. (2019) used commercial activated carbon and reported 1.86 mg/g sorption capacity for CIP. A magnetic biochar-based manganese oxide composite was reported that having 8.37 mg/g sorption capacity for CIP (Li et al., 2018b). Elsewhere, Zhao et al. (2019) synthesized magnetic biochar from potato leaves and CIP adsorption capacity was found 11.46 mg/g. Also, the adsorption capacities of MTC obtained for CIP in this study can

be compared with the removal capacity of magnetic herbal biochar, rice husk biochar, and magnetic commercial activated carbon/chitosan which have shown higher adsorption capacities compared with MTC (Danalıoğlu et al., 2017; Kong et al., 2017; Zeng et al., 2018). For example, maximum adsorption capacities of PRO were estimated to be 13 and 146.6 mg/g for corn straw biochar and activated charcoal, respectively (Wang et al., 2017b; Zhao et al., 2019). The higher saturated adsorption capacities are likely due to the result of more specific surface area and pore volume that provided more active adsorption sites. Also, the differences could be attributed to the employment of a lower initial concentrations for the selected pharmaceuticals in comparison to other studies.
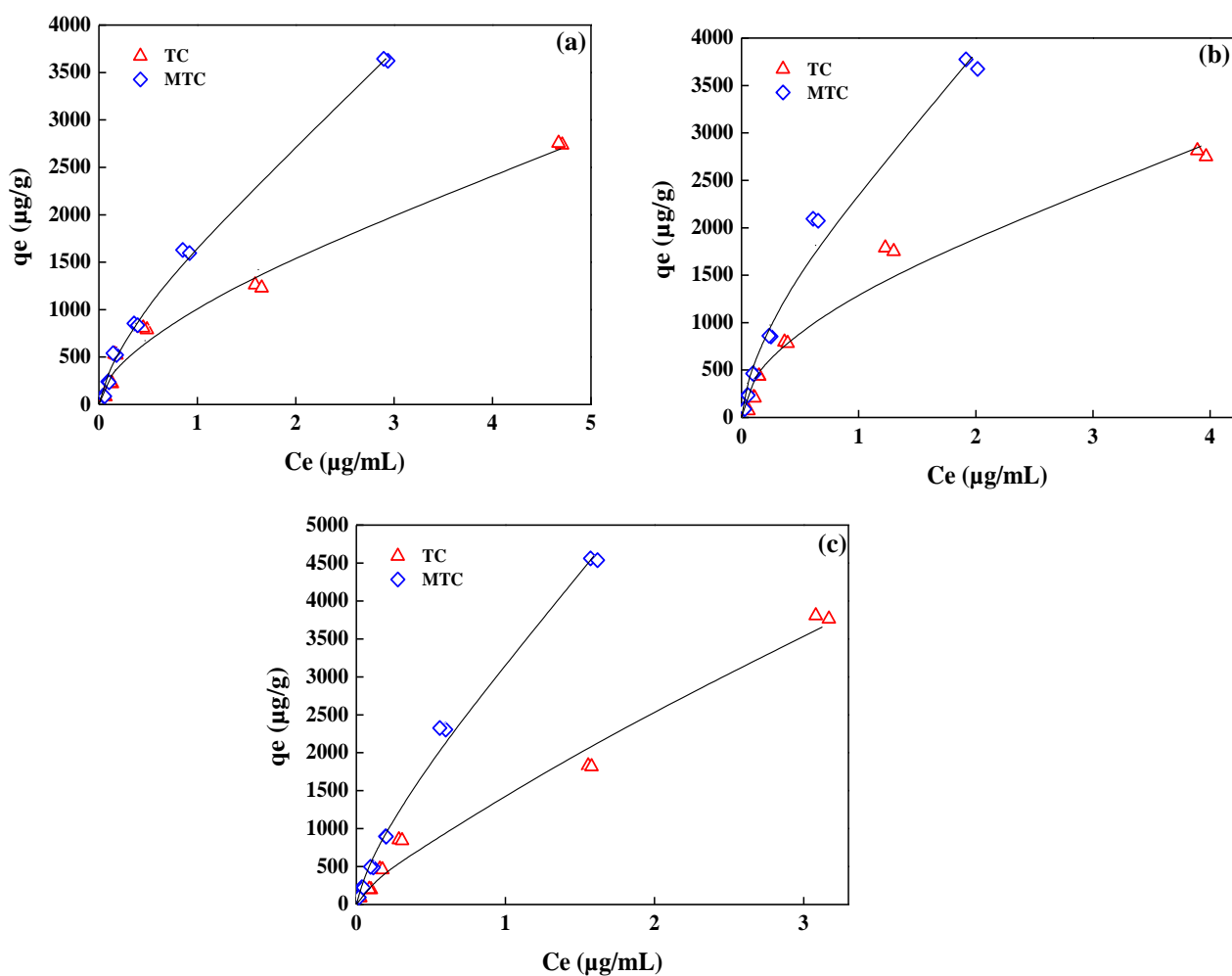
Figure 3. 9. Multi-concentration adsorption isotherms of CIP (a), PRO (b) and CLO (c) onto synthesized adsorbents. Symbols represent measured data, while solid lines are Freundlich isotherm model fits.

Table 3. 4. Sorption isotherm parameters of CIP, PRO and CLO onto different adsorbents.

Adsorbent	Adsorbate	Langmuir			Freundlich			Temkin			Dubinin-Raduskevich			
		K_L	q_m	R^2	K_f	n	R^2	A	B	R^2	q_t	B	E_a	R^2
		$L/\mu g$	g/g		$(\mu g/g)(mL/\mu g)^{1/n}$			$(mL/\mu g)$			$(\mu g/g)$	(mol^2/kJ^2)	(kJ/mol)	
	CIP	0.40	4000	0.82	13.04	0.63	0.96	0.013	557.57	0.87	1020	0.0016	17.67	0.73
TC	PRO	0.48	4360	0.82	27.11	0.56	0.95	0.024	654.52	0.97	1140	0.0016	17.67	0.76
	CLO	0.50	5540	0.75	5.60	0.80	0.97	0.034	717.13	0.82	900	0.0003	40.82	0.51
	CIP	0.39	6940	0.84	8.12	0.77	0.99	0.053	823.4	0.88	1160	0.0009	23.57	0.67
MTC	PRO	0.65	6600	0.96	24.20	0.66	0.98	0.051	813.9	0.89	1160	0.0003	40.82	0.64
	CLO	0.50	10550	0.92	19.84	0.74	0.98	0.084	975.91	0.84	1180	0.0001	70.71	0.57

3.3.6. Plausible adsorption mechanisms

Adsorption mechanisms of pyrochars depend on both the nature and type of adsorbent and sorbate physiochemical properties (Wang et al., 2016). The compounds under investigation; CIP, PRO and CLO, are all ionisable compounds, with different physical and chemical properties. Multiple methods and characterisations were used to obtain quantitative information in an attempt to identify and elucidate the different sorption mechanisms of the three compounds onto MTC. Of these, zeta potential, point of zero charge pH (pH_{pzc}) as shown in Figure 3.10, and FTIR data were useful in explaining the underlying sorption mechanisms which may have been responsible for the observed trend in the data obtained. A pictorial diagram in Figure 3.11 is proposed to elucidate the sorption mechanisms involved with detailed discussion below.
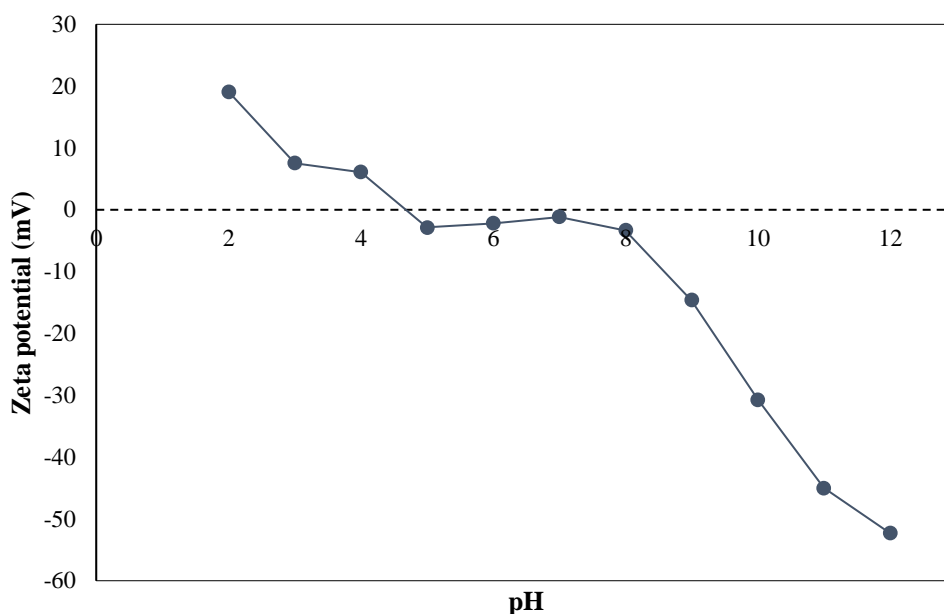
Figure 3. 10. Zeta potential of MTC under varying pH.

3.3.6.1. π-π Electron Donor Acceptor (EDA) interaction

One of the major adsorption mechanisms for organic chemicals interaction with benzene rings on carbonaceous surface in some studies has been described by π-π Electron Donor Acceptor (EDA) interaction (Ma et al., 2015; Moreno-Castilla, 2004; Wang et al., 2014; Zhu et al., 2004). All three compounds used in the present study possess benzene rings; however, the electronegativity of the molecular atom or atoms attached to the benzene ring may indicate the role of benzene ring during the adsorption mechanism. For example, CIP has fluorine group and N–heteroaromatic ring connected to benzene ring that may function as a π-electron-acceptor due to the strong electronegativity of F and N. Whereas, the presence of –OH group on the surface of MTC as determined through the FTIR analysis makes the benzene rings as π-electron donors, resulting in π-π electron EDA interaction between the adsorbent and adsorbate. Meanwhile, aromatic C=C bond on the MTC surface (1650 cm^{-1}) could be strong π-electron-donor which might be related with the π-π EDA interaction (Hu et al., 2019; Liu et al., 2019; Wang et al., 2017a). This type (π-π EDA) of interaction was found to be an important driving force for the sorption of CIP on carbon surface in a number of studies reported earlier (Afzal et al., 2018; Li et al., 2014a; Ma et al., 2015; Ramil et al., 2010; Wang et al., 2016; Yu et al., 2016).

Similarly, the benzene rings in CLO molecules may also act as π- acceptor due to the chlorine atoms substitution and this may interact with electron donor moieties of the biochar via π-π EDA interaction. Based on the PRO structure, π–π EDA interaction via the naphthalene rings of PRO could also contribute to the sorption promotion. Except for π-π EDA interaction as described above, cation–π should be another important mechanismresponsible for the adsorption of the pharmaceuticals by MTC. Under the low pH values (pH < pKa), the positively charged CIP, PRO and CLO may cause cation-π bonding with π electrons on the MTC, which

was demonstrated to be a specific adsorption mechanism in some studies (Li et al., 2016; Pei et al., 2012).

3.3.6.2. Cation exchange and electrostatic repulsion

In addition, CIP, PRO and CLO uptake could be explained by cation exchange and electrostatic repulsion driven mechanisms. For instance, at pH < 6.18, cationic species of CIP were dominant and as the surface of pyrochar (pH$_{pzc}$ = 4.65 < solution pH) was oppositely charged (Figure 3.10), cation exchange could be attributing to the sorptive behaviour of CIP. When pH of solution ranged between 6.18 and 8.76, zwitterionic form of CIP was dominant, however, contribution of this form CIP for sorption was found to be negligible. At pH > 8.76, CIP behaved as anion and due to electrostatic repulsion between ionic CIP molecules and pyrochar, adsorption capacity reduced. For PRO at the pH range from 4.65 to 9.42, positively charged PRO (pKa ~ 9.42) easily attracted the adsorbent carrying negative charges which could be attributed to cation exchange. By increasing pH to above 9, adsorption capacity of pyrochar decreased slightly probably due to the electrostatic repulsion. For CLO with pKa value 9.20, the electrostatic attraction between the protonated CLO and the oppositely charged pyrochar was one of the possible interactions at 4.65 < pH < 9.2. However, for pH > 9.2, repulsive interaction can take place between negatively charged CLO and the adsorbent. In all the pharmaceuticals studied, the cation exchange is possible when the compounds are positively charged based on the pH of the solution and the pH$_{pzc}$ of MTC (Figure 3.10). However, the reduction of the adsorption capacity of MTC at high pH or at pH where the pharmaceuticals are negatively charged may indicate electrostatic repulsion. In addition, it also implies that other sorption mechanism are involved at high pH since MTC can still absorb some of the adsorbates.

3.3.6.3. K_{ow} dependency

The octanol-water partition coefficient (K_{ow}) is often used as an index to show chemical hydrophilicity and hydrophobicity (Peng et al., 2012). As it can be observed from Table 3.1, the K_{ow} value of CLO is higher than that of CIP and PRO indicating CLO higher hydrophobicity. Also, the lower content of O/C of MTC (0.127) indicates its high hydrophobicity. Highly hydrophobic adsorbates in water solutions have a strong tendency to be adsorbed on carbon surface (Liu et al., 2010). As the highest hydrophobicity of CIP has been shown to be around pH 7 (Yu et al., 1994), hydrophobic surface interactions can also be considered as one of the plausible sorption mechanisms of CIP onto MTC at around pH 7 (Peng et al., 2016). PRO adsorption could be also affected by hydrophobic effect. At a typical neutral environmental pH, PRO exists as a cationic species, and it may behave like a cationic surfactant with the protonated amine and naphthalene ring as hydrophilic and hydrophobic moiety, respectively (Wang et al., 2016). Hence, hydrophobic tail of PRO (the naphthalene ring) could be sorbed via hydrophobic interactions in addition to the cationic exchange. Also, as CLO has high hydrophobicity ($3.5 < \log K_{ow}$) (Choi et al., 2018), its adsorption onto MTC may be dominated by hydrophobic partitioning.
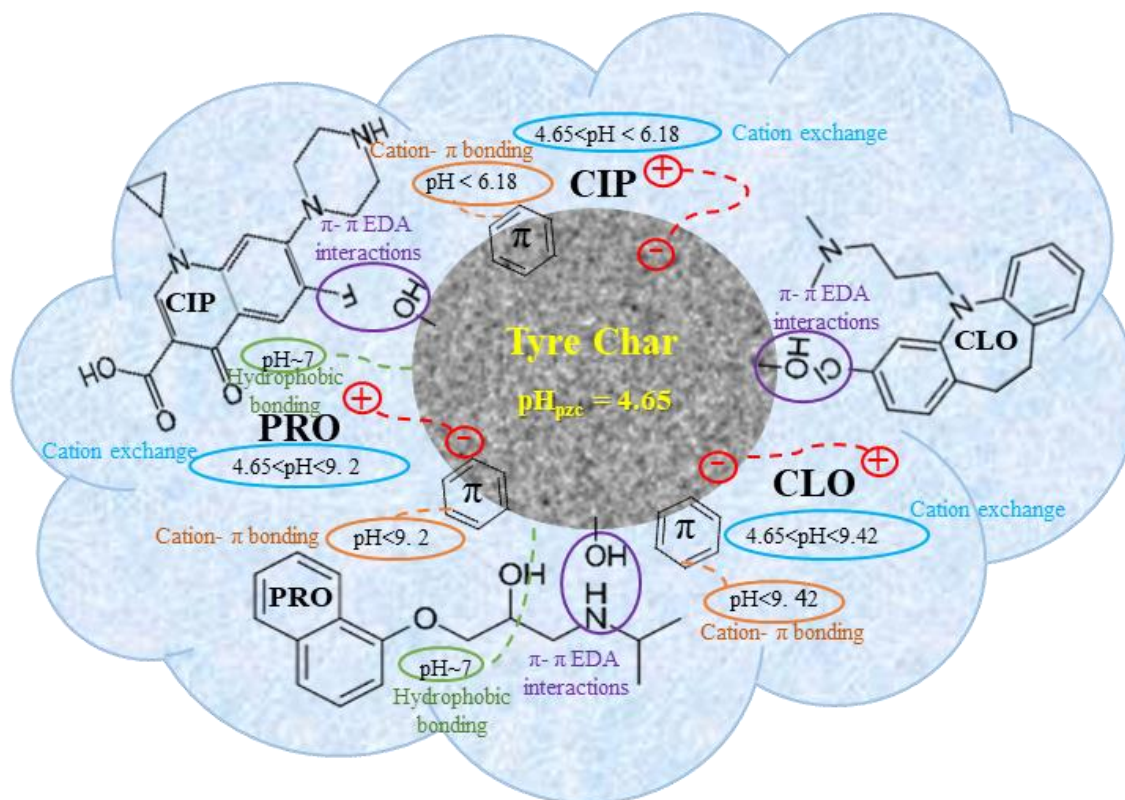
Figure 3. 11. Proposed plausible sorption mechanisms of CIP, PRO and CLO onto tyre pyrochar.

3.4. Preliminary techno-economic assessment

A preliminary feasibility study for the pyrochar production was conducted using data of the experimental study that was performed at TRL3-7. For the economic assessment, first, the pyrolysis products yields were considered which according to the pyrolysis pilot plant outputs, are: gas (14.5 ± 2 wt. %), liquid (37.5 ± 1 wt. %) and pyrochar (48.0 ± 2 wt. %). A full analysis of the economic assessment is provided in the Appendix B. Briefly, the production cost of tyre pyrochar for a plant capacity of 6 tonne/day was determined by summing capital charges in the form of ACC (Annualized capital cost/Capital charges) to the fixed and variable operating costs (Table 3.5). Estimation of capital and the operating costs for ELTs collection, steel separation, shredding and pyrolysis process in a pilot-scale Plant determined tyre pyrochar production cost (Islam et al., 2011).

Market cost of pyrochar ranges from 350–1200 US$/tonne which is a value lower than that of the powdered activated carbon (1100–1700 US$/tonne) (Thompson et al., 2016). Revenue income of selling oil by-product taken from the plant should be considered in total production cost. Pyrolysis oil can be sold at 400 US$/tonne (Fels and Pegg, 2008), and by deducting the revenue income from the total production cost, the pyrochar unit production cost can be decreased to 299 US$/tonne which is a much lower value that the market price 350–1200 US$/tonne (Figure 3.12).

Table 3. 5. Economic analysis of ELTs Pyrolysis in Pilot Scale Plant (6 tonne/day).

Parameters used in cost Bases		Production Cost	
Location, time, currency	New Zealand, 2020, USD	Base equipment cost	120,000
Annual operating time	7512 h	Fixed capital investment (FCI)	273,000
Maintenance	2.5% of FCI	Total capital required	313,950
Overheads	2% of FCI	Annualized capital cost/Capital charges	58,848
Taxes and insurance	1.5% of FCI	Annual fixed operating cost	
Other fixed operating costs	1% of FCI	Maintenance + overheads + taxes and insurance + other fixed operating costs	19,110
Labour rate [1]	11.74 USD/h (regular duty @ 8 h/day)	Salary for employee	176,382
Total labours (in equivalent of shift operators)	6	Annual variable operating cost	
Feedstock cost	20 US$/ton	Feedstock	37,560
Electricity price [2]	0.098 USD/ kWh	Electricity	22,085

	(30 kW for pilot plant)				
General overheads	60% of total salaries			General overheads	105,829
Interest rate	10%			Total annual operating cost	360,966
Plant life	8 years			Total annual production cost	419,814
Product yield (Pyrochar)	48%			Unit production cost (US$/tonne)	466
By-products	Oil	375 tonne/year	400 US$/tonne	Revenue income	150,000
				Unit production cost after considering revenue (US$/tonne)	299

[1] https://www.govt.nz/browse/work/workers-rights/minimum-wage/

[2] https://www.mbie.govt.nz/building-and-energy/energy-and-natural-resources/energy-statistics-and-modelling/energy-statistics/energy-prices/electricity-cost-and-price-monitoring/
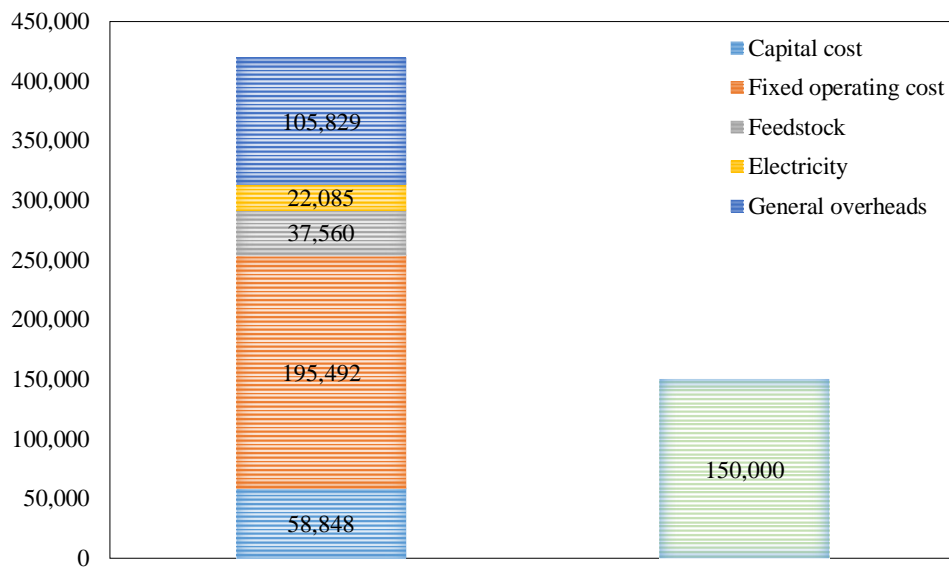
Figure 3. 12. Cost and revenue distribution of tyre char production in Pilot Scale Plant (6 tonne/day).

3.5. Conclusions

Through this study the production and synthesis of a novel magnetic adsorbent using pyrochar from ELTs at TRL7-3 plant was demonstrated. As compared to TC, MTC presented better performance in the removal of the three pharmaceuticals from water. The adsorption efficiency was greatly affected by the solution pH and the maximum adsorption was found to occur at pH 7 for CIP and pH 9 for PRO and CLO. The adsorption onto magnetic adsorbent was also dependent on ionic strength wherein the removal at lower concentrations of ionic strength was more favourable. The kinetics and isotherm data could be best described by pseudo-second order kinetic and Freundlich isotherm models. Maximum adsorption capacities were 6.94, 6.6 and 10.55 mg/g for CIP, PRO and CLO, respectively. It was postulated that π-π electron donor–acceptor interactions, electrostatic interactions and hydrophobic bonding are some of the key driving forces for sorption of CIP, PRO and CLO onto MTC. An economic assessment revealed that the pyrochar is economically viable as it is found to be low-cost with production cost was estimated to be 299 US$/tonne, much lower than existing biochar market price 350–1200 US$/tonne. The concept of circular economy fits well with the approach of ELTs pyrolysis in conjunction with environmental remediation benefits such as the utilisation of the pyrochar for magnetisation as a low-cost adsorbent for pollutant removal demonstrating with good recyclability and reusability performance. However, the present proof of concept needs upscaling from lab to pilot level before true potential of such technology comes to fruition. Indeed, various challenges lie ahead in terms of scale-up and the process parameters that need to be optimised and this could be a focus for future research.

CHAPTER 4: Adsorption of pharmaceuticals in a fixed-bed column using tyre-based activated carbon: Experimental investigations and numerical modelling

4.1. Introduction

Pharmaceuticals and other emerging contaminants such as personal care products have raised international concerns because of their low biodegradability, high persistence, and facile bioaccumulation (Zhang et al., 2016). These contaminants are generally present in water at trace levels (e.g., ng/L), and can have adverse effects on both human and the ecosystem health (De Andrade et al., 2018). Conventional wastewater treatment plants are not designed and in effective in the removal/degradation of majority of pharmaceuticals (Bagheri et al., 2014). Among existing advanced treatments, adsorption has been considered as an attractive technology due to its simple and effective operation without generation of toxic by-products (Tong et al., 2010).

Environmental risks posed by ELTs or scrap tyres have attracted increasing global attention due to the environmental threat following their disposal to landfill or open burning. In New Zealand, nearly 5 million ELTs are disposed of in landfills, stockpiles, and often are illegally dumped or unaccounted for each year (Tasalloti et al., 2020). Therefore, the use of ELTs as precursor for carbon-based adsorbents has added advantages of both waste minimization and reduction in processing costs. Activated carbon from waste tyres has been found to be effective for adsorptive removal of pharmaceuticals (Acosta et al., 2016; Azman et al., 2019), dyes (Hakimi Mohd Shaid et al., 2019; Mukherjee et al., 2019; Tuzen et al., 2018) and heavy metals (Adio et al., 2019; Kim et al., 2018; Makrigianni et al., 2017) under batch experiments using aqueous solutions. Magnetisation of carbonaceous adsorbents facilitates their application at full-scale industrial wastewater treatment as they can be easily separated and regenerated after treatment. Furthermore, magnetic adsorbent can have higher surface area and adsorption capacity than non-magnetic adsorbents as have been described in Chapter 3. Magnetic

carbonaceous adsorbents can be synthesised by chemical co-precipitation or pyrolysis activation (Chen et al., 2011; Devi & Saroha, 2014)

Fixed-bed granular activated carbon has been identified as a "Best Available Technology" by the United States Environmental Protection Agency (USEPA) for the removal of organic contaminants from aqueous solution (Westerhoff et al., 2005). Majority of pharmaceuticals removal studies in aqueous phase using carbon-based adsorbents has been done under static conditions (batch mode), and there are limited number of studies on pharmaceuticals adsorption in dynamic operational conditions using packed-bed columns (Darweesh & Ahmed, 2017a; Darweesh & Ahmed, 2017b; de Franco et al., 2018; Mondal et al., 2016; Nazari et al., 2016). These studies have mainly investigated the effect of operating conditions (inlet concentrations, flow rate and adsorbent bed height) on adsorption capacity. For example, Darweesh & Ahmed (2017b) illustrated the adsorption dynamics of levofloxacin on date-stone carbon and investigated the influence of inlet concentration (75–250 mg/L). The authors observed that at high initial concentrations, breakthrough curves shifted toward the origin. Nazari et al. (2016) studied the continuous adsorption of cephalexin on a walnut shell-based carbon under flow rates of 4.5, 6, and 7.5 mL/min and a rapid breakthrough was observed at high flow rates. Mondal et al. (2016) tested the adsorption of ranitidine on activated mung bean husk derived biochar at different bed heights and the authors observed that the breakthrough time was prolonged with increasing bed height. A much earlier study by Liao et al. (2013) illustrated the adsorption dynamics of tetracycline and chloramphenicol on bamboo charcoal at flow rates of 3.3, 6.6, and 10 mL/min and rapid breakthroughs were obtained at high flow rates for both pharmaceuticals.

Dynamic adsorption experiments allow prediction and modelling of breakthrough curves in simple operation mode and easy to scale-up for industrial applications. Moreover, they are capable of treating large volume of solution and more realistic for calculating design

parameters in real-life applications especially by using appropriate numerical models (Jaria et al., 2019, Köhne et al., 2009; Reynel-Avila et al., 2015). Mathematical models correlating the experimental breakthrough curve are needed to design and optimise adsorption columns (de Franco et al., 2017). To predict organic and inorganic pollutants transport in porous media and analyse breakthrough data for continuous adsorption, various numerical models have been developed and exploited, such as the Adams–Bohart, Thomas, Yoon–Nelson, Hydrus-1D and Hydrus-2D models (de Franco et al., 2017; Engelhardt et al., 2015; Jaria et al., 2019; Liao et al., 2013; Suárez et al., 2013). Adsorption in fixed-bed occurs by several simultaneous phenomenon such as mass transfer and dispersion of solutes. Therefore, the models that ignore either the adsorption parameters or non-equilibrium processes cannot effectively describe breakthrough curves, especially for scale-up purposes.

The Adams–Bohart model assumes that mass transfer or axial dispersion of solute is insignificant, and adsorption is proportional to the residual capacity of the adsorbent and the adsorbate concentration (Chu, 2010). In contrast, the Thomas model which assumes a Langmuir isotherm and a pseudo-second-order kinetics without axial dispersion in the adsorption column (Ahmed & Hameed, 2018) is suited for adsorption processes with limitations of no external and internal diffusion. Meanwhile, the Yoon–Nelson model (Yoon and Nelson, 1984), a simple breakthrough model, assumes that decreasing rate of adsorption is directly proportional to adsorbate adsorption and the adsorbate breakthrough on the adsorbent. Additionally, the model does not consider the properties of adsorbate, type of adsorbent and the physical properties of the adsorbent bed. However, Hydrus model allows the numerical solution of equilibrium and non-equilibrium convective dispersive equations considering mass transfer, molecular diffusion and hydrodynamic dispersion (Šimůnek & van Genuchten, 2008).

Previous studies (Hanna et al., 2010; Jellali et al., 2016; Suárez et al., 2007), have shown that predicting the fate and transport of chemicals in porous media using physical and/or chemical non-equilibrium models can be successful and more realistic. Unlike equilibrium models where adsorption is an instantaneous process, chemical non-equilibrium models assume that adsorption is time dependent and a kinetic rate process (Jellali et al., 2010; Šimůnek & van Genuchten, 2008). To date, modelling the fate and transport of pharmaceuticals using non-equilibrium processes in column studies for wastewater treatment applications has not yet been explored. Additionally, in spite of increasing volume of research on dynamic adsorption of contaminants from aqueous solution, to-date, there have been only a few studies investigating the effect of particle size of adsorbent on diffusion pattern of the adsorbate molecules (Gupta & Garg, 2019) and the effect of nano-particle adsorbents on fate of contaminants has been hitherto neglected. On the other hand, to have a better representation of what occurs during the wastewater treatment and to understand the competitive effects on the removal of the targeted compound, the performance of adsorption process needs to be assessed for solution containing pharmaceuticals with different chemical properties.

The overarching aim of this study is therefore to evaluate the performance of synthesised MTC for the removal of three pharmaceuticals from aqueous solution under dynamic operating conditions. The specific objectives are: (1) to compare the performance of commercial activated carbon (CAC) and activated tyre char (ATC) with MTC in packed-bed columns for removal of PRO, (2) to assess the importance of non-equilibrium processes on pharmaceuticals transport using the Hydrus-1D model and compare the results with those obtained from Adams–Bohart, Thomas, and Yoon–Nelson models, (3) to investigate the dependence of adsorption dynamics on operation parameters (flow rate, initial concentrations,

bed heights, pH), presence of competitive adsorbates (CIP and CLO), and the particle size of adsorbents and (4) to formulate a conceptual design for large-scale fixed-bed columns of tyre-based activated carbon for wastewater treatment.

4.2. Materials and methods

4.2.1. Materials

ELTs samples were mixtures of passenger car tyres and truck tyres (ratio of 90:10) and were supplied by PK Rubber (a tyre recycling company in Cork, Ireland). Coal based commercial granular activated carbon used in this study was purchased from Chemviron, New Zealand. Prior to its application in column studies, it was ground, sieved (75–300 μm), washed with deionized (DI) water, and dried in oven at 100 °C overnight. CIP, PRO, CLO, and methanol (LCMS grade, 99.9% purity) were purchased from Sigma–Aldrich (Auckland, New Zealand). Formic acid (CH_2O_2), potassium hydroxide (KOH), sodium bromide (NaBr), hydrochloric acid (HCl), sodium hydroxide (NaOH) and NaCl were analytical grade and were used as received.

4.2.2. Preparation of adsorbents

The MTC used in this study was synthesised and characterised as reported in Chapter 3. Briefly, the ELTs were pyrolysed in a prototype pilot plant (constructed by the Irish PGE company) at 550 °C temperature, heating rate 20 °C min^{-1} and particle size 20 mm under oxygen-free and atmospheric pressure. TC produced from ELTs pyrolysis was crushed, sieved (75-300 μm), and 10 g of sieved pyrochar was stirred in 200 mL of DI water containing 1.5 g of $FeCl_2.4H_2O$ and 3.5 g of $FeSO_4 \cdot 7H_2O$ at 900 rpm for 1 h. Then, the mixture was heated to 60 °C and pH was increased to 9-11 with dropwise addition of KOH solution (3.0 M) and stirred for an

additional hour. Following rinsing with DI water for five times, the obtained pyrochar was dried in a vacuum oven (50 °C for 48 h) and sieved (75-300 μm).

In the present study, ATC was prepared using a modified version of chemical activation method (Antoniou & Zabaniotou, 2015). TC and KOH flakes were mixed (ratio 1:4), heated in a muffle furnace for 1 h at 400 °C, followed by pyrolysis in a tube furnace for 1 h at 850 °C under N^2 atmosphere (100 ml/min). After cooling, the sample was collected and added into a solution containing 1 L of 0.5 N HCl with continuous stirring (900 rpm) for 1 h at 85 °C. Finally, ATC was rinsed five times with deionized water and dried in a vacuum oven at 100 °C for 24 h.

To produce nano chars, 5 g of MTC was placed in a planetary ball mill machine (Retsch PM100 Planetary Ball Mill) within stainless steel jars (50 cm^3) and balls (diameter 10 mm) (mass ratio of steel balls: char powder = 4.65:1) and operated (575 rpm for 1.6 h) in ambient air with rotation direction altered every 0.5 h. The milling time was optimized for the preparation of MTC in the size of 250 nm. To gain bigger size (500-1000 nm), the speed and milling time was reduced to 300 rpm and 30 min, respectively.

4.2.3. Characterization

Average particle size and pore size distributions of the adsorbents were measured by laser beam scattering technique using a Zetasizer Nano S90 apparatus (Malvern Instruments, UK). Samples were prepared by dispersing in distilled water containing 1% ethanol and 0.5% Tween 80, using Vibra-Cell VCX-130 Ultrasonic Processor (Sonics & Materials, USA) for 60 min. The samples were kept cold by an external ice bath during the sonication. The Brunauer-Emmett-Teller (BET) surface area and Barrett–Joyner–Halenda (BJH) cumulative pore

volumes of the ATC were obtained by N_2 adsorption at $-196\,°C$ using a Micromeritics Tristar 3000 instrument.

4.2.4. Analytical methods

The concentrations of bromide were measured using ion-chromatography (IC) equipped with an AS18 column, Dionex Corporation, at a flow rate of 1 mL/min and run time of 20 min. The detection limit of bromide was 0.1 mg/L. Concentrations of CIP, PRO and CLO were determined by liquid chromatography tandem mass spectrometer (LC-MS/MS) using an Eclipse plus C18 column (100×2.1 mm, particle size 3.5 μm). Prior to the analysis, all samples were filtered through 0.20μm cellulose acetate filters. The mobile phase was a mixture of 0.1% formic acid in water (A) and 100% methanol (B) and was used at a flow rate of 0.2 mL/min and a column temperature of 40 °C. The runtime was 14 min with CIP, PRO and CLO retention time of 6.12, 7.19 and 7.89 minutes, respectively.

4.2.5. Column experiments

4.2.5.1. Fixed-bed column experimental protocol

The fixed-bed column was made of Plexiglas tube with an inside diameter of 1.4 cm and an adjustable length of 20 cm. For each experiment, the column was uniformly packed with adsorbent with particle size of 75-300 µm. The adsorbent layer was sandwiched by sand from both sides to maintain a uniform flow. Before each experiment, the column was equilibrated with a continuous flow of DI using a peristaltic pump (Masterflex®, USA) at up-flow operation mode for 24 h. Then, conductivity (WTW meter) and TOC (Shimadzu, model TOC-VCPH,

SSM-5000A) of samples were determined and the stability of the effluent was confirmed based on the conductivity and TOC values.

To determine the longitudinal dispersivity and the dispersion of adsorbates and to check the effect of physical non-equilibrium processes, conservative tracer experiments were performed using 10 mg/L of sodium bromide (NaBr). The aqueous solutions containing the known concentrations of CIP, PRO and CLO were continuously pumped into the column at a fixed flow rate of 3 mL/min, equivalent to empty bed contact time (EBCT) of 0.42 min. BTCs were obtained by collecting 3 mL of aqueous solutions at the outlet of the column at set time intervals using a programmable fraction collector (OMNICOLL single channel collector). All experiments were stopped when the saturation state occurred, and outlet column concentration became constant with the time. The initial pH and the temperature were kept constant to 7 and 20 ± 2 °C, respectively.

4.2.5.2. Effect of operational conditions on BTCs

The tested operational adsorption parameters under continuous mode were volumetric flow rates, initial concentrations, mass of adsorbents, single component and ternary solutions, adsorbent particle size and solution pH. Different flow rates (1, 3 and 5 mL/min) were studied to determine the impact of flow rate at a constant initial PRO concentration of 2 mg/L and adsorbent mass of 1.5 g. To determine the effect of initial concentrations, the fixed-bed column was fed with a single solution of PRO at different concentrations (1, 2, and 5 mg/L) at a constant flow rate of 3 mL/min and adsorbent mass of 1.5 g (2.1 cm). Three adsorbents mass of 1 (1.55 cm), 1.5 (2.1 cm) and 2 g (2.7 cm) were used to investigate the dependence of adsorption dynamics on adsorbent mass with set PRO initial concentration and flow rate at 2 mg/L and 3 mL/min, respectively. Adsorption of PRO from single or ternary solutions (PRO, CIP, CLO)

studies were carried out on individual component solutions of PRO (2 mg/L) and ternary

mixtures of PRO, CIP and CLO (2 mg/L of each pharmaceutical) at the flow rate of 3 mL/min

and adsorbent mass of 1.5 g. To investigate the effect of adsorbent particle size on the

breakthrough profile of PRO adsorption, two different size range of 200-500 nm and 500-1000

nm were employed at initial PRO concentration = 2 mg/L, flow rate: 3 mL/min and adsorbent

mass: 1.5 g. Finally, dependence of adsorption dynamics of PRO as affected by solution pH

(4.0 and 10.0) was studied at a constant PRO initial concentration, flow rate and adsorbent

mass of 2 mg/L, 3 mL/min and 1.5 g, respectively.

4.2.5.3.   Fixed-bed column data analysis

BTCs were obtained by plotting C/C_0 (C and C_0 are the effluent and influent concentration in

mg/L) as a function of operating time (t, min) to assess the pharmaceuticals adsorption onto

MTC in a fixed-bed system under different operational conditions. The volume of effluent

treated by the system is determined by breakthrough point (t_b) defined as the time at which

C/C_0 becomes 0.1. The time at which the ratio of effluent concentration (C) to the influent

concentration (C_0) reaches a determined value is considered the saturation point (corresponding

to a saturation time (t_s)).

The total mass of adsorbate adsorbed per gram of adsorbent at the saturation time in column

(q_s (mg/g)) was calculated from the area above the BTC by the equation below:

$$q_s = \frac{QA}{1000m} = \frac{Q}{1000m} \int_{t=0}^{t=t_s} C_{ad} dt = \frac{Q}{1000m} \int_{t=0}^{t=t_s} (C_0 - C_t) dt \qquad (4.1)$$

Where Q and t_s are the volumetric flow rate (mL/min) and saturation time (min), respectively.

C_0 is inlet pharmaceuticals concentration, C_t is the measured pharmaceuticals concentration at

the column outlet as a function of time and m is the dry weight of adsorbent (g). Other useful

parameters for the BTCs analysis such as adsorption capacity at breakthrough time (q_b), contact

time (CT), effluent volume until breakthrough (V_{eff_b}), effluent volume until saturation (V_{eff_s}) and length of mass transfer zone (MTZ) were determined using following expressions.

$$q_b = \frac{Q}{1000m} \int_{t=0}^{t=t_b} (C_0 - C_t)dt \tag{4.2}$$

$$CT = \frac{V_c}{Q} \tag{4.3}$$

$$V_{eff\_s} = Qt_s \tag{4.4}$$

$$V_{eff\_b} = Qt_b \tag{4.5}$$

$$MTZ = h(1 - \frac{t_b}{t_s}) \tag{4.6}$$

where V_c is the adsorbent volume (L) and h is the bed height (cm) and all other terms are as defined earlier.

4.2.5.4.   Breakthrough curves modelling

The solute transport equations in Hydrus model can consider equilibrium and/or non-equilibrium conditions between the liquid and solid phases, thus improving the description of solute transport in porous medium. The description of one-dimensional solute transport in either fully saturated or non-saturated zone is usually described using the convection–dispersion equation (Šimůnek & van Genuchten, 2008):

$$\frac{\theta \partial C}{\partial t} + \rho \frac{\partial S}{\partial t} = \theta D \frac{\partial^2 C}{\partial z^2} - q \frac{\partial C}{\partial z} \tag{4.7}$$

$$D = \lambda v = \lambda \frac{q}{\theta} \tag{4.8}$$

where C is concentration of the solute (g/cm^3), t is time (min), ρ (g/cm^3) is the medium bulk density, S is the sorbed concentration (g/g), θ is the volumetric water content (cm^3/cm^3), D is dispersion/diffusion coefficient (cm^2/min), q is the volumetric fluid flux density (Darcy's

velocity) (cm/min), λ is the longitudinal dispersion coefficient [cm], v the average pore velocity (cm/min) and Z is the distance (cm).

The equilibrium sorption of solutes can be represented by the following equation below (Baskaran et al., 1996).

$$S = \frac{K_d C^\beta}{1+\eta C^\beta} \qquad (4.9)$$

where K_d (cm^3/g) is the distribution coefficient, and β (-) and η (cm^3/g) are adsorption coefficients that can be best represented by the isotherm model. When β=1, the adsorption becomes the Langmuir, when η=0, the equation becomes the Freundlich, and when both β=1 and η=0, it leads to a linear adsorption.

Two-site chemical non-equilibrium model that is available in Hydrus-1D was used to represent chemical non-equilibrium processes in solute transport. Some studies have successfully used two-site chemical non-equilibrium models to predict BTCs of organic compounds (Briones & Sarmah, 2019; Caceres-Jensen et al., 2019; Davidson & McDougal, 1973; Parker & Jardine, 1986) and metals (Fu et al., 2019; Jellali et al., 2016; Žukauskaitė et al., 2019) in porous media. According to two-site model, assuming that the sorption sites can be divided into two fractions, sorption on one fraction of the sites is assumed to be instantaneous and in equilibrium with the solution (S^e), while time-dependent kinetic sorption (S^k) occurs on the second fraction (Šimůnek & van Genuchten, 2008). Total solute transport, instantaneous sorption, and rate-limited or kinetic sorption, modelled by a first order equation, are described in Eq. 4.10 to Eq.4.11, respectively.

$$S = S^e + S^k \qquad (4.10)$$

$$S^e = f_e \frac{K_d C^\beta}{1+\eta C^\beta} \qquad (4.11)$$

$$\frac{\partial S^k}{\partial t} = \alpha_k[(1-f_e)K_d C - S^k] \qquad (4.12)$$

where, f_e (-) is the fraction of equilibrium sites, and α_k (1/min) is a first-order rate coefficient. Other terms are as described earlier.

To determine the values for λ and q, simulation of conservative tracer BTCs was performed by inverse approach using the Levenberg-Marquardt algorithm. Initial and boundary conditions used in this study were: a concentration flux at the inlet and a zero-concentration gradient at the outlet respectively. In addition, the adsorbents inside the column were assumed to be exempt of solute concentration, and constant water content which were equal to the porosity of adsorbents.

To compare the predicted values obtained by Hydrus-1D with other models, three common models, Thomas, Yoon-Nelson and Adams-Bohart, were applied as follows:

Thomas model: $\dfrac{C}{C_0} = \dfrac{1}{1+\exp(K_T q_0 M/Q - K_T C_e t)}$ $\qquad (4.13)$

Adams−Bohart model: $\dfrac{C}{C_0} = \exp(K_A C_0 t - K_A N_0 H/u)$ $\qquad (4.14)$

Yoon−Nelson model: $\dfrac{C}{C_0} = \dfrac{\exp(K_T t - K_T \tau)}{1+\exp(K_T t - K_T \tau)}$ $\qquad (4.15)$

Where k_T is the Thomas rate constant (mL/min mg), q_0 is the adsorption capacity (mg/g), M is the mass of adsorbent (mg), Q is the inlet flow rate (ml/min), k_A is the Adams- Bohart constant (l/min.mg), N_0 is the saturation concentration (mg/L), H is bed depth of the column (cm), u is the superficial velocity (cm/min), K_T is Yoon-Nelson rate constant (1/min), and τ is the time required for 50% adsorbate breakthrough (min).

4.3. Results and discussions

4.3.1. Characterisation of adsorbents

According to N_2 isotherm of the ATC as shown in Figure. F.1, adsorption increased considerably at relative pressures (p/p$_0$) above 0.9 and a well-developed micro-porosity was observed due to N_2 adsorption at low relative pressures. The surface area of Tyre char was 38.17 m^2/g as reported in Chapter 3 and after thermal and chemical activation, it had a substantial jump to 453.81 m^2/g and the total pore volume at P/P$_o$ =0.98 was 0.6551 cm^3/g was higher than that were reported earlier (Abdelbassit et al., 2020; Kim et al., 2018; Makrigianni et al., 2015). The particle size distribution for the samples in experiments with milling condition 1.6 h, 575 rpm, 5 g and 0.75 h, 400 rpm, 5 g were illustrated in Figure. F.2, with the particles ranging from 100-500 nm and 500-1000 nm, respectively.

4.3.2. Tracer experiment

Before doing the column experiments for the selected pharmaceuticals, the bromide BTC was established to check the presence of physical non-equilibrium conditions and determine the longitudinal dispersivity (λ) and the Darcy's flow velocity (q). The bromide BTCs showed a nearly symmetrical shape without any tailing when C/C_0 was close to 1 (Figure 4.1), indicating saturation of column and negligible immobile water fraction for transport under the used hydraulic conditions (Briones & Sarmah, 2019; Jellali et al., 2010). Hydrodynamic properties of the column were optimized using Hydrus-1D inverse method, assuming an equilibrium state. Water contents (θ) were assumed constant and set equal to 0.39, 0.42, 0.46 cm^3/cm^3 for MTC, ATC and CAC, respectively which is the porosity of packed char. The estimated values of λ and q for MTC, ATC and CAC are presented in Table F.1. The predicted low λ indicated that the adsorbent was relatively homogenous. In addition, the smaller fitted value for q by Hydrus-

1D than the experimental one could be attributed to the column packing and presence of two layers of sand at column boundaries. Based on R^2 value, the equilibrium model was a good fit to the bromide BTCs, and the predicted λ was used for the subsequent solute transport through the same column.
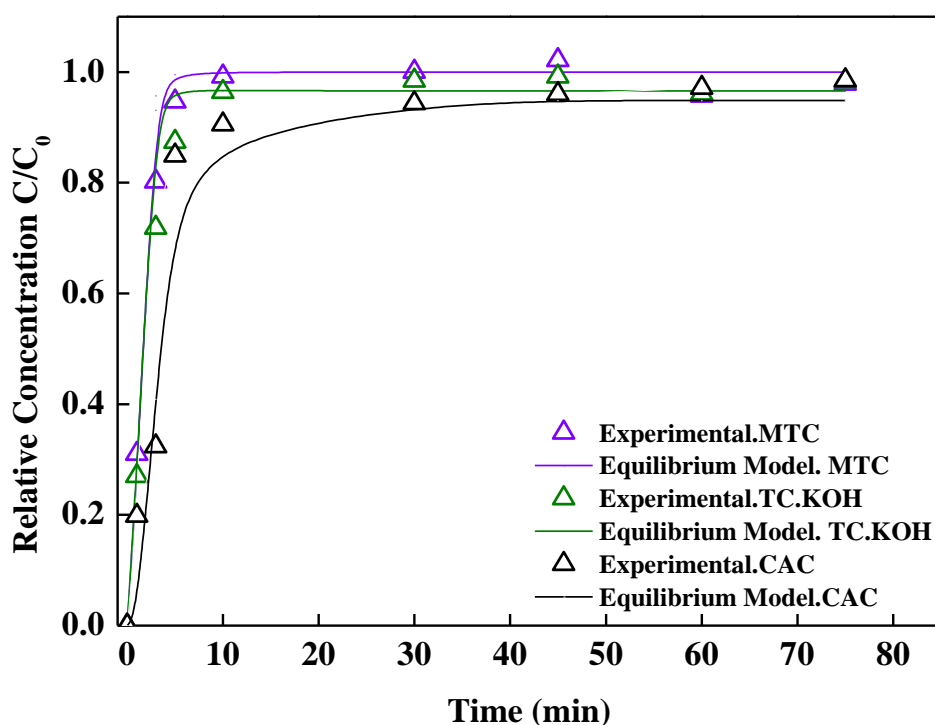
Figure 4. 1. Experimental and fitted breakthrough curve of bromide tracer with Hydrus-1D model for MTC, ATC and CAC (NaBr=10 mg/L; Flow rate=3 mL/min; adsorbent mass=1.5 g).

4.3.3. Comparison of models

The three models introduced in Section 4.2.5.4 were applied to analyse the breakthrough curve data of PRO adsorption onto MTC at a constant initial PRO concentration of 2 mg/L, flow rate of 3 mL/min and adsorbent mass of 1.5 g (Figure. F.3). Non-equilibrium Hydrus-1D model was able to well predict the experimental trends, as indicated by the error analysis (Table F.2).

Conversely, the predicted values through equilibrium Hydrus-1D, Yoon–Nelson, Thomas, and Adams-Bohart models were not in agreement with the experimental data. The predicted values obtained using Thomas and Yoon–Nelson models were quite similar. The lowest root-mean-square error (RMSE), average percentage error ($\varepsilon\%$) and Chi square (X^2) and highest correlation coefficient (R^2) were for the non-equilibrium Hydrus-1D model (Table F.2). Indeed, the experimental data fitting non-equilibrium Hydrus-1D model was successful, and this can be related to the effect mass transfer and dispersion mechanisms which were taken into account.

Table 4. 1. Efficiency and mass transfer parameters determined from the breakthrough curves corresponding to the fixed-bed adsorption of pharmaceuticals onto MTC.

	Adsorbent	Particle Size	C_{in} (mg/L)	Q (mL/min)	m (g)	t_b (min)	pH	V_{eff_b} (L)	q_b (mg/g)	t_s (min)	q_s (mg/g)	MTZ (cm)
Single Solution												
PRO	MTC	75-300 μm	2	**1**	1.5	950	7	0.95	0.0732	11610	5.86	1.95
	MTC	75-300 μm	2	**3**	1.5	310	7	0.93	0.0410	3660	4.53	1.92
	MTC	75-300 μm	2	**5**	1.5	108	7	0.54	0.0365	3096	3.04	2.02
	MTC	75-300 μm	2	3	**1**	180	7	0.54	0.0334	2160	4.11	1.42
	MTC	75-300 μm	2	3	**2**	540	7	1.62	0.1382	5760	8.25	2.44
	MTC	75-300 μm	**1**	3	1.5	420	7	1.26	0.0555	4620	3.44	1.90
	MTC	75-300 μm	**5**	3	1.5	150	7	0.45	0.0771	3480	7.12	2.01
	MTC	75-300 μm	2	3	1.5	120	**4**	0.36	0.002	3480	1.88	2.02
	MTC	75-300 μm	2	3	1.5	720	**10**	2.16	0.0594	5760	5.04	1.83
	MTC	**100-500 nm**	2	3	1.5	540	7	1.62	0.1522	5220	8.43	1.88
	MTC	**500-1000 nm**	2	3	1.5	360	7	1.08	0.0636	4320	5.40	1.92
	ATC	75-300 μm	2	3	1.5	4800	7	14.40	1.0770	23280	25.32	1.66
	CAC	75-300 μm	2	3	1.5	7620	7	22.86	1.8330	39420	61.31	1.69
CIP	MTC	75-300 μm	2	3	1.5	180	7	0.54	0.0682	3540	4.34	1.99
CLO	MTC	75-300 μm	2	3	1.5	3120	7	9.36	1.1060	6600	16.11	1.10
Ternary solution							7					
PRO	MTC	75-300 μm	2	3	1.5	73	7	0.22	0.0081	1500	1.93	2.01
CIP	MTC	75-300 μm	2	3	1.5	60	7	0.18	0.0002	720	1.11	1.92
CLO	MTC	75-300 μm	2	3	1.5	960	7	2.88	0.1685	3600	7.70	1.54

4.3.4. Fixed-bed adsorption of pharmaceuticals

To predict pharmaceutical breakthrough curves, Hydrus-1D was used under different experimental conditions. For all conditions, both equilibrium and non-equilibrium modelling were performed by using hydrodynamic parameters determined from the tracer experiment and adsorption parameters estimated using inverse simulations based on the Levenberg-Marquardt algorithm. Table 4.1 shows efficiency and mass transfer parameters of experimental breakthrough curves on the fixed-bed adsorption of PRO from synthetic wastewater.

4.3.4.1. Effect of flow rates on adsorption of PRO

BTCs of the PRO varied with flow rates and in general, higher the flow rate, the steeper and the shorter exhaustion time were observed for the BTCs (Figure 4.2a). A plausible explanation is that the increasing flow rate from 1 to 3 mL/min tends to lead a shorter contact time from 3.2 to 0.65 min between the adsorbent particles and the adsorbate ions and consequently results in early arrival of the related BTCs. Additionally, higher adsorption capacities at exhaustion time were obtained at smaller flow rates (5.86, 4.53 and 3.04 mg/g for applied flow rates of 1, 3 and 5 mL/min, respectively). This can be attributed to the higher rate of mass transfer at lower flow rate. These findings are consistent with those obtained using other biomasses during pharmaceutical removal from water (Jaria et al., 2019). Also, by decreasing the flow rate from 1 to 5 mL/min, the collected volume at the column outlet at t_b increased from 0.54 to 0.95 L (Table 4.1). Table 4.1 shows that MTZ values are strongly dependent on the bed depth and equilibrium point (t_b) and the values for MTZ increased with an increase in bed height. As discussed in Chapter 3, the same adsorbate-adsorbent system was used in batch mode to investigate kinetic and equilibrium adsorption experiments. Based on the results, the adsorption capacity of PRO (6.6 mg/g) in batch mode was higher compared with column operation. A

plausible explanation for this could be that in the batch mode, adsorbates have better interactions with active sites of adsorbents as they can move freely in the aqueous solutions and the external diffusion is favoured under the stirring conditions.

The non-equilibrium adsorption resulted in a better fit to the BTCs compared to the simple equilibrium for all flow rates and the correlation coefficients were > 0.98. The estimated transport parameters using non-equilibrium model are summarised in Table 4.2. By decreasing the flow rate from 5 to 1 mL/min, an increase in mass transfer and K_d values were observed. Higher f_e values for lower velocities confirm that more adsorbent sites were at equilibrium with the solution. Similar results were also reported by Jellali et al. (2016) using raw sawdust and magnesium pre-treated biochar for removal of lead from aqueous solutions.

4.3.4.2.   Effect of initial concentrations on PRO adsorption

Increasing initial concentration of PRO led to decreased breakthrough and exhaustion times which could be attributed to rapid saturation of adsorption sites and presence of diffusive flux at higher concentrations (Figure 4.2b). The experimental adsorption capacities obtained by Eq. (1) increased from 3.44 to 7.12 mg/g when the used initial concentration was increased from 1 to 5 mg/L (Table 4.3). However, there was no marked increase in MTC values (1.90 to 2.01) with increased initial concentration.

Higher K_d values were obtained for higher initial concentrations which was supported by the observed increase in adsorption capacity (q_b) in Tables 4.1 and 4.3 when initial concentration increased from 1 to 5 mg/L. Given that concentration gradient plays an important role in adsorption process at high initial concentration, driving force of adsorption is likely to be greater due to high concentration difference facilitated by high MTZ values. The simulated BTCs by equilibrium model could not fit the experimental data well with simulated BTCs

appearing before the measured BTCs indicating a faster transport of the solute. However, BTCs simulated by the chemical non-equilibrium model could predict PRO adsorption well, implying that the PRO adsorption is a chemical non-equilibrium process. As can be observed Table 4.3, f_e values tended to be lower at higher concentrations. This could be attributed to the fact that the diffusive and dispersive flux tended to be higher at higher concentrations and therefore, a smaller fraction of adsorbent would be in equilibrium with the solute.

4.3.4.3.   Effect of adsorbent mass on PRO adsorption

The experimental and BTCs modelling of PRO adsorption as a function of varied adsorbent mass is plotted in Figure 4.2c. A close examination revealed that BTCs shifted towards the origin at smaller bed heights. The observed trend in BTCs can be attributed to early saturation of the fixed-bed due to presence of less sorption sites and acceleration of adsorption rate at smaller bed heights (Baral et al., 2009). Furthermore, with an increase in bed height, adsorption capacity also increased by two-fold (4.11 to 8.25 mg/g) as the adsorbent mass was raised from 1 g to 2 g (Table 4.1). This increase may be attributed due to more binding sites and higher contact time implying greater diffusion of adsorbate into the solid particles (Darweesh & Ahmed, 2017a).

For the numerical simulations, transport of PRO at different adsorbent mass was predicted better by chemical non-equilibrium model than equilibrium model. With the increases in adsorbent mass from 1 g to 2 g, f_e increased from 0.39 to 0.51 implying that more sorption sites were in equilibrium with the adsorbent particles (Table 4.4).

Figure 4. 2. Breakthrough curves and fittings of the experimental data to the Hydrus-lD for the adsorption of PRO onto MTC (pH=7, particle size: 75-300 um) (a) at different flow rates, (b) initial concentrations, and (c) adsorbent mass

Table 4. 2. Fixed and estimated parameters from PRO transport through column using two-site chemical non-equilibrium models in Hydrus-1D for different flow rates (f: fixed parameters and e: estimated parameters).

Q (mL/min)	λ^f (cm)	q^e (cm/min)	K_d^e (cm³/g)	η (cm³/g)	β (-)	α^e (1/min)	f_e^e (-)	R^2 (%)
1	0.63	0.51	2381	0.27	0.90	1.27E-03	0.61	0.98
3	0.63	1.70	2270	0.25E-04	0.95	8.43E-04	0.41	0.98
5	0.63	3.10	1362	0.66E-01	0.91	1.46E-04	0.25	0.98

Table 4. 3. Fixed and estimated parameters from PRO transport through column using two-site chemical non-equilibrium models in Hydrus-1D for different initial concentrations (f: fixed parameters and e: estimated parameters).

C_{in} (mg/L)	λ^f (cm)	q^e (cm/min)	K_d^e (cm³/g)	η (cm³/g)	β (-)	α^e (1/min)	f_e^e (-)	R^2 (%)
1	0.63	1.75	2132	0.60E-01	0.89	1.08E-03	0.45	0.98
2	0.63	1.70	2270	0.25E-01	0.95	8.43E-04	0.41	0.98
5	0.63	1.81	2719	0.13E-01	0.98	6.27E-04	0.35	0.99

Table 4. 4. Fixed and estimated parameters from PRO transport through column using two-site chemical non-equilibrium models in Hydrus-1D for different adsorbent mass (f: fixed parameters and e: estimated parameters).

m (g)	λ^f (cm)	q^e (cm/min)	K_d^e (cm³/g)	η (cm³/g)	β (-)	α^e (1/min)	f_e^e (-)	R^2 (%)
1	0.63	1.81	2623	0.12	0.96	3.60E-03	0.39	0.99
1.5	0.63	1.70	2270	0.25E-01	0.95	8.43E-04	0.41	0.98
2	0.63	1.73	1996	0.56	0.83	7.45E-04	0.51	0.98

4.3.4.4.   Adsorption of PRO, CIP and CLO with single and ternary solutions

The experimental and modelling of BTCs on the adsorption of PRO, CIP and CLO using single and tertiary solutions are shown in Figure 4.3, and the effect of competition on the PRO adsorption was investigated by comparing the BTCs of all pharmaceuticals. Under single solution, the BTCs of PRO and CIP exhibited similar trend with early arrival and were much steeper than CLO, with BTC for CLO peaked its exhaustion time much later than PRO and CIP; 3660, 3540 and 6600 min, respectively. Similar steeper BTCs were observed for tertiary adsorption, and higher BTCs were observed for CIP and PRO, however, an opposite trend was found for CLO. Compared to data from single component solution, the saturation time and adsorption capacity of PRO, CIP and CLO decreased in the ternary solution which could be likely due to the competitive adsorption of pharmaceuticals in the mixture for the adsorption sites.

The plots of BTCs in Figure 4.3 and summarised fitted parameters in Table 4.5 using chemical non-equilibrium models for the experimental results lend further support that chemical non-equilibrium model described the experimental data better than equilibrium model. In the single solution, the fitted K_d values of pharmaceuticals followed an order CLO>PRO>CIP. In the case of ternary solution, a decrease in all K_d values was observed that might be attributed to the competitive effects amongst the adsorbates. Although the order of K_d values in ternary solution slightly changed (CLO> CIP >PRO), CIP still exhibited the lowest adsorption capacity. A general trend observed was the consistent lower values of K_d for all three compounds under ternary solution suggesting the competition for the molecules for the available sites in the adsorbents. The lower adsorption of CIP in both single and ternary solution can be explained by its pKa values (6.18 and 8.76). At pH 7, zwitterionic form of CIP is dominant and there is no electrostatic attraction between MTC and CIP molecules. However, higher adsorption of

PRO and CLO can be related to electrostatic attraction as their pKa values are 9.42 and 9.2, respectively. Also, the octanol-water partition coefficient (K_{ow}) of CLO is higher than CIP and PRO indicating its high hydrophobicity. Therefore, CLO has higher tendency of adsorption onto carbon surface in comparison to CIP and PRO (Liu et al., 2010).
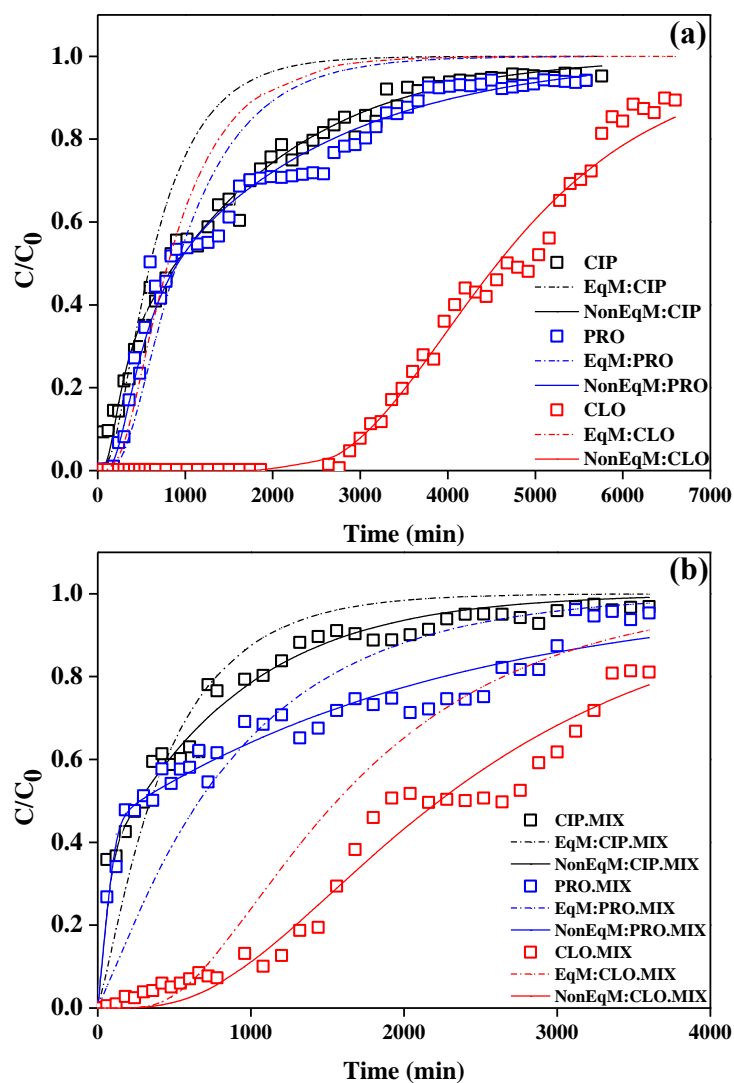
Figure 4. 3. Breakthrough curves and fittings of the experimental data to the Hydrus-lD for the adsorption of PRO onto MTC from (a) single solution and ternary solution (Q= 3 mL/min, Cin= 2 mg/L, m= 1.5 g, pH=7, particle size: 75-300 μm)

Table 4. 5. Fixed and estimated parameters from PRO, CIP and CLO transport through column using two-site chemical non-equilibrium models in Hydrus-1D in single and ternary solution (f: fixed parameters and e: estimated parameters).

	Compound	λ^f (cm)	q^e (cm/min)	K_d^e (cm³/g)	η (cm³/g)	β (-)	α^e (1/min)	f_e^e(-)	R^2 (%)
Single solution	CIP	0.63	1.81	2174	0.98E-01	0.96	1.34E-03	0.28	0.99
	PRO	0.63	1.70	2270	0.25E-01	0.95	8.43E-04	0.41	0.98
	CLO	0.63	2.08	3024	0.54	0.75	9.07E-03	0.18	0.99
Ternary solution	CIP	0.63	1.78	2041.8	0.19	0.98	7.95E-04	0.22	0.97
	PRO	0.63	1.74	1993.2	0.23	0.92	2.35E-03	0.35	0.97
	CLO	0.63	1.89	2723	0.30	0.90	9.96E-03	0.16	0.98

4.3.4.5.   Effect of pH on adsorption of PRO

The effect of pH on the adsorption of PRO was studied at pH 4, 7 and 10 and illustrated in Figure 4.4. With increasing pH, the breakthrough time was higher, and the BTCs shifted away from the origin. Breakthrough points were achieved at 720, 310, 120 min at pH 10, 7 and 4, respectively (Table 4.1). At pH 4, the surface of MTC was positively charged with a point of zero charge (pH$_{pzc}$) value of 4.65 as obtained in Chapter 3. At this pH value, the cationic species of PRO were dominant, and adsorption capacity reduced due to electrostatic repulsion between cationic PRO molecules and MTC. In addition, higher pH values resulted in the enhancement of the adsorption capacities. This could be attributed to the electrostatic attraction between the solutes and adsorbent binding sites as PRO exists as a cationic species at around pH 10 and the adsorbent is negatively charged. At pH >10, however, the electrostatic interactions would be expected to have little effect on the sorption process due to neutral molecule of propranolol. It is noteworthy that the highest pH used in this study was 10, which was about 0.5 log unit higher

than the pKa of PRO, and it could assumed that higher adsorption observed could be still within reasonable expectation that pH is near the pKa value of PRO (9.42) and thus the species is still in positively charged.
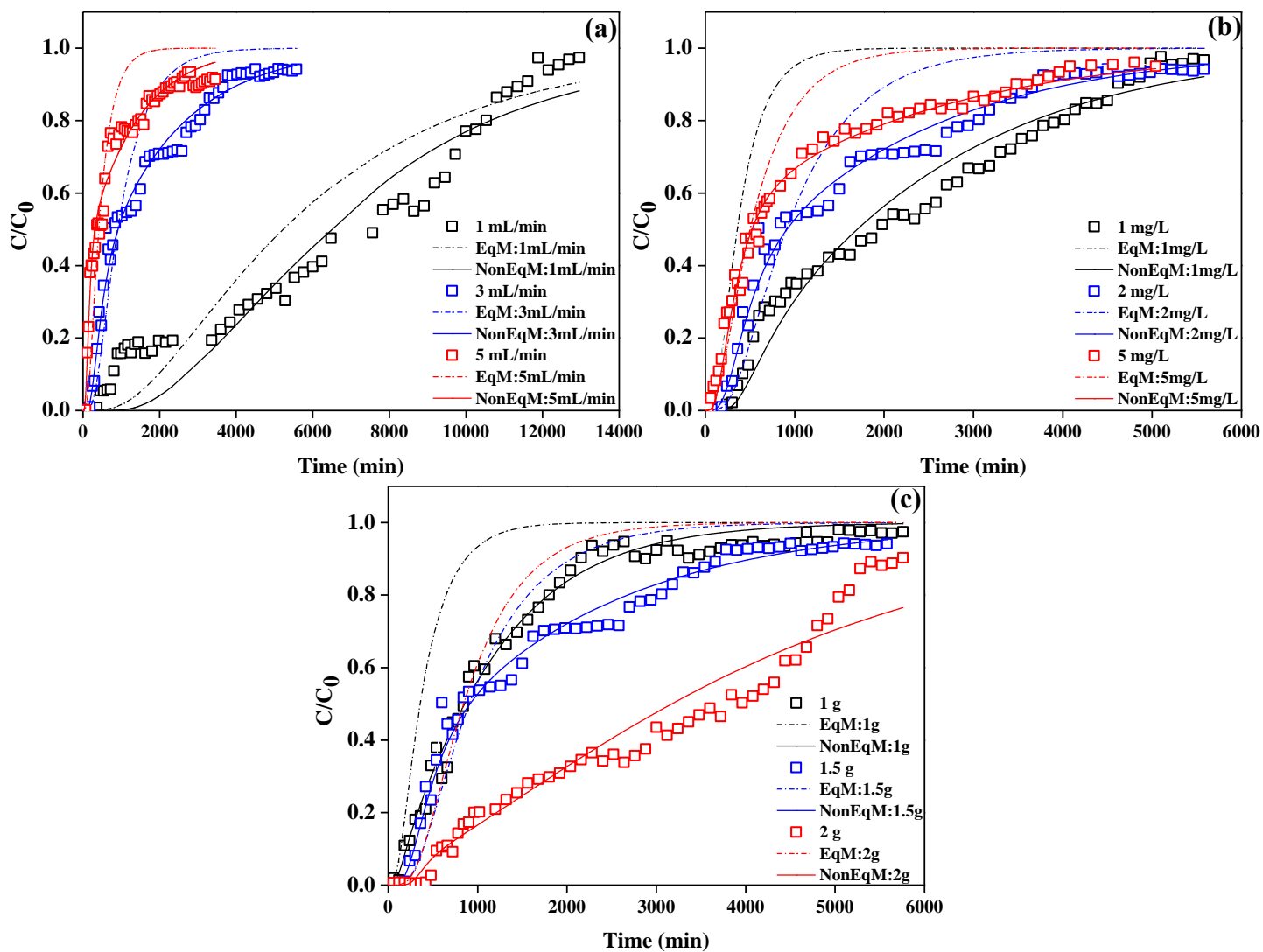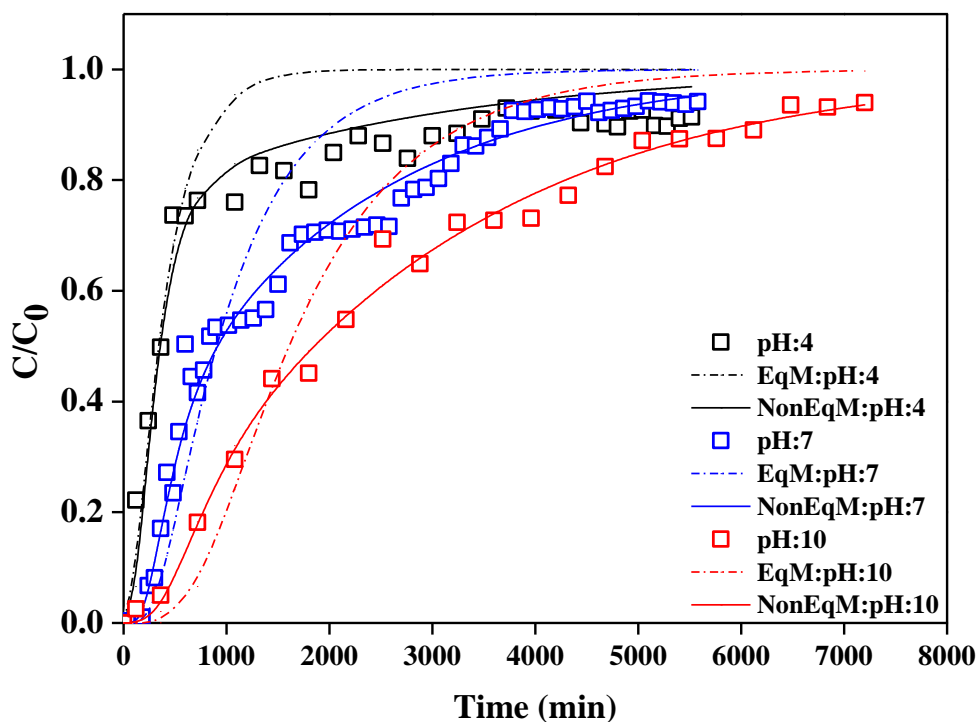

Figure 4. 4. Breakthrough curves and fittings of the experimental data to the Hydrus-lD for the adsorption of PRO onto MTC at pH 4, 7 and 10 (Q= 3 mL/min, Cin= 2 mg/L, m= 1.5 g, particle size: 75-300 µm)

4.3.4.6.   Effect of adsorbent particle size on adsorption of PRO

To observe the effects of particle size on BTCs, column tests were performed at different particle sizes of MTC (100-500 nm, 500 nm-1µm and 75-300 µm). By decreasing the particle size from 75-300 µm to 100-500 nm, breakthrough time rose from 310 min to 540 min. Similar findings were reported by Gupta & Garg (2019). A plausible explanation for the increased breakthrough time with reduction in particle size could well be attributed to the fact that the

smaller particle sizes have shorter diffusion paths for adsorbate molecules, leading to an increase in adsorbate penetration into adsorbent pores and higher adsorption (Gupta & Garg, 2019). Moreover, ball milling is expected to enhance the specific surface area of the chars and increase the number of active sites for adsorbing the adsorbate molecules (Lyu et al., 2018a). As it can be observed from Figure 4.5, the BTCs are much closer to the experimental ones when non-equilibrium modelling was used; however, the simulated BTCs are totally different from the experimental ones when assuming equilibrium state between adsorbents and adsorbate.
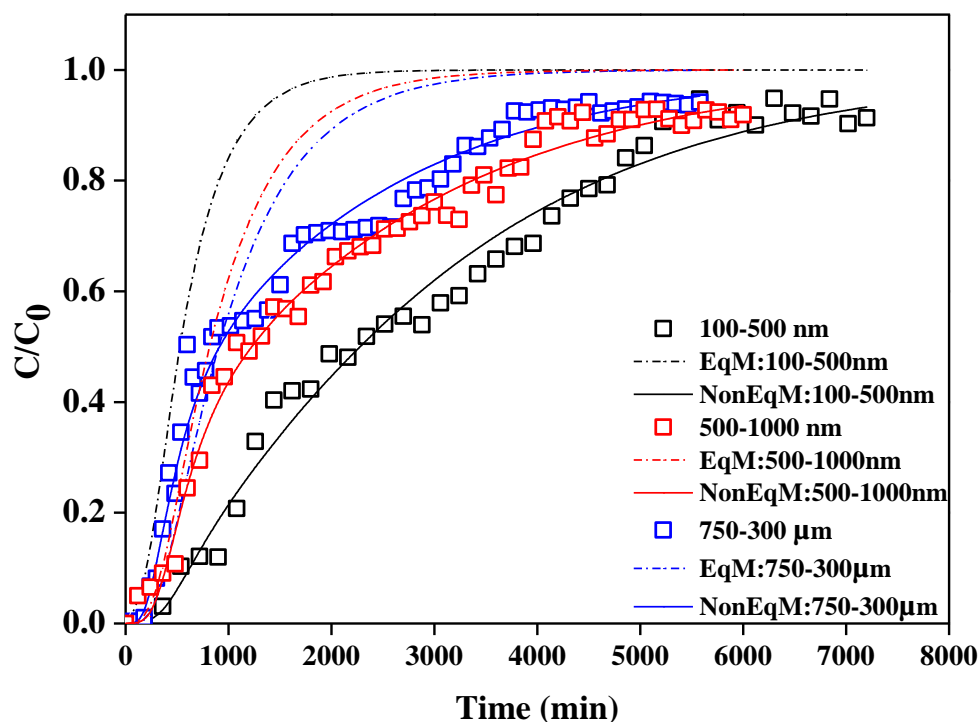
Figure 4. 5. Breakthrough curves and fittings of the experimental data to the Hydrus-lD for the adsorption of PRO onto MTC at different adsorbent particle size (Q= 3 mL/min, Cin= 2 mg/L, m= 1.5 g, pH=7)

Table 4. 6. Fixed and estimated parameters from PRO transport through column using two-site chemical non-equilibrium models in Hydrus-1D for different adsorbent particle size (f: fixed parameters and e: estimated parameters).

Adsorbent particle size	λ^f (cm)	q^e (cm/min)	K_d^e (cm³/g)	η (cm³/g)	β (-)	α^e (1/min)	f_e^e(-)	R^2 (%)
100-500 nm	0.63	1.72	2955	0.19	0.90	1.18E-03	0.37	0.98
500-1000 nm	0.63	1.81	2401	0.16	0.88	9.19E-04	0.36	0.99
75-300 um	0.63	1.70	2270	0.25E-01	0.95	8.43E-04	0.41	0.98

4.3.4.7. Adsorption of PRO in a fixed-bed column using CAC and ATC

Figure 4.6 shows the BTCs of PRO in the fixed-bed columns filled with the different adsorbents. The t_b for MTC, ATC and CAC were 0.21, 3.3, 5.3 day while t_s for MTC, ATC and CAC were 2.54, 16.1 and 27.37 day, respectively (Table 4.1). BET surface area of ATC increased considerably after chemical activation enabling treatment of larger volume of contaminated water than MTC under the same operating condition. Also, the ATC demonstrated much higher adsorption capacity for PRO (25 mg/g) than MTC (4.5 mg/g), and its adsorption was comparable to the CAC (61 mg/g).

The model simulated BTCs assuming equilibrium between PRO ions and the adsorbents appeared much too early compared to the experimental ones; however, the non-equilibrium model described the experimental data from the column study well for all adsorbents. Chemical non-equilibrium model parameters are summarised in Table 4.7, and it can be observed that f_e values for ATC and CAC are smaller than MTC implying that smaller fraction of the solid matrix is in equilibrium with PRO due to higher diffusive and dispersive flux. Contrary to

MTC, higher α^e for ATC and CAC shows that mass transfer of PRO from the aqueous solutions to the adsorbents was relatively fast. Overall, the experimental findings showed that ATC could be considered as a potential promising adsorbent due to its high surface area and pore volume for adsorption of pharmaceuticals.
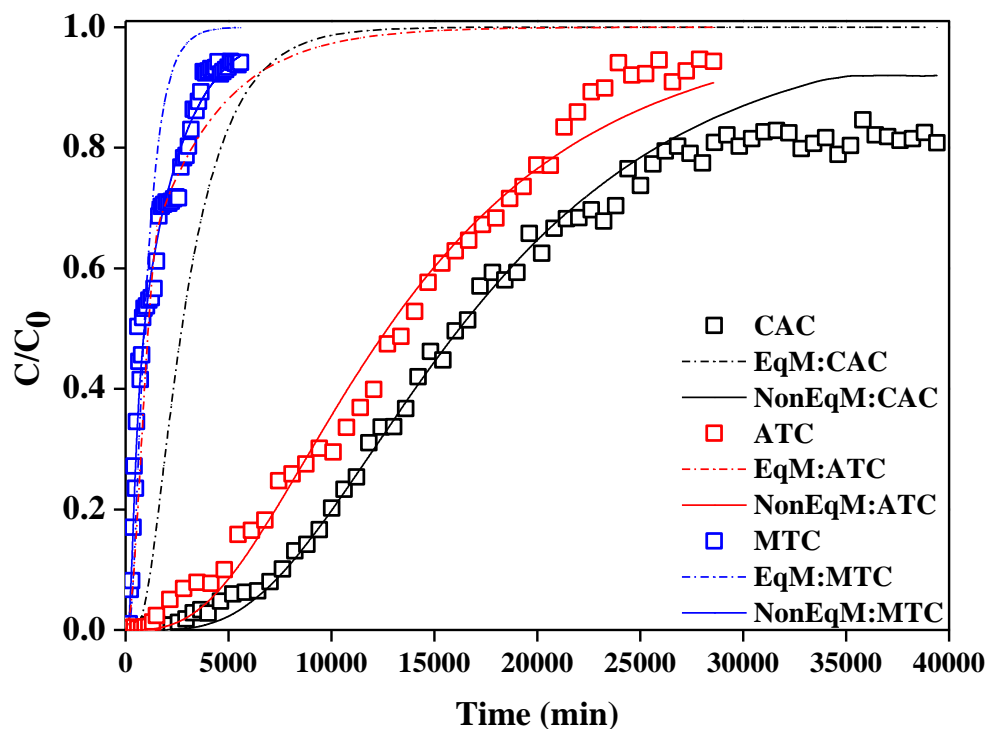
Figure 4. 6. Breakthrough curves and fittings of the experimental data to the Hydrus-lD for the adsorption of PRO onto different adsorbents (Q= 3 mL/min, Cin= 2 mg/L, m= 1.5 g, pH=7, particle size: 75-300 um)

Table 4. 7. Fixed and estimated parameters from PRO transport through column using two-site chemical non-equilibrium models in Hydrus-1D for different adsorbents (f: fixed parameters and e: estimated parameters).

Adsorbent	λ^f (cm)	q^e (cm/min)	K_d^e (cm³/g)	η (cm³/g)	β (-)	α^e (1/min)	f_e^e(-)	R^2 (%)
MTC	0.63	1.70	2270	0.25E-01	0.95	8.43E-04	0.41	0.98
ATC	0.74	1.75	8616	0.42	0.81	1.22E-03	0.27	0.99
CAC	0.44	1.79	19143	0.75	0.90	1.97E-03	0.16	0.99

4.3.5. Scale-up challenges and techno-economic assessment

Low-cost, easily available and environmentally friendly precursors for adsorbent preparation always are in great demand water and wastewater treatment industries. On the other hand, expensive, eco-unfriendly and less available materials would be irreproducible on a commercial scale. As about 4 billion tyres are landfilled or discarded in solid waste streams worldwide, producing adsorbents from waste tyres and activating them would be potentially beneficial for minimizing tyre wastes and treating large volume of contaminated water. Furthermore, the high removal efficiency of tyre char, its low-cost and simple application in treatment systems could make it economically profitable. Recognising the importance of technical and socio-economic constraints and techno-economic feasibility, an attempt was made to briefly discuss this aspect below.

There is a dearth of information on estimation of the cost of adsorbent-based water and wastewater treatment systems involving several cost elements, volume of treated water, degree of purification, different techniques, and operating conditions. In this study, economic analysis of a fixed-bed column of tyre char for wastewater treatment has been conducted to translate experimental data into economic figures and develop new market accessibility for tyre chars. Due to the absence of scale correlations, input data were extrapolated from pilot-scale to large-scale and therefore, the column dimension, flow rate, initial concentration and adsorbent mass were considered as 2.1×2.75 m, 35 m³/h, 50 mg/L and 4 tonnes, respectively. The breakthrough time estimated by non-equilibrium Hydrus model (R^2: 99%) for the scaled-up column with mentioned specification and input data was 28 days. The production cost of tyre char (299 US$/tonne) was obtained from Chapter 3. The feasibility of the scale-up was estimated by adding capital charges in the form of annualized capital cost (ACC) to the fixed and variable operating costs (Table 4.8) (Islam et al., 2011). The data of cost analysis was used to determine the treatment cost of per cubic meter of wastewater. The estimated treatment costs for a fixed-

bed column using tyre-based activated carbon showed good potential for wastewater treatment even though there is variation depending on the specific location, time, and low-cost feed material.

Table 4. 8. Economic analysis of a fixed-bed column of tyre char for wastewater treatment

Location, time, currency	New Zealand, 2021, USD	
Annual operating time	7512 h	
Base Plant Cost (BPC)	185,000	
Interest rate (I)	10%	
Plant life (N)	8 years	
Total labours (in equivalent of shift operators)	6	
Treated wastewater (m³/day)	840	
Parameters used in cost estimation		**Treatment Cost**
Fixed capital investment (FCI)	1.75*1.3*BPC	420,875
Total capital Requirement (TCR)	1.15* FCI	484,006
Annualized capital cost/Capital charges	$TCR/\{1- [\![(1+I)]\!] \char`^(-N) \} \times I$	90,724
Maintenance	2.5% of FCI	10,522
Overheads	2% of FCI	8,418
Taxes and insurance	1.5% of FCI	6,313
Other fixed operating costs	1% of FCI	4,209
Labour rate	13.57 USD/h (regular duty @ 8 h/day)	203,876
Electricity price	0.098 USD/ kWh (30 kW for pilot plant)	22,085
General overheads	60% of total salaries	1,196
Tyre char	299 US$/tonne	2,990
Wastewater treatment cost (US$/m³)	**1.57**	

4.4. Conclusions

The performance of MTC, ATC and CAC fixed-bed columns was evaluated to determine the removal of three selected pharmaceuticals from aqueous solution. The adsorption performance was dependent on operating factors such as bed height, initial concentration, influent pH, and especially volumetric flow rate and particle size. Low flow rate and nano particle size were demonstrated to significantly increase the removal rate of contaminants from wastewater. Moreover, the presence of other pharmaceuticals affects PRO removal from synthetic wastewater which must be related to the competitive effects of other pharmaceuticals. Furthermore, the column packed with ATC adsorbent had higher adsorption capacity (25.32 mg/g) and was able to treat a notable volume of effluent (69.84 L) in comparison to MTC. The non-equilibrium Hydrus model was able to predict the experimental BTCs well under the tested experimental conditions; however, Adams–Bohart, Thomas, and Yoon–Nelson model were not in agreement with the experimental ones. The results of this study have significant implications for the application of activated tyre char for wastewater treatment. Tyre chars activated by thermal and chemical treatment had much greater specific surface area and adsorption capacity in comparison to pristine tyre char and could be potentially used as an adsorbent for treating pharmaceutical-contaminated waters under dynamic conditions. A more complete study is still warranted to investigate the application of tyre char in larger scale columns with real wastewater effluents and degradation and desorption of adsorbed contaminants for regeneration and recovery of used adsorbent. Additional studies should be undertaken to characterise adsorbents before and after adsorption through characterisation tests such as X-ray photoelectron spectroscopy, Fourier Transform Infrared Spectroscopy and X-Ray Diffraction Analysis in order to gain new insights into the adsorption mechanisms.

Chapter 5: Effects of effluent organic matter on adsorptive removal of propranolol under fixed-bed column using magnetic tyre char as packing material

5.1. Introduction

The presence of organic micro pollutants (OMPs) such as pharmaceuticals in surface and ground waters at trace levels can be harmful due to their toxic effects on invertebrates, fish, mussels, algae and human embryonic cells (Dieter & Mückter, 2007; Pal et al., 2010). Advanced wastewater treatment minimizes the negative impacts of the receiving aqueous compartments and therefore has been accentuated as a strategy to protect the aquatic environment (Shon et al., 2006). Although activated carbon adsorption as an advanced technology has received considerable attention to eliminate OMPs from water bodies, activated carbon is not an eco-friendly and cost-effective adsorbent. Tyre char obtained from ELTs can be a cheap and environmentally friendly adsorbent and has been successfully tested in adsorptive removal of pharmaceutical from water (Acosta et al., 2016; Azman et al., 2019).

Effluent organic matter (EfOM) which originates from wastewater treatment plant effluents can be a potential threat for the ecosystem and human health. The presence of EfOM in water bodies can negatively affect water quality and cause formation of carcinogenic disinfection by-products during treatment, disruption of water treatment processes, and bacterial regrowth as well as formation of problematic biofilm in water distribution systems (Winter et al., 2018). EfOM is a complex mixture of natural organic matter (NOM), soluble microbial products (SMPs), and trace harmful chemicals (Yu et al., 2012). Carbon-based adsorbents have been found to be effective in the elimination of EfOM (Cheng et al., 2005; Nguyen et al., 2013) and range of OMPs (Reguyal et al., 2017; Shanmuganathan et al., 2017) from water. Adsorption of EfOM by carbon-based adsorbents (powdered activated carbon) has been found to have negative affect on OMPs adsorption as demonstrated by Zietzschmann et al., (2014). The underlying mechanisms involved during the adsorption of both EfOM and OMPs for the sorbents could be associated with the adsorption sites or due to the blockage of adsorbent pores

by larger molecules (Li et al., 2003). OMPs and EfOM consist of chemical compounds with different molecular weight, hydrophobicity, electrical charge, and functional groups. Therefore, concentrations of EfOM and OMPs and their affinity on adsorbents can make considerable differences in their adsorption (Delgado et al., 2012; Matsui et al., 2003). Adsorption mechanisms such as π-π electron donor acceptor (EDA) interactions, hydrogen bonding, hydrophobicity and electrostatic interactions have been used to explain the adsorption behaviour of various organic chemicals onto carbon-based adsorbents (Heo et al., 2019; Velten et al., 2011; Yazdani et al., 2019).

In most published studies to date, the removal of individual fractions of EfOM and its characterization have been hitherto neglected and much emphasis was placed on the aspects of removal of composite NOM (Nguyen et al., 2013; Shanmuganathan et al., 2017). Among different methods available for EfOM characterization, liquid chromatography with organic carbon detector (LC-OCD) has gained increasing acceptance. LC-OCD is based on three separation processes, namely, size exclusion, ion interaction, and hydrophobic interaction. The method of LC-OCD analysis calculates organic carbon concentrations of biopolymers (e.g. polysaccharides, proteins and amino sugars), humic substances (e.g. fulvic and humic acids), building blocks (hydrolysates of humic substances), low molecular weight (LMW) acids, and neutrals fractions of EfOM based on area integration of the fractional peaks (Huber et al., 2011).

In Chapter 4, the dynamic adsorption behaviour of MTC, activated tyre char and commercial activated carbon for the removal of PRO from aqueous solution under varied operating conditions (e.g. particle size and pH) was investigated with observation of high adsorption of PRO onto MTC. However, to demonstrate the usefulness of fixed-bed column packed with tyre char for industrial applications, large-scale column studies are warranted. Furthermore, saturated adsorbents should be regenerated and reused for economic feasibility. Ball milling

using mechanical energy can be used for mechanochemical degradation of chemical species and regeneration of used adsorbents (Shan et al., 2016).

In spite of ongoing substantial rise in published research on dynamic adsorption for contaminants removal from aqueous solutions, there are just a limited number of studies that investigated the compatibility of the adsorbents for real wastewater treatment and the competitive effect of EfOM on OMPs adsorption (Jaria et al., 2019; Zusman et al., 2020). Although adsorption of EfOM by fixed-bed columns has been reported, differences in adsorption of various fractions of EfOM and the effects of EfOM on transport parameters of OMPs have been hitherto neglected. Therefore, new information on the influence of EfOM on the OMPs removal using adsorbents under fixed-bed column could provide new insights into their management strategies and the development and application of carbon-based fixed-bed columns for removal of EfOM and OMPs from aqueous solutions. In addition, there have been only a few studies on the use of fixed-bed columns in industrial context and determining the key parameters in scaling up the column treatment system (Vilardi et al., 2019). Regeneration and reuse of exhausted adsorbents using green methods, such as ball milling also an area that are yet to be explored (Shan et al., 2016).

The overarching goal of this Chapter is to study the competitive effects of EfOM on PRO adsorption in a fixed-bed column packed with MTC. Specific objective is to investigate the effects of water matrix constituents on the PRO removal using MTC and identified EfOM fractions contributing most to adsorption inhibition on the adsorbent. The effect of EfOM presence on OMPs transport parameters and the adsorption mechanisms of EfOM and OMPs onto MTC were also investigated. Additionally, following specific objectives are explored as part of this chapter:

(i) The applicability of laboratory data as the basis for designing a pilot-scale adsorption column and the effect of important design parameters (contact time, linear velocity and bed

height/diameter ratio) on break through curves (BTCs), and (ii) To determine the practical feasibility of regeneration of MTC using ball milling, with special emphasis on its destruction efficiency, reaction process, final by-products and intermediates, and also the influence of different additives on degradations of PRO.

5.2. Materials and methods

5.2.1. Materials

PRO was purchased from Sigma-Aldrich, New Zealand. All the reagents used in this study were of analytical grade and commercially available. MTC was synthesised according to the procedure discussed in Chapter 3. Tyre char made of ELTs was constructed in a pyrolysis pilot plant by the Irish PGE company in collaboration with the University College of Cork.

5.2.2. Water samples characteristics

The wastewater effluent used in this study was collected from the outlet of Mangere WWTP, located in Auckland, New Zealand. The Mangere WWTP comprises inlet screening, grit tanks, primary sedimentation tanks, clarifiers, filters and UV disinfection. The collected samples, correspond to the UV treated effluent, were stored in dark at a temperature of 2 °C. The samples were characterised by measuring conductivity (WTW meter), pH, TOC (Shimadzu, model TOC-VCPH, SSM-5000A), and UV_{254}. In addition, the background concentrations of PRO were measured and was below the detection limit. Prior to the adsorption experiments, the respective concentrations of PRO were determined, and distilled water and wastewater

samples were spiked to similar PRO concentrations using 1000 mg/L PRO stock solutions.

Characterization results of real wastewater effluents are shown in Table 5.1.

Table 5. 1. Characterization of wastewater effluent.

Parameter	Unit	Value
pH		7.79
UV_{254}	1/m	22.10
Conductivity	mS/cm	0.73
NO_3^-	mg/L	3.90
TOC	mg/L	13.30
Hydrophobic DOC	mg/L	1.79
Hydrophilic DOC	mg/L	9.85
Biopolymers	mg/L	1.39
Humic substances	mg/L	4.72
Building blocks	mg/L	1.71
LMW neutrals	mg/L	2.03
LMW acids	mg/L	<4

5.2.3. Adsorbent characteristics

Brunauer–Emmett–Teller (BET) and Barrett–Joyner–Halenda (BJH) methods was used to determine Specific surface areas, and cumulative pore volumes and pore diameters. Surface electrical properties of the adsorbent was determined using a zeta sizer analyser (Nano ZS90, Malvern, UK). Main physical and chemical properties of MTC is summarised in Table 5.2.

Table 5. 2. Summary of characteristics of MTC (According to Chapter 3) .

Parameter	Value
Carbon (wt. %)	59.45
Hydrogen (wt. %)	1.25
Nitrogen (wt. %)	<0.3
Oxygen (wt. %)	10.13
Sulfur (wt. %)	1.42
Iron (wt. %)	27.45
BET surface area (m^2/g)	49.23
BJH cumulative pore volume (cm^3/g)	2.66
BJH average pore diameter (nm)	19.65
Point of zero charge	4.65

5.2.4. Analytical methods

The concentrations of PRO were measured by liquid chromatography tandem mass spectrometer (LC-MS/MS). LC-MS/MS was carried out on an Eclipse plus C18 column (100×2.1 mm, particle size 3.5 μm) with a linear gradient at 0.2 mL/min from a mixture of 0.1% formic acid in water (mobile phase A) and 100% methanol (mobile phase B). The runtime was 14 min with retention time 7.19 minute. Prior to the analysis, all samples were filtered through 0.20 μm cellulose acetate filters.

In order to characterize EfOM fractions quantitatively and qualitatively, LC-OCD analyses were employed following the method of Huber et al., (2011). A weak cation exchange column ($250mm \times 20$ mm, TSK HW 50S, 3000 theoretical plates, Toso, Japan) with a phosphate buffer

(0.01 M, pH 7) containing 0.1 M of NaCl was used for separation of EfOM fractions by molecular weight, biopolymers (>20,000 g/mol), humic substances (1200-500 g/mol), building blocks (500-350 g/mol), and LMW neutrals (<350 g/mol). Flow rate and injection volume were 1.1 mL/ min and 1 mL, respectively. A software program provided by the manufacturer (ChromCALC, DOC-LABOR, Karlsruhe, Germany) was used for data acquisition and processing, and quantification of each fraction was determined from each chromatogram. Prior to LC-OCD analysis, samples were filtered through 0.45 μm PTFE filters.

5.2.5. Column adsorption experiment

MTC was packed in a plexiglas column (adjustable length 10 cm, inner diameter 1.4 cm) to a bed height of 2.1 cm, containing sand and glass wool. The aqueous solutions containing the 2 mg/L of PRO were operated in up-flow mode at a constant flow rate of 1 mL/min. The flow velocity was maintained using a peristaltic pump (Masterflex®, USA). Treated effluents were collected at set time intervals using a programmable fraction collector (OMNICOLL single channel collector). All experiments were stopped when effluent concentrations became constant with the time.

5.2.6. Amounts adsorbed and partition coefficient

Amounts of the PRO and EfOM adsorbed onto MTC per gram of adsorbent at the saturation time (q_s (mg/g)) in column were calculated from the area above the BTC using the following equation:

$$q_s = \frac{QA}{1000m} = \frac{Q}{1000m} \int_{t=0}^{t=t_s} C_{ad} dt = \frac{Q}{1000m} \int_{t=0}^{t=t_s} (C_0 - C_t) dt \qquad (5.1)$$

Where Q is volumetric flow rate (mL/min), t_s is saturation time (min), C_0 is inlet pharmaceuticals concentration, C_t is the measured pharmaceuticals concentration at the column outlet as a function of time and m is the dry weight of adsorbent (g).

Where Q and t_s are the volumetric flow rate (mL/min) and saturation time (min), respectively. C_0 is inlet pharmaceuticals concentration, C_t is the measured pharmaceuticals concentration at the column outlet as a function of time and m is the dry weight of adsorbent (g). Other useful parameters for the BTCs analysis such as contact time (CT), effluent volume until saturation (V_{eff}) and length of mass transfer zone (MTZ) were determined using following expressions.

$$CT = \frac{V_c}{Q} \tag{5.2}$$

$$V_{eff} = Qt_s \tag{5.3}$$

$$MTZ = h(1 - \frac{t_b}{t_s}) \tag{5.4}$$

where V_c is the adsorbent volume (L) and h is the bed height (cm) and all other terms are as defined earlier.

5.2.7. Modelling

Experimental breakthrough curves were fitted to Non-equilibrium Hydrus-1D model as described in Chapter 4. Chemical non-equilibrium processes in solute transport is represented by two-site chemical non-equilibrium model that is available in Hydrus-1D. This model is based on the assumption that sorption sites can be divided into two fractions, sorption on one fraction of the sites is assumed to be instantaneous and in equilibrium with the solution (S^e), while time-dependent kinetic sorption (S^k) occurs on the second fraction. This model is expressed using the convection–dispersion equation (Šimůnek & van Genuchten, 2008):

$$\frac{\theta \partial c}{\partial t} + \rho \frac{\partial s}{\partial t} = \theta D \frac{\partial^2 c}{\partial z^2} - q \frac{\partial c}{\partial z} \tag{5.5}$$

$$D = \lambda v = \lambda \frac{q}{\theta} \tag{5.6}$$

$$S = S^e + S^k \tag{5.7}$$

$$S^e = f_e \frac{K_d C^\beta}{1 + \eta C^\beta} \tag{5.8}$$

$$\frac{\partial S^k}{\partial t} = \alpha_k [(1 - f_e) K_d C - S^k] \tag{5.9}$$

where C is concentration of the solute (g/cm^3), t is time (min), ρ (g/cm^3) is the medium bulk density, S is the sorbed concentration (g/g), θ is the volumetric water content (cm^3/cm^3), D is dispersion/diffusion coefficient (cm^2/min), q is the volumetric fluid flux density (Darcy's velocity) (cm/min), λ is the longitudinal dispersion coefficient [cm], v is the average pore velocity (cm/min), Z is the distance (cm), f_e (-) is the fraction of equilibrium sites, α_k (1/min) is a first-order rate coefficient, K_d (cm^3/g) is the distribution coefficient, and β and η are adsorption coefficients that determine the shape of isotherm.

5.2.8. Scale-up

In order to investigate the effect of scale-up on pharmaceuticals removal, three scale-up tests (SCL1, SCL2 and SCL 3) were carried based on different geometric (bed height/diameter ratio), kinematic (contact time) and physical (linear velocity) criteria and compared to lab-scale performance. Design of the columns and parameters selected for the experiments are summarised in Table 5.3.

Table 5. 3. Columns design and parameters.

Parameter	Lab SCL	SCL1	SCL2	SCL3
h/d	1.5	0.75	1.5	1.5
CT (min)	3.23	3.23	6.46	3.23
v(cm/min)	0.64	0.64	0.64	1.29
d(cm)	1.4	2.8	2.8	2.8
Q(mL/min)	1	4	4	8
h(cm)	2.1	2.1	4.2	4.2
m(g)	1.5	6	12	12

5.2.9. Valorisation of the exhausted adsorbent

Following the pharmaceutical adsorption experiments and subsequent characterisation, the spent MTC adsorbents were dried at 50 °C for 3 hours. Once dried, the adsorbent was accurately weighed to ~3 g and placed into a 50 cm^3 stainless-steel jar, along with 8 stainless-steel balls (10 mm diameter, 4.0 g each). Once sealed with a stainless-steel lid, the jar was placed into a planetary ball mill (Retsch PM100, Germany) which was operated at 300 rpm or 550 rpm for various time trials. These parameters were selected based on delivering the maximum amount of kinetic energy to the spent MTC adsorbent, creating defects in the matrix, and significantly influencing chemical reactivity. TiO_2 and SiO_2 (quartz sand, 99.2% silica) were used as additives in these trials (300 mg additive per 1 g of adsorbent) to determine any enhanced degradation effects. The directional spinning of the jar was programmed to alternate every 15 minutes to reduce caking on the inside of the jar. All trials were conducted under ambient conditions in air. An appropriate amount of the milled and non-milled adsorbents (0.2 g) were added to 20 mL solvents (water, methanol, acetone) separately in glass centrifuge tubes

and were sonicated for 1 h, followed by shaking in an end-over-end shaker for 24 h to extract the adsorbed PRO from the spent adsorbents. Samples were filtered subsequently through a 0.20 μm cellulose acetate filters and the concentrations of PRO in the extracts were determined by LC-MS/MS as described earlier.

5.3.   Results and discussion

5.3.1. Adsorption of EfOM and PRO from municipal wastewater

The LC-OCD chromatogram of the wastewater sample as influent of column studies is shown in Figure 5.1. The analysis of wastewater sample showed that EfOM contained 1.79 mg/L of hydrophobic fraction and 9.85 mg/L of hydrophilic fraction which comprised of 15.4% and 84.6% of DOC, respectively. The hydrophilic fraction was composed of 4.72 mg/L (40.5%) of humic substances; 2.03 mg/L (17.4%) of LMW neutrals; 1.71 mg/L (14.7%) of building blocks; and 1.39 mg/L (11.9%) of biopolymers. LMW acids were not detected (Table 5.1).

Complete breakthrough of EfOM was obtained after 24 hours which showed the capability of tyre char column in the removal of EfOM. Characterisation of EfOM fractions in column effluents at three different time (1, 8, 16 hour) were carried out using the LC-OCD analysis and shown in Figure 5.2. A close examination of the data in Figure 5.2 suggest that the BTC of DOC increased three-fold (from 0.21 to 0.64) with the increased contact time (from 1 to 16 hour) because of reduced adsorption. The removal of hydrophobic fraction was lower than hydrophilic fraction at the start of the experiment; however, BTCs of both the hydrophobic and hydrophilic fractions reached about 68% after 16 hours. Adsorption of hydrophilic fraction can be explained by ion exchange, surface complexation and hydrogen bonding mechanisms

(Nguyen et al., 2012); while hydrophobic interactions could play an important role in hydrophobic fraction removal (Moreno-Castilla, 2004).

Molecular weight of EfOM and pore size of adsorbents can greatly affect adsorption of EfOM (Newcombe et al., 1997; Karanfil and Kilduff, 1999). Adsorption of EfOM fractions mainly occur in mesopores (2-50 nm width) and large micropores (1-2 nm width) (Summers and Roberts, 1988; Cheng et al., 2005). The average pore size of MTC is 19.65 nm as reported in Table 5.2. As shown in Figure 5.2, removal degree of DOC fractions were based on their molecular weight and followed an order: LMW organics > building blocks > humic substances. This can be attributed to the difficulty of large molecules moving into the micro and meso pores of the adsorbents. Humic substances with high molecular weight (500-1200 g/mole) exhibited the least removal rate and reached 81% breakthrough after 16 hours. However, biopolymers with the highest molecular weight had shown lower breakthrough than building blocks and humic substances which is in contrast with size exclusion effect. Some hydrophobicity-independent mechanisms, such as H-bonding, anion exchange or surface complexation can be reasons for high removal of biopolymers. As LMW neutrals fraction of EfOM access easily to most of MTC pore volume, its adsorption is higher based on its size exclusion effects alone.

The BTCs of the fixed-bed adsorption of PRO onto MTC from wastewater and distilled water are shown in Figure 5.3. Due to competitive effect between PRO molecules and EfOM fractions in wastewater for adsorption sites, steeper curves were observed in wastewater matrix in comparison to distilled water. The presence of EfOM in wastewater caused an inhibition on PRO sorption and decreased its adsorption capacity (5.86 mg/g) compared with PRO adsorption from distilled water (2.03 mg/g). Moreover, both t_b and t_s decreased to 4 hours and 94 hours, respectively in wastewater matrix (Table 5.4). For the numerical simulations, the transport of PRO through MTC adsorbent was predicted well using non-equilibrium Hydrus model (Table 5.5). The fitted Kd value in wastewater was lower than the one corresponding to

the distilled water, indicating less adsorption of PRO in wastewater by MTC. Also, mass transfer coefficient decreased in wastewater matrix that shows a limited mass transfer of PRO from the wastewater to the adsorbent. Low values of the mass transfer coefficients lead to less adsorption due to slower equilibration between the solution and adsorbent (Šimůnek & van Genuchten, 2008).
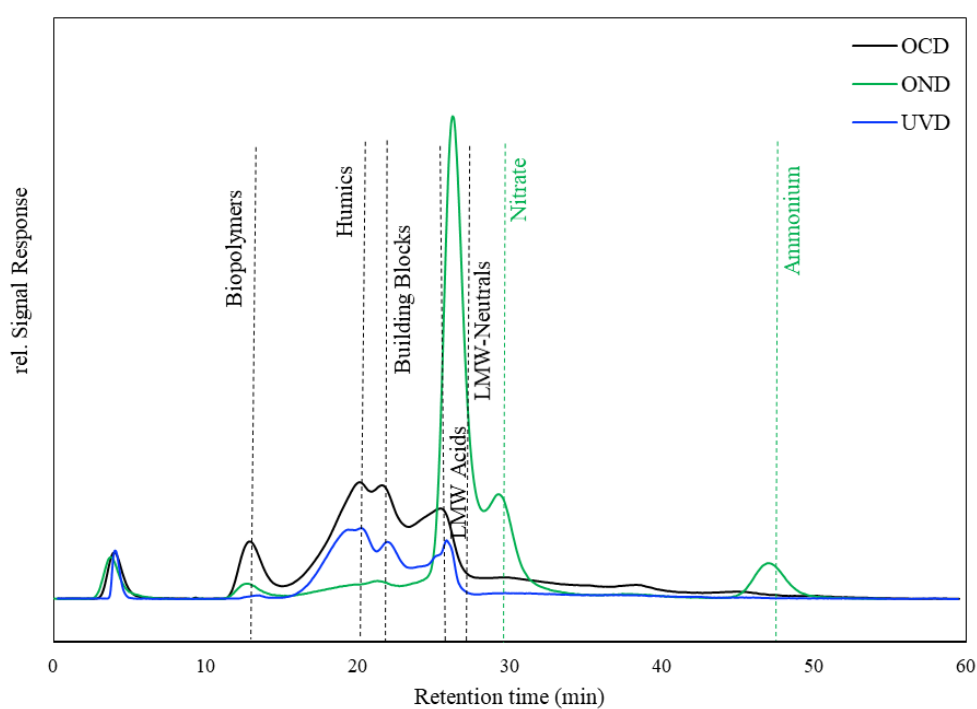
Figure 5. 1. Chromatogram of influent wastewater sample illustrating the different peaks observed by LC-OCD.
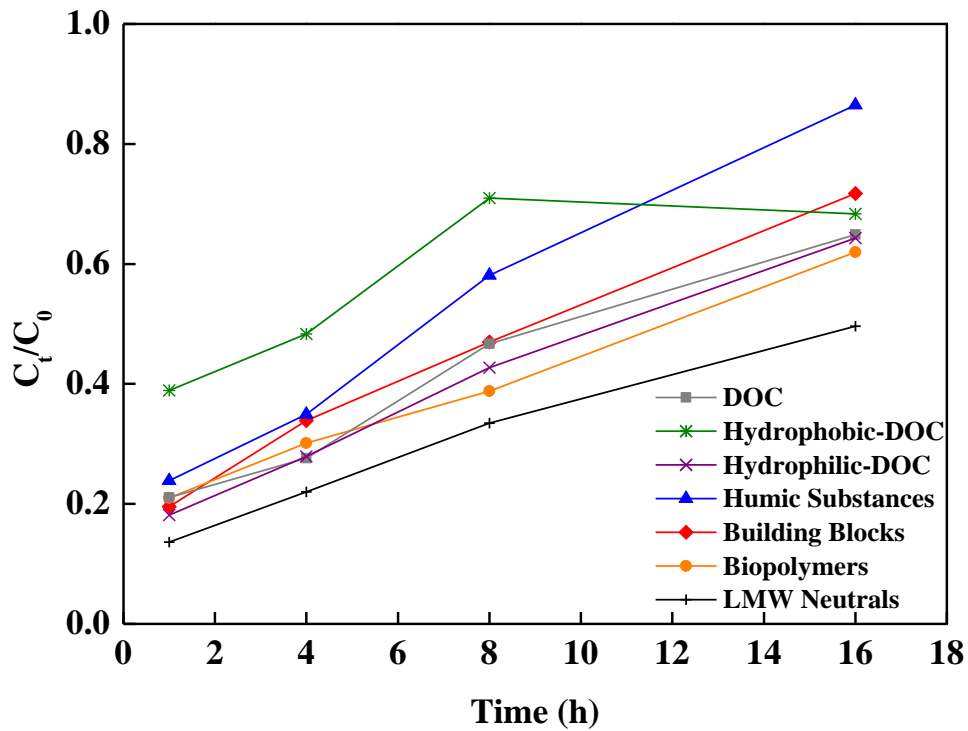
Figure 5. 2. BTCs of EfOM fractions in wastewater effluent.

Figure 5. 3. BTCs and fittings of the experimental data to the Hydrus-lD for the adsorption of PRO onto MTC in distilled water and wastewater.

Table 5. 4. Efficiency and mass transfer parameters determined from the breakthrough curves corresponding to the fixed-bed adsorption of pharmaceuticals onto MTC.

	Q (mL/min)	h (cm)	t_b (hr)	t_s (hr)	$V_{eff\_}$ (L)	q_s (mg/g)	MTZ (cm)
Base Scenario	1	2.1	15.8	193.5	11.61	5.86	1.95
WWTP effluent	1	2.1	4	94.01	5.64	2.03	2.01
SCL1	4	2.1	23.75	212.16	50.92	8.17	1.86
SCL2	4	4.2	136.80	396.00	95.04	12.16	2.74
SCL3	8	4.2	62.70	315.40	151.39	22.58	3.36

Table 5. 5. Fixed and estimated parameters from PRO transport through column using two-site chemical non-equilibrium models in Hydrus-1D for different scenario (f: fixed parameters and e: estimated parameters).

	λ^f (cm)	q^e (cm/min)	K_d^e (cm³/g)	η (cm³/g)	β (-)	α^e (1/min)	f_e^e (-)	R^2 (%)
Base Scenario	0.63	0.51	2381	0.27	0.90	1.27E-03	0.61	0.98
WWTP effluent	0.63	0.59	2255	0.33	0.98	6.20E-04	0.14	0.99
SCL1	0.63	0.56	2431	0.41	0.88	1.53E-03	0.55	0.99
SCL2	0.63	0.69	2596	0.22	0.84	1.51E-03	0.71	0.99
SCL3	0.63	1.21	2485	0.44	0.85	6.62E-03	0.24	0.99

5.3.2. Competition mechanisms between PRO and EfOM

Hydrophobicity and electrical charge of the OMPs can be explained by Log D (distribution coefficient) and pK_a (acid dissociation constant) values that affect OMPs adsorption onto carbon-based adsorbents (Shanmuganathan et al., 2015). Hydrophobic compounds having higher LogD values (>3.2) are more thoroughly adsorbed through hydrophobic interactions than OMPs with lower LogD values. Although PRO has low hydrophobicity (logD = 1.26), its hydrophobic tail (the naphthalene ring) can be adsorbed through hydrophobic interactions. Moreover, OMPs with high pK_a values (>7) are positively charged in wastewater (pH~ 7) and can be highly adsorbed by negatively charged adsorbents through electrostatic interactions. Cationic species of PRO (pK_a~9.42) can be easily attracted onto the adsorbent as the surface of tyre char (pH_{pzc} = 4.65 < solution pH) is negatively charged. In contrast to PRO, EfOM in wastewater is negatively charged due to existence of phenolic groups and carboxylic acid (Perdue and Lytle, 1983; Velten et al., 2011) and electrostatic repulsion can take place between negatively charged EfOM and the adsorbent. Consequently, as the electrostatic attractions cannot play a role in EfOM removal, the principal factor controlling EfOM adsorption is pore size distribution that can compete with PRO adsorption mechanisms and decrease PRO uptake as shown in Figure 5.3. The strongest competitive effects happen by small fractions of EfOM such as LMW neutrals while the least interfering fractions are larger ones like humic substances. As expected from the BTC of PRO in wastewater effluent, rapid increase in Ct/Co during the first hours was observed which can be related to the high competition between PRO and EfOM molecules due to blockage by smaller EfOM fractions. However, the BTC showed reduced EfOM competitiveness that can be attributed to the remaining larger EfOM molecules that are unlikely to compete with PRO molecules.

5.3.3. Scale-up study

The BTCs obtained for larger scale columns for adsorption of PRO onto MTC exhibited similar trend in lab SCL and SCL1, however, had considerably less variation of t_b and t_s. Lower bed height/diameter ratio had a little effect on the BTC and increased the adsorption capacity slightly (from 5.86 to 8.17 mg/g) that could be related to better liquid holdup in SCL1 (Table 5.4). In contrast, higher contact time in SCL2 (keeping the same linear velocity and bed height/diameter ratio) made the shape of BTC flatter and increased t_b (15 to 136.8 hours), t_s (194 to 396 hours) and q_s (5.86 to 12.16 mg/g) substantially. In SCL2, mass transfer and hydrodynamic conditions were kept constant and just contact time was increased. Generally, at higher contact time, the adsorbate molecules obtain a sufficient time to diffuse into the adsorbent and leading to a better uptake. Similar results have been observed and reported by Kumar & Jena (2016). The BTC of SCL3 shifted to the right at a higher linear velocity when contact time and bed height/diameter ratio were kept constant. Results also showed a higher adsorption capacity and a later saturation of the adsorbent in comparison to lab SCL. When the velocity was increased from 0.64 cm/min in lab SCL to 1.29 cm/min in SCL3, the t_s and q_s value increased from 193.5 hours and 5.86 mg/g to 315.4 hours and 22.58 mg/g, respectively (Table 5.4). A plausible explanation for this could be due to higher mass transfer and dispersion at higher velocity (Fernández-González et al., 2019).

Due to the simultaneous existence of several phenomenon (mass transfer and pollutant diffusion and dispersion) in adsorption of contaminants onto carbon-based fixed-bed columns, numerical models considering kinetic and dispersion parameters should be used for higher scale or real field situation. As mentioned in Chapter 4, non-equilibrium Hydrus-1D model was successfully used for modelling the transport of pharmaceuticals onto fixed-bed columns of tyre char. In this study, the scale-up experimental data for PRO removal were modelled by non-equilibrium Hydrus-1D model using dispersion and mass transfer mechanisms to evaluate the

scale-effect and estimate model parameters. All predicted parameters in the small-scale column were then used as input values for the model to simulate larger column experimental data. Results showed that predicted values using non-equilibrium Hydrus-1D model were completely in agreement with scale-up experimental data ($R^2 > 0.98$). The estimated transport parameters using non-equilibrium model are summarised in Table 5.5. The higher mass transfer and dispersion values obtained through modelling SCL3 experimental data confirms the reason for higher adsorption capacity and exhaustion time. Moreover, an increase in K_d value were observed in SCL2 as it is proportional to contact time between PRO and the adsorbent matrix. The modelling results showed the suitability of the non-equilibrium Hydrus-1D model to model the large-lab-scale BTCs of PRO adsorption onto MTC.
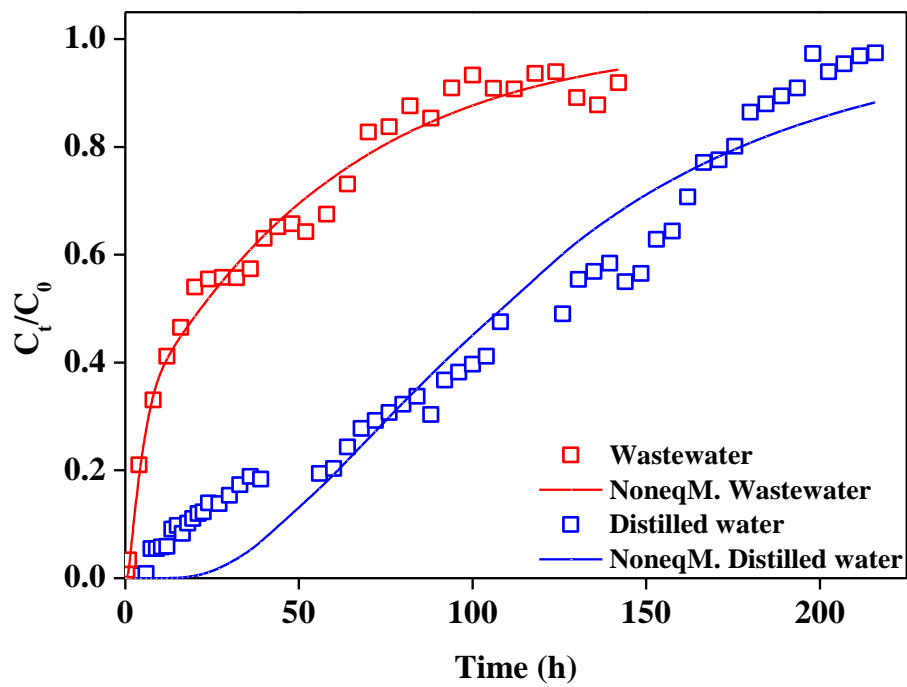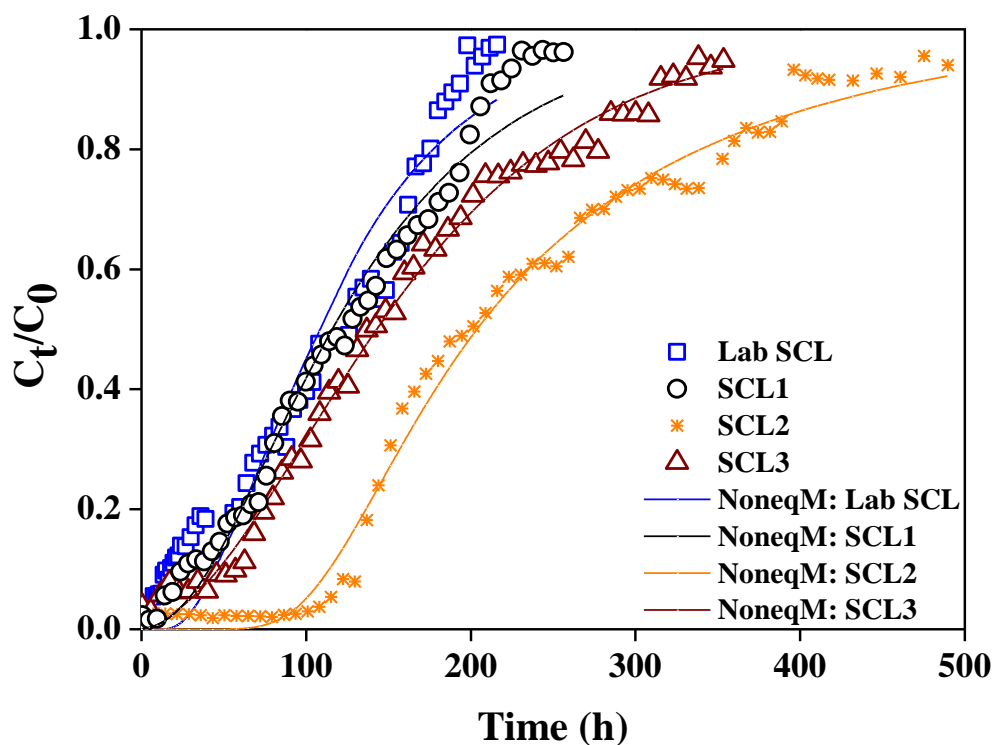

Figure 5. 4. BTCs and fittings of the experimental data to the Hydrus-lD for the adsorption of PRO onto MTC in small and large-lab-scale.

5.3.4. Regeneration of adsorbent

Figure 5.5 indicates the results of the PRO desorption from spent MTC before ball milling using water, methanol and acetone. As the percentage of PRO desorption in water is very low (6%), water was found to be unfavourable for regeneration of MTC. Using acetone for extraction of PRO had a much better performance (61%) than water; however, it is less effective than methanol (76%). Therefore, methanol was selected and used as the most effective solvent for desorption of PRO following ball milling of MTC.
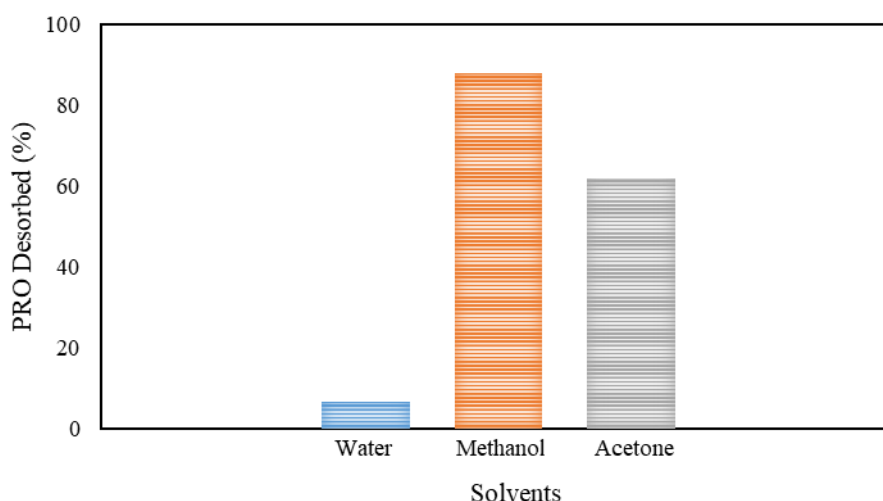
Figure 5.5. Regeneration of PRO saturated MTC using three solvents.

High energy ball milling is a mechanochemical treatment technology which can effectively mineralise organic compounds, including pharmaceuticals, persistent organic pollutants, and polycyclic aromatic hydrocarbons (Cagnetta et al., 2016). In previous studies, ball milling of spent adsorbents has shown high rates of degradation of the target compound (>98%), leading to the regeneration and subsequent reuse of the adsorbent (Shan et al., 2016). Furthermore, spent adsorbents subjected to ball milling conditions exhibit an increase in specific surface area

and oxygen-containing functional groups, which enhance the removal efficiencies of target compounds from water (Lyu et al., 2017; Meng et al., 2019; Pan et al., 2017).

Initially, the rotational settings of the ball mill were varied to determine optimum speed (rpm) for the remainder of the ball milling trials (Table 5.7). After 5 hours milling time at 300 rpm, 46.0% of PRO adsorbed to MTC had degraded, while 5 hours at 550 rpm led to 79.2% PRO degradation (Table 5.7). As such, 550 rpm was chosen as the optimum speed setting for subsequent trials. Figure 5.6 shows the degradation of PRO during mechanochemical treatment of the spent MTC adsorbent at 550 rpm over extended milling times. After 10 hours, quantitative LC-MS/MS analysis revealed 82.8% PRO destruction, following roughly pseudo-first order degradation kinetics. This kinetic rate of degradation aligns with general trends observed during ball milling of other organic compounds (Cagnetta et al., 2017).
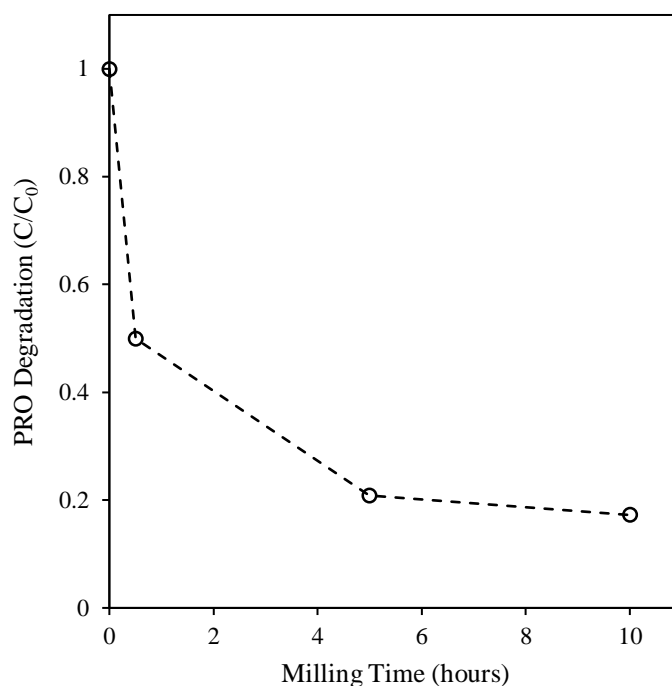
Figure 5.6. Mechanochemical degradation of PRO adsorbed to MTC (550 rpm).

Additives like TiO_2 and SiO_2 are generally used to enhance degradation rates of the target compound. In this case, TiO_2 showed negligible enhanced effect in comparison with the MTC-

only trial, with 81.0% PRO degradation after 5 hours milling. However, the addition of SiO_2 led to a marked increase in PRO degradation after 5 hours milling, with a destruction efficiency of 92.0% (Table 5.7). This enhanced rate of PRO destruction can be attributed to the homolytic cleavage of covalent silica bonds which occurs during mechanochemical collision events, resulting in the generation of silyl (Si$^\bullet$) and siloxyl (Si-O$^\bullet$) radicals on the surfaces of freshly fractured quartz particles (Zhang et al., 2001). These reactive surfaces interact with organic compounds, such as PRO, leading to fragmentation and eventual mineralisation of the target molecule (Yu et al., 2013).
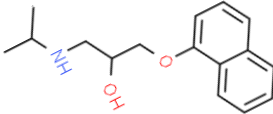
Table 5.6. Effect of speed and additives on mechanochemical degradation efficiencies for PRO.

	Speed		Additive*	
	300 rpm	550 rpm	TiO_2	SiO_2
PRO Degradation (%)	46.0	79.2	81.0	92.0

Degradation intermediates of PRO after ball milling were analysed and investigated by LC-MS/MS (Figure 5.7). Interpretation of MS/MS spectra of PRO after milling and comparisons with the spectra before milling showed that a series of transformation products were generated as shown in Table 5.7. The m/z 274, with the proposed structural composition shown in Figure 5.7, was previously reported as one the photocatalytic degradation by-products of PRO (Li et al., 2019).

Table 5.7. Degradation byproducts of PRO identified by LC-MS/MS.

Compound	Formula	Retention time	Molecule weight	m/z ratios of byproducts	Structure
PRO	$C_{16}H_{21}NO_2$	6.95	259.34	274,318, 338,360,376	

 Ball milling of exhausted adsorbents is not only effective in their regeneration and reusability (Shan et al., 2016), but also it can increase surface area and oxygen containing functional groups of adsorbents enabling increased removal efficiency as reported in some studies (Lyu et al., 2017).

Table 5.7. Degradation byproducts of PRO identified by LC-MS/MS.
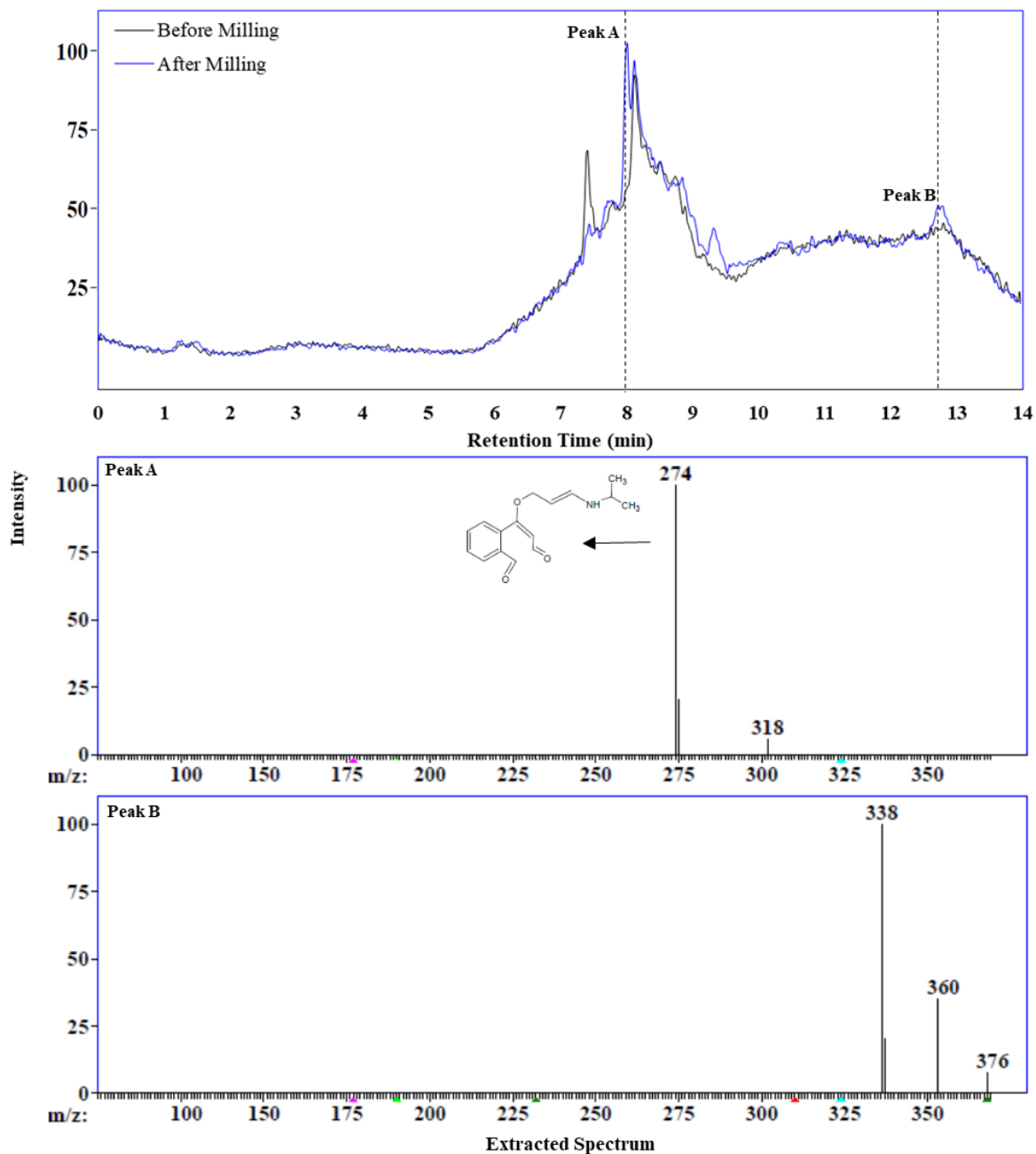
Figure 5.7. The MS/MS spectra of PRO after milling.

5.4. Conclusion and Environmental Significance

The impact of the competitive adsorption of EfOM fractions and PRO molecules in urban wastewater onto a tyre-based adsorbent packed in a fixed-bed column was studied in this Chapter. Various EfOM components in real water samples were characterized using LC-OCD

approach. Compared to distilled water, the adsorption of PRO onto adsorbent decreased (5.86 to 2.03 mg/g) in real wastewater sample which can be attributed to its competitive effects with EfOM fractions. Molecular weight of EfOM fractions played an important role in their removal. The smaller fractions of EfOM like LMW organics provoked more competition with other fractions; however, larger molecules like humic substances had least removal rate. Higher removal of biopolymer fraction than humic substances can be related to other adsorption mechanisms, such as H-bonding, anion exchange or surface complexation. Hydrophobic effect and electrostatic attraction can be the main adsorption mechanisms of PRO onto MTC. In a larger scale column, the effect of contact time, linear velocity and bed height/diameter ratio on breakthrough and adsorption capacity of PRO on MTC were investigated. Higher adsorption capacity in larger scale column was obtained when the linear velocity increased from 0.64 to 1.29 cm/min, which was attributed to higher mass transfer and dispersion at higher linear velocity. In addition, increasing contact time (3.23 to 6.46 min) led to ~two-fold adsorption capacity (5.86 to 12.16 mg/g) and longer breakthrough time (15 to 136.8 hours) due to having more time for diffusion of adsorbate molecules into adsorbent.

Efficiency of non-equilibrium Hydrus model for simulating the breakthrough of scaled-up columns was tested and fundamental transport properties, such as mass transfer and dispersion coefficient were evaluated. The results demonstrated that Hydrus-1D model could fit the experimental data well. Ball milling study showed excellent performance for the degradation of PRO and regeneration of exhausted adsorbent. 92% of adsorbed PRO was degraded after milling for 5 hours at the speed of 500 rpm and presence of quartz sand (SiO_2).

Despite many studies presently reported that biochar has an excellent capacity for removal of organic pollutants from aqueous solutions, biochar still is an untapped technology for water remediation. In order to bring application of biochar technology into schedule, more persuasive

studies such scale-up, regeneration of exhausted biochars and its application for real water and wastewater treatment are required.

Inadequate information on pilot-scale, small and large scale biochar-based systems to show their feasibility and performance compared to conventional systems and also lack of enough information on design parameters and operating conditions has impeded the application of biochar for water and wastewater treatment. Bulk of existing studies are on batch adsorption experiments and there is limited literature on scaled up fixed-bed columns especially using appropriate and reliable numerical modelling. Scale-up information used for validation of models can be further utilized for subsequent scale-up and predicting breakthrough at unknown operating conditions which will be major advance. In addition, biochar's capacity for contaminants removal from real multi-component aqueous solutions has not been reported in many past studies.

Presence of different organic and inorganic contaminants with different concentrations make the adsorption process more challenging and complex. Understanding the process is important for developing design parameters for biochar-based water treatment technologies. Moreover, feasible and environmentally friendly techniques for regeneration of spent biochars are still lacking. As biochars have a finite capacity for adsorption, therefore their reuse and regeneration is necessary for economic, environmental and energy benefits. An effective, environmentally friendly and economical regeneration method, such as ball milling technology, can avoid entering new pathways of pollutants which are desorbed in some regeneration studies to the environment.

Consequently, validated protocols for application of biochar for water remediation and its regeneration are yet to be developed. Addressing these knowledge gaps, limitations and uncertainties may dispel negative public perceptions and create further research and supportive

policy framework to unlock the application of biochar in removing contaminants from water bodies.

CHAPTER 6: Summary, conclusions, and recommendations for future studies

6.1. Summary and significant findings

This thesis introduces a novel, environmentally friendly and low-cost magnetic char derived from waste tyres for remediating wastewater. The research presents ELTs pyrolysis and converting them to tyre char as an adsorbent for removal of pharmaceuticals in batch and fixed-bed column experiments, followed by modelling and scale-up designing, techno-economic feasibility assessment and regeneration of exhausted adsorbents.

Chapters 3, 4 and 5 provide details of the major contributions of this thesis. In Chapter 3, synthesis, characterisation and application of MTC for batch adsorption of three selected pharmaceuticals, CIP, PRO and CLO in aqueous solution was investigated. CIP, PRO and CLO are considered as emerging contaminants and are frequently detected in different aqueous environment. The occurrence and fate of these pharmaceuticals in waterbodies are considered as one of the emerging issues because they can have toxic effects on human health and environment. Among various water treatment methods, adsorption technology is considered as the best one due to its advantages such as low-cost, high efficiency, and simple operation and design. The adsorbent used in this study was from waste tyres. Durability of waste tyres has made their disposal as one of the major environmental issues worldwide. TC was obtained from pyrolysis of ELTs in a continuous-operation pilot plant at TRL 7 and then magnetised by chemical co-precipitation of Fe^{3+}/Fe^{2+} at TRL 3. SEM-EDS, BET, elemental analysis, VSM, FTIR, and zeta potential were used for characterisation of TC and MTC. The surface area of TC increased after magnetisation and MTC showed higher adsorption capacities for all three compounds compared to TC. Adsorption mechanisms of CIP, PRO and CLO onto MTC were investigated using FTIR and zeta potential. Cation-π, π-π EDA, cation exchange, electrostatic interactions and hydrophobic effect were shown to be the main mechanisms for the adsorption of the pharmaceuticals onto the adsorbent. Additional adsorption experiments analysing the

effects of environmental parameters such as pH and ionic strength showed high dependence of pharmaceutical adsorption on pH and high adsorption capacities were obtained at low ionic strength. Techno-economic feasibility study demonstrated tyre char as a feasible substitute for activated carbon. This ELTs based low-cost magnetic adsorbent (estimated at $299/tonne) can be potentially used at full-scale industrial wastewater treatment for elimination of drugs from aqueous solutions, offering sustainable environmental remediation. However, there is a need to perform fixed-bed column studies to obtain practical information in terms of breakthrough curves and demonstrate the effectiveness of this adsorbent in industrial applications. Analysing this information using appropriate models is useful for calculating the design parameters in real-life applications and identifying the best operating conditions in columns packed with adsorbents. Moreover, development of more efficient adsorbents for water and wastewater treatment is required to replace commercial activated carbons.

Therefore, Chapter 4 focuses on dynamic adsorption of the pharmaceuticals in a fixed-bed column packed with MTC, ATC and CAC. The breakthrough curves corresponding to the adsorption of PRO at different operational conditions (initial concentration, flow rate and bed height), adsorbent particle size and presence of competitive pharmaceuticals were determined. ATC with high surface area (453.81 m^2/g) was prepared by thermal and chemical activation of TC with surface area (38.17 m^2/g). The removal efficiency of ATC was found to be comparable with CAC. The Hydrus model that incorporates chemical non-equilibrium process was utilised to predict the pharmaceutical transport through fixed-bed columns and investigate the key process controlling their removal. Efficiency of commonly used fixed-bed models (Adams-Bohart, Thomas, Yoon-Nelson) and Hydrus-1D model was tested and compared. Techno-economic feasibility of a fixed-bed column packed with tyre char for wastewater treatment has been also briefly discussed in this chapter. Future research should be directed in seeking design and development of effective fixed-bed columns for real wastewater treatment at pilot and

industrial scales, as well as various aspects of scaling up of fixed-bed columns should be covered. Additionally, novel adsorbents should be utilisedfor treating real wastewater which contains different contaminants such as EfOM. In addition, to make the adsorption process more economical, there is a demand to regenerate and reuse exhausted adsorbents using environmentally friendly and effective techniques.

For the above reasons, Chapter 5 demonstrates the competitive effect of EfOM on adsorption of a MOP, PRO, onto MTC packed in a fixed-bed column. EfOM present in real wastewater was characterized and monitored during adsorption onto MTC using LC-OCD technique. Different fractions of EfOM named as biopolymers, humic substances, building blocks, LMM neutrals and LMM acids were quantified and distinguished based on relative molecular weights. Process scale-up studies were also carried out in this chapter utilising the lab-scale optimization values in larger scale columns. The impact of important design parameters such as contact time, linear velocity and bed height/diameter ratio on breakthrough and adsorption capacity of MTC were tested. Non-equilibrium Hydrus model which considers dispersion and mass transfer mechanism was used to simulate the transport of PRO in a fixed-bed column and investigate the effect of scale-up on transport parameters. Regeneration of MTC using ball milling technology also was demonstrated in this study as an effective and green technique for recovery of spent adsorbents. Quartz sand was used as a cheap and efficient additive to increase the degradation of PRO adsorbed onto the adsorbent.

6.2. Conclusions

In this thesis, development of a novel and cost-effective magnetic tyre char as effective adsorbent for the removal of three selected pharmaceuticals in aqueous solution was demonstrated. The major findings of this study are drawn as follows:

- The surface area and micropore volume of tyre char increased after magnetisation.

- MTC showed higher adsorption efficiency for all three pharmaceuticals, 85%, 90% and 92% for CIP, PRO and CLO respectively.

- Pseudo-second order kinetic and Freundlich isotherm models best described the adsorption of the pharmaceuticals onto MTC. Maximum adsorption capacities of 6.94, 6.6 and 10.55 mg/g were obtained for CIP, PRO and CLO, respectively.

- Solution pH had a great effect on adsorption efficiency of the pharmaceuticals onto MTC, with maximum adsorption at pH 7 for CIP and pH 9 for PRO and CLO. The removal efficiency of the compounds were more favourable at lower concentrations of ionic strength.

- Cation-π, π-π EDA, cation exchange, electrostatic repulsion and hydrophobic effect were shown as main adsorption mechanisms for adsorption of pharmaceuticals onto MTC, confirmed by the FTIR and zeta potential analyses.

- Tyre char was shown to be economically viable with the estimated cost of 299 US\$/tonne which is much lower than commercial activated carbon.

- Thermal and chemical activation of tyre char increased its surface area about twelve-fold (38.17 to 453.81 m^2/g). The adsorption capacity of ATC also was much higher than TC and comparable to commercial activated carbon which can be related to high surface area of ATC.

- In the fixed-bed column experiments, higher bed height of adsorbent and solution pH increased adsorption of PRO on MTC. Ball milled nano particles size of adsorbent and lower flow rate were shown to be very effective in the removal rate of PRO. In the single solution, adsorption capacity of pharmaceuticals followed an order CLO>PRO>CIP. Compared to single solution, the presence of other pharmaceuticals in the ternary solution decreased the adsorption capacity of all compounds which can be related to the competitive effects for adsorption onto adsorbent sites. In both single and ternary solution, CIP had lower adsorption capacity than PRO and CLO that can be related to the lack of electrostatic attractions at solution pH (7).

- Hydrus model which incorporates chemical non-equilibrium process successfully predicted the transport of all three pharmaceuticals ($0.97 < R^2 < 0.99$). However, the equilibrium Hydrus model and also other common models such as Adams–Bohart, Thomas and Yoon–Nelson did not fit the experimental data well. This shows the importance of considering non-equilibrium processes, mass transfer, and hydrodynamic dispersion in modelling the transport of contaminants in fixed-bed columns which were considered in non-equilibrium Hydrus model.

- The unit cost for treatment of wastewater by a tyre char fixed-bed column was estimated to be 1.57 US\$/m^3 which shows it as a commercially feasible technology for wastewater treatment.

- Compared to PRO adsorption in aqueous solution, the competitive effects of different fractions of EfOM in real wastewater decreased the adsorption capacity of PRO into MTC from 5.86 to 2.03 mg/g. Based on the characterization of EfOM components using LC-OCD technique, pore size distribution was determined the main factor affecting the adsorption of EfOM fractions. Humic Substances had the least removal rate while low molecular weight neutrals were the most interfering fraction. Hydrophobic effect and

electrostatic attraction were shown to be the main potential adsorption mechanisms for adsorption of PRO onto MTC.

- Contact time, linear velocity and bed height/diameter ratio as important design parameters were determined to be effective in scale-up purposes. Higher linear velocity and contact time increased adsorption capacity and breakthrough time of PRO in the fixed-bed column packed with MTC. Lower bed height/diameter ratio did not change removal rate and breakthrough time as much as the other two parameters. Non-equilibrium Hydrus model was demonstrated to fit the experimental data in larger columns well and was validated for subsequent scale-up purposes under unknown operating conditions.

- Ball milling was shown as an efficient and green method for degradation of adsorbed PRO onto the adsorbent and recovery of spent adsorbent. 79% of PRO was degraded after milling for 5 hours at 550 rpm and then it increased to 92% after addition of quartz sand. This increase can be attributed to presence of free Si– or SiO–radicals as the breakdown of SiO_2 structure which react with organic compounds and speed up mechanochemical reactions.

6.3. Recommendations for future studies

Despite successful application of magnetic tyre char for adsorption of CIP, PRO and CLO in aqueous solution under static and dynamic mode, further questions have been arisen about its application in water treatment. Therefore, more information is needed, and the following recommendations have been identified for future:

- Results of adsorption mechanisms in batch studies may be extended and confirmed with carrying out more characterisation tests such as X-ray photoelectron microscopy (XPS) and X-Ray Diffraction (XRD) before and after adsorption to provide more insights into the adsorption mechanisms involved.

- It has been demonstrated that predicting the transport of pharmaceuticals with equilibrium model was not satisfactory while the two-site chemical non-equilibrium model predicted the experimental data well. More accurate simulations may be obtained considering both physical and chemical non-equilibrium processes in Hydrus model. Suitability of other numerical models that incorporate mass transfer, diffusion and dispersion mechanisms in modelling the transport of contaminants should be tested and compared with non-equilibrium Hydrus model.

- There is little information on scale-up of fixed-bed columns packed with carbon-based adsorbent for contaminants removal from water solutions. Larger scale columns with different design parameters should be utilised to assess the effect of scale-up. Full-scale adsorption systems including series of column should be tested to have higher efficiency for industrial purposes.

- Given the complex nature of EfOM, comprehensive EfOM characterization approaches such as fluorescence excitation and emission matrices (FEEM) should be employed to reveal EfOM behaviour better during adsorption process.

- A more detailed regeneration study using ball milling may be warranted to investigate mechanisms of degradation and potential degradation pathways of pharmaceuticals with different physiochemical properties. Degradation using different additives may be further explored. Moreover, the effect of ball milling on adsorption capacity of regenerated adsorbent should be investigated and magnetisation of magnetic adsorbents after ball milling for future application should be tested.

- A more complete and an in-depth techno economic feasibly study using tyre char for wastewater treatment should be carried out to make the project more pliable in the future. The cost of the magnetisation and modification process and their utilisation for removal of contaminants from aqueous solutions should be accounted. Assessment of the economic and technical viability of adsorbents regeneration using ball milling should be carried out for full-scale applications.

Appendices

Appendix A
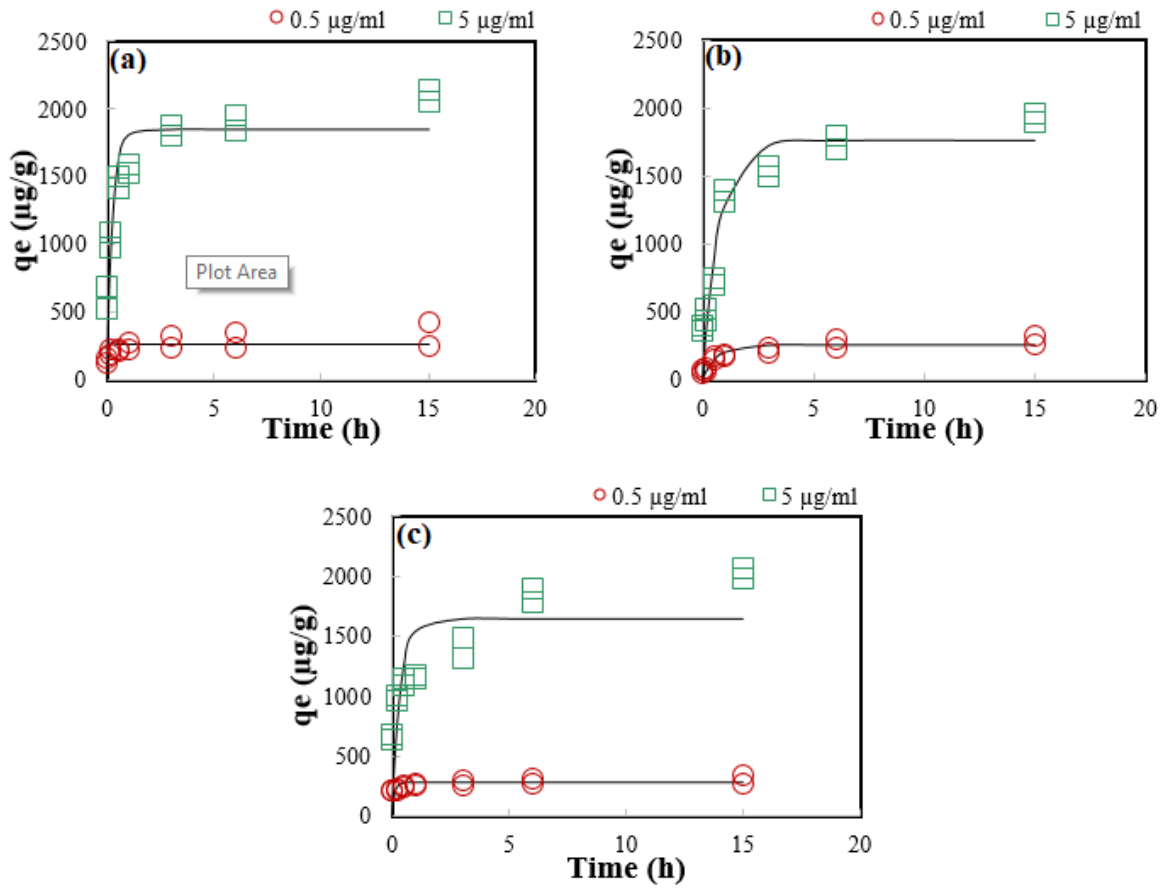
Figure A.1. Adsorption kinetics of CIP (a), PRO (b) and CLO (c) onto MTC fitted with Pseudo-first-order kinetics.
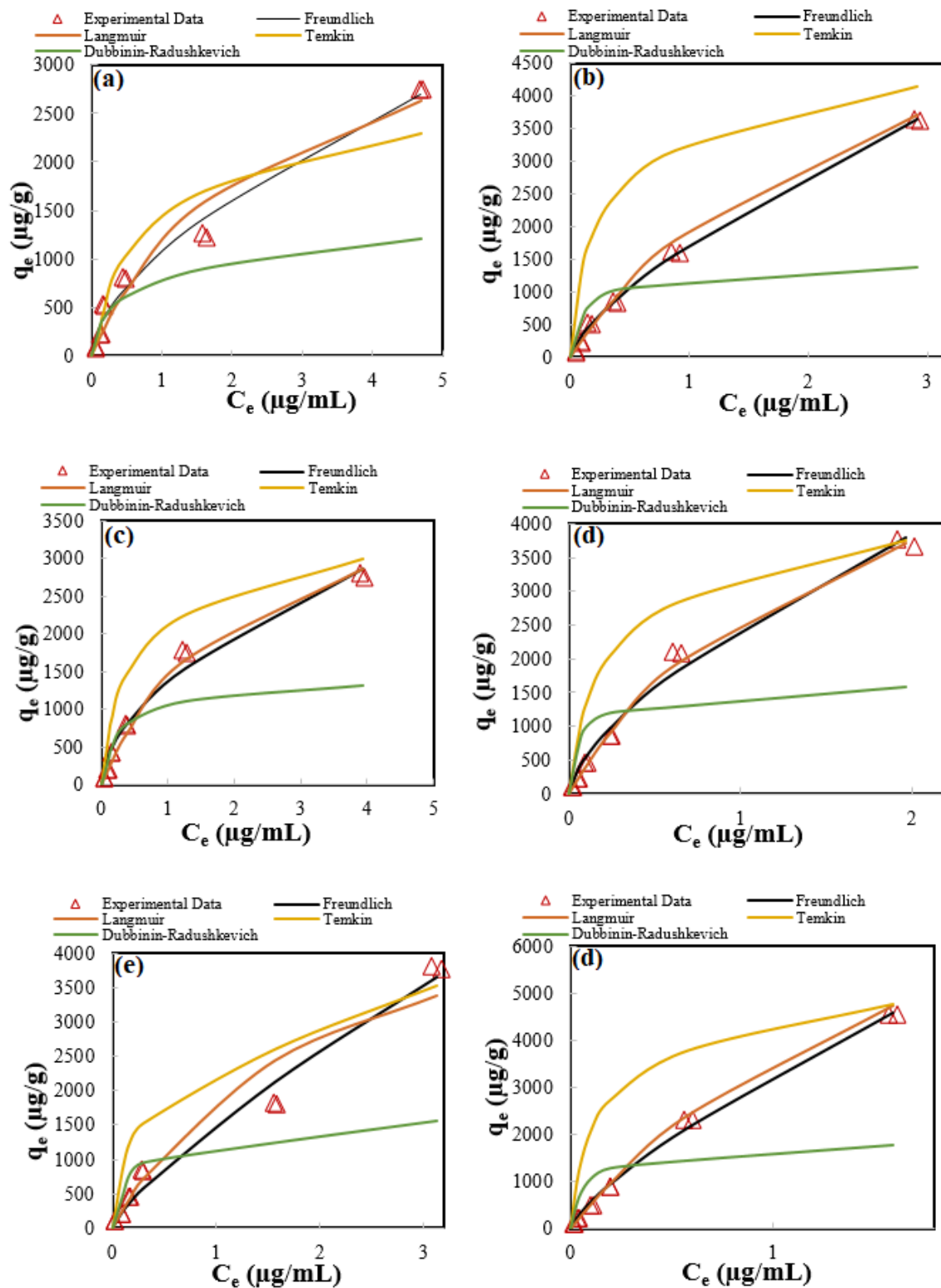
Figure A.2. Multi-concentration adsorption isotherms of CIP onto TC (a), CIP onto MTC (b), PRO onto TC (a), PRO onto MTC (b) CLO onto TC and CLO onto MTC (c) fitted with Freundlich, Langmuir, Temkin and Dubinin-Radushkevich isotherm models.

Appendix B

Techno-economic feasibility of this study

Published data and manufacturers quotes determine the base equipment costs. In this study, the equipment cost for pilot plant is US$ 120,000. Capital costs for the plant was determined based on the costs related to the major pieces of base equipment. Capital cost was estimated based on both direct costs (a building factor, piping and instrumentation factor, a site improvement factor, and a utilities factor) and indirect costs (covering engineering costs and construction overheads). The direct plant cost was calculated by multiplying a piping and instrumentation factor, a structure and building factor, a site improvement factor, and a utilities factor, 15%, 25%, 15% and 20% of base equipment costs, respectively. Indirect cost was determined by multiplying factor of 30% of direct costs, and then was added to direct plant cost to give the fixed capital investment (*FCI*). All factors related to direct and indirect plant cost were obtained from Elliott et al., 1990 and Islam et al., 2011. Start-up costs (10% of *FCI*) and working capital (5% of *FCI*) were added to the FCI to obtain Total Capital Requirement (TCR) for the plant.

To calculate annualised capital cost (*ACC*), annuity method was used to obtain distributed-levelled capital charge equally which is represented in Eq. (1):

$$ACC = \frac{TCR}{\{1-(1+I)^{-N}\}} \times I \qquad \text{(B.1)}$$

I is the interest rate and *N* is the plant life time.

According to the Table 5, percentages of the *FCI* found from previous studies (Aden et al., 2002, Elliott et al., 1990) were used to calculate fixed operating costs including maintenance, overheads and, taxes and insurance. Current wage rate in New Zealand is 11.74 USD/h, and 7 Shift operators were involved in the pilot-scale plant. Feedstock price, interest rate, electricity

price and general overhead factor which covers safety, general engineering, general plant maintenance, payroll overhead (including benefits), plant security, phone, light, heat and plant communications are given in the Table 3.5.

Appendix C

Breakthrough curves modelling

For modelling the fate and transport of pharmaceuticals in a column packed with tyre char, two-site chemical non-equilibrium model implemented into HYDRUS-1D was used. Solute transport in numerical models is usually described using the relatively standard advection–dispersion equation as described below:

$$\frac{\theta \partial C}{\partial t} + \rho \frac{\partial S}{\partial t} = \theta D \frac{\partial^2 C}{\partial Z^2} - q \frac{\partial C}{\partial Z} \qquad (C.1)$$

$$D = \lambda \nu = \lambda \frac{q}{\theta} \qquad (C.2)$$

where C is concentration of the solute (g/cm^3), t is time (min), ρ (g/cm^3) is the medium bulk density, S is the sorbed concentration (g/g), θ is the volumetric water content (cm^3/cm^3), D is dispersion/diffusion coefficient (cm^2/min), q is the volumetric fluid flux density (Darcy's velocity) (cm/min), λ is the longitudinal dispersion coefficient (cm), ν the average pore velocity (cm/min) and Z is the distance (cm).

HYDRUS-1D considers a general nonlinear sorption equation that can be simplified into a Langmuir or Freundlich isotherm (Šimůnek et al., 2008).

$$S = \frac{K_d C^\beta}{1 + \eta C^\beta} \qquad (C.3)$$

where K_d (cm^3/g) is the distribution coefficient, and β and η are adsorption coefficients that can be best represented by the isotherm model. When $\beta=1$, the adsorption becomes the Langmuir, when $\eta=0$, the equation becomes the Freundlich, and when both $\beta=1$ and $\eta=0$, it leads to a linear adsorption.

The two-site assumes that the sorption on one fraction of the sorption sites is instantaneous, while kinetic sorption occurs on the second fraction.

$$S = S^e + S^k \tag{C.4}$$

$$S^e = f_e \frac{K_d C^\beta}{1 + \eta C^\beta} \tag{C.5}$$

$$\frac{\partial S^k}{\partial t} = \alpha_k [(1 - f_e) K_d C - S^k] \tag{C.6}$$

where, f_e (-) is the fraction of equilibrium sites, and α_k (1/min) is a first-order rate coefficient. Other terms are as described earlier.

Levenberg–Marquardt algorithm was used for inverse parameters estimation in Hydrus 1-D model. The numerical solution of the advective-dispersive transport equation for different boundaries and initial conditions is carried out in Hydrus 1-D model. The upper and bottom boundary conditions in this study were a concentration flux at the inlet and a zero-concentration gradient at the outlet, respectively. In addition, the adsorbents inside the column were assumed exempt of solute concentration, and constant water contents that were equal to the porosity of adsorbents were considered in the model.

A value of longitudinal dispersivity was determined through inverse estimation using BTCs of the conservative tracer and then was considered constant for pharmaceuticals transport. The initial used volumetric fluid fluxes (q: cm/min) which were obtained by dividing flow rate to column cross-sectional area (cm2), have been adjusted in order to fit the experimental lead BTCs. The other parameters (K_d, β, η, f_e and α_k), were obtained through inverse simulation.

Appendix D

Analyses of CIP, PRO and CLO

A new and accurate multi-residue analytical method was developed and validated for the determination of Ciprofloxacin (CIP), a broad-spectrum antibiotic, Propranolol (PRO), one of the most common beta-blockers detected in water bodies, and Clomipramine (CLO), which is among the most widely prescribed antidepressants, in synthetic wastewater using liquid chromatography/tandem mass spectrometry (LC/MS–MS). Simultaneous detection and identification of these three organic compounds in environmental samples have not been studied to date. The analytes were determined in the positive mode electrospray ionisation (ESI). These pharmaceuticals were analysed using a C18 column (100×2.1 mm, particle size 3.5 μm). Ultra-pure water acidified with 0.1 % volume of formic acid and 100% methanol were used as mobile phases, at a flow rate of 0.2 mL min−1 and a temperature of 40 °C. Sample injection volume was set at 1 μL and retention times were 5.77, 6.97 and 7.79 minutes for CIP, PRO and CLO, respectively. Optimised collision energy for CIP's daughter compounds was -19 and -35 eV, for PRO's daughter compounds was -17 and -18 eV, and for CLO's daughter compounds was -40 and -21 eV. The detection limit for all three compounds is 2 ppb. This new analytical methodology can be used for the further research on the fate, occurrence and distribution of these pharmaceuticals in aqueous environmental matrices.

Appendix E

Error Analysis

The average percentage errors (ε%) are used to show the fit between the experimental and modelling values of C_t/C_0 used for plotting breakthrough curves and they are calculated according to equation (1) (Malkoc, Nuhoglu, & Abali, 2006):

$$\varepsilon = \frac{\sum_{i=1}^{N}[(\left(\frac{C_t}{C_0}\right)_{exp} - \left(\frac{C_t}{C_0}\right)_{model})/\left(\frac{C_t}{C_0}\right)_{exp}]}{n} \times 100 \qquad (E.1)$$

The correlation coefficient (R^2) is a measure of analytical accuracy and its value is within the range of $0 < R^2 \leq 1$, where higher values shows a better fit. R^2 can be mathematically determined as (Islam et al., 2017):

$$R^2 = 1 - \frac{\sum_{i=1}^{n}(\frac{C_t}{C_0}_{exp} - \frac{C_t}{C_0}_{model})^2}{\sum_{i=1}^{n}(\frac{C_t}{C_0}_{exp})^2 - [\frac{(\sum_{i=1}^{n}\frac{C_t}{C_0}_{exp})^2}{n}]} \qquad (E.2)$$

The root-mean-square error (*RMSE*) is also used to judge the models. A smaller value for RMSE reflects an accurate analysis. This error can be expressed as follows (Largitte & Pasquier, 2016):

$$RMSE = \sqrt{\frac{1}{n}\sum_{i=1}^{n}(\frac{C_t}{C_0}_{exp} - \frac{C_t}{C_0}_{model})^2} \qquad (E.3)$$

Chi square (X^2) is also used to evaluate the best fit model. Smaller values of X^2 also indicates a better fit of the model. The X^2 value was calculated by equation below. (Munagapati & Kim, 2016):

$$X^2 = \sum_{i=1}^{n}\frac{(\frac{C_t}{C_0}_{exp} - \frac{C_t}{C_0}_{model})^2}{\frac{C_t}{C_0}_{model}} \qquad (E.4)$$

In the all equations, *n* is the number of measurements, and C_t/C_{0exp} and C_t/C_{0model} are the experimental and modelling values of relative concentration, respectively.

Appendix F
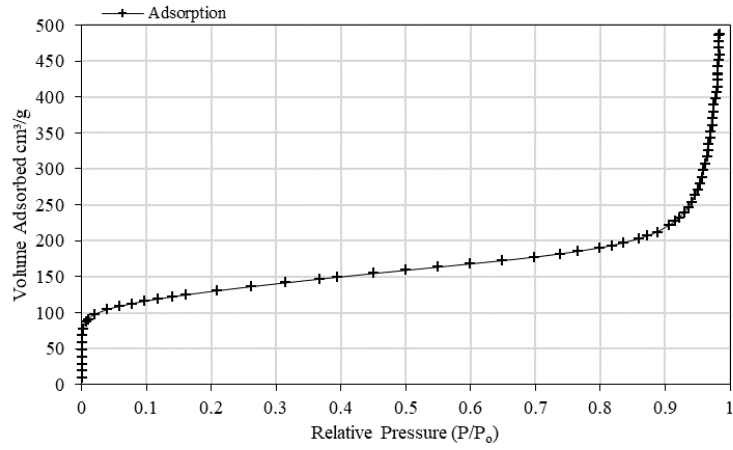
Figure. F.1. Nitrogen adsorption isotherms at 77 K for ATC (P/P0 is the partial pressure of nitrogen and the adsorbed gas onto ATC is measured as a function of P/P0).
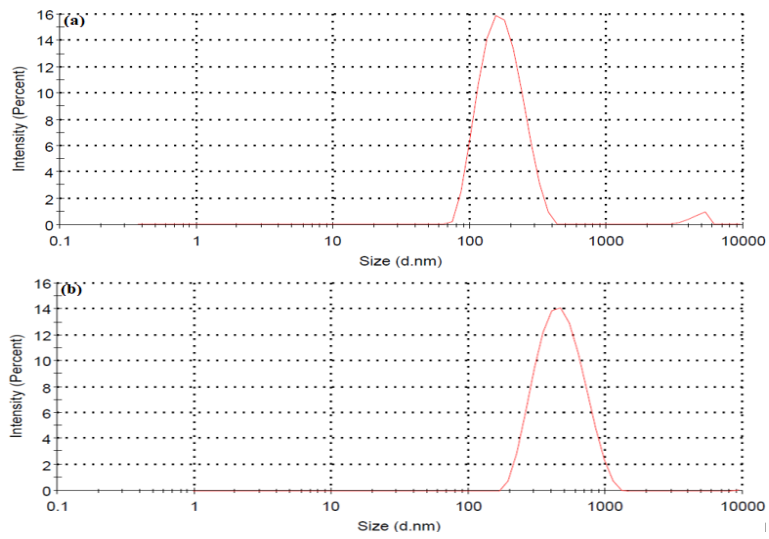
Figure. F.2. Size distribution by volume (a: 100-500 nm and b: 500-1000 nm).
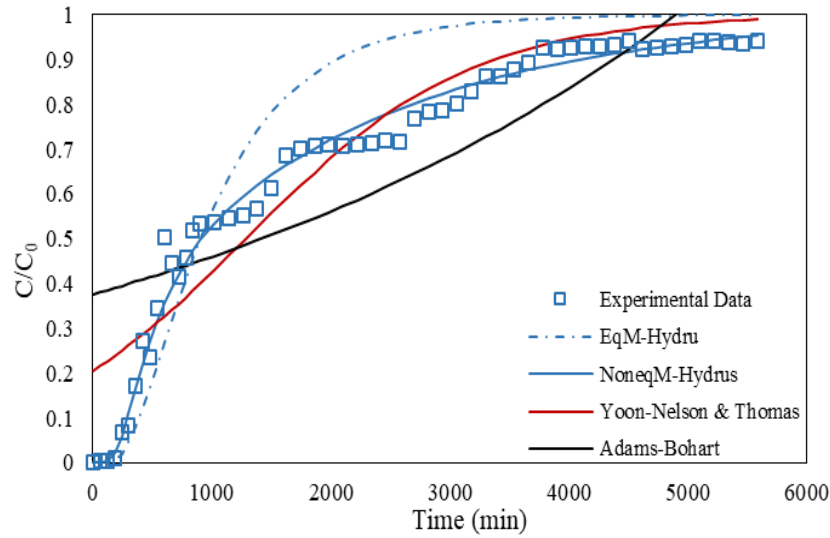
Figure. F.3. Breakthrough curves and fittings of the experimental data to the Hydrus-lD, Yoon–Nelson, Thomas, and Adams-Bohart for the adsorption of PRO onto MTC.

Table F.1. Fixed and estimated parameters from the conservative tracer transport through column using the equilibrium model in Hydrus-1D (f: fixed parameters; e: estimated parameters; c: calculated parameters).

Adsorbent	λ^e (cm)	q^e (cm/min)	θ^f (cm³/cm³)	D^c (cm²/min)	R^2
MTC	0.63	1.53	0.39	2.47	0.98
ATC	0.74	1.65	0.42	2.91	0.99
CAC	0.44	1.41	0.46	1.35	0.98

Table F.2. Error analysis for different models

Models	RMSE	X^2	R^2	ε (%)
Adams–Bohart	0.26	4.52	0.47	14.8
Thomas	0.15	2.29	0.83	8.74
Yoon–Nelson	0.15	2.29	0.83	8.74
Hydrus-NonEq	0.05	0.95	0.98	0.25
Hydrus-Eq	0.21	4.40	0.65	68.35

References

Abdelbassit, M. S., Popoola, S. A., Saleh, T. A., Abdallah, H. H., Al-Saadi, A. A., & Alhooshani, K. R. (2020). DFT and Kinetic Evaluation of Chloromethane Removal Using Cost-Effective Activated Carbon. *Arabian Journal for Science and Engineering*. https://doi.org/10.1007/s13369-020-04458-x

Acevedo, B., Rocha, R. P., Pereira, M. F. R., Figueiredo, J. L., & Barriocanal, C. (2015). Adsorption of dyes by ACs prepared from waste tyre reinforcing fibre. Effect of texture, surface chemistry and pH. *Journal of Colloid and Interface Science*, *459*, 189–198. https://doi.org/10.1016/j.jcis.2015.07.068

Acosta, R., Fierro, V., Martinez de Yuso, A., Nabarlatz, D., & Celzard, A. (2016). Tetracycline adsorption onto activated carbons produced by KOH activation of tyre pyrolysis char. *Chemosphere*, *149*, 168–176. https://doi.org/10.1016/j.chemosphere.2016.01.093

Adio, S. O., Asif, M., Mohammed, A. R. I., Baig, N., Al-Arfaj, A. A., & Saleh, T. A. (2019). Poly (amidoxime) modified magnetic activated carbon for chromium and thallium adsorption: Statistical analysis and regeneration. *Process Safety and Environmental Protection*, *121*, 254–262. https://doi.org/10.1016/j.psep.2018.10.008

Afzal, M. Z., Sun, X. F., Liu, J., Song, C., Wang, S. G., & Javed, A. (2018). Enhancement of ciprofloxacin sorption on chitosan/biochar hydrogel beads. *Science of the Total Environment*, *639*, 560–569. https://doi.org/10.1016/j.scitotenv.2018.05.129

Ahmad, M., Lee, S. S., Dou, X., Mohan, D., Sung, J. K., Yang, J. E., & Ok, Y. S. (2012). Effects of pyrolysis temperature on soybean stover- and peanut shell-derived biochar properties and TCE adsorption in water. *Bioresource Technology*, *118*, 536–544. https://doi.org/10.1016/j.biortech.2012.05.042

Ahmad, M., Rajapaksha, A. U., Lim, J. E., Zhang, M., Bolan, N., Mohan, D., … Ok, Y. S. (2014). Biochar as a sorbent for contaminant management in soil and water: A review. *Chemosphere*, *99*, 19–23. https://doi.org/10.1016/j.chemosphere.2013.10.071

Ahmed, M. B., Zhou, J. L., Ngo, H. H., Guo, W., & Chen, M. (2016). Progress in the preparation and application of modified biochar for improved contaminant removal from water and wastewater. *Bioresource Technology*, *214*, 836–851. https://doi.org/10.1016/j.biortech.2016.05.057

Ahmed, M. J., & Hameed, B. H. (2018). Removal of emerging pharmaceutical contaminants by adsorption in a fixed-bed column: A review. *Ecotoxicology and Environmental Safety*, *149*(December 2017), 257–266. https://doi.org/10.1016/j.ecoenv.2017.12.012

Akhtar, A., & Sarmah, A. K. (2018). Novel biochar-concrete composites: Manufacturing, characterization and evaluation of the mechanical properties. *Science of the Total Environment*, *616–617*, 408–416. https://doi.org/10.1016/j.scitotenv.2017.10.319

Al-Degs, Y. S., El-Barghouthi, M. I., El-Sheikh, A. H., & Walker, G. M. (2008). Effect of solution pH, ionic strength, and temperature on adsorption behavior of reactive dyes on activated carbon. *Dyes and Pigments*, *77*(1), 16–23. https://doi.org/10.1016/j.dyepig.2007.03.001

Ali, I., Asim, M., & Khan, T. A. (2012). Low cost adsorbents for the removal of organic

pollutants from wastewater. *Journal of Environmental Management*, *113*, 170–183. https://doi.org/10.1016/j.jenvman.2012.08.028

Álvarez, P. M., Beltrán, F. J., Gómez-Serrano, V., Jaramillo, J., & Rodríguez, E. M. (2004). Comparison between thermal and ozone regenerations of spent activated carbon exhausted with phenol. *Water Research*, *38*(8), 2155–2165. https://doi.org/10.1016/j.watres.2004.01.030

Antoniou, N., Stavropoulos, G., & Zabaniotou, A. (2014). Activation of end of life tyres pyrolytic char for enhancing viability of pyrolysis - Critical review, analysis and recommendations for a hybrid dual system. *Renewable and Sustainable Energy Reviews*, *39*, 1053–1073. https://doi.org/10.1016/j.rser.2014.07.143

Antoniou, N., & Zabaniotou, A. (2018). Re-designing a viable ELTs depolymerization in circular economy: Pyrolysis prototype demonstration at TRL 7, with energy optimization and carbonaceous materials production. *Journal of Cleaner Production*, *174*, 74–86. https://doi.org/10.1016/j.jclepro.2017.10.319

Antoniou, Nikos, & Zabaniotou, A. (2015). Experimental proof of concept for a sustainable End of Life Tyres pyrolysis with energy and porous materials production. *Journal of Cleaner Production*, *101*, 1–14. https://doi.org/10.1016/j.jclepro.2015.03.101

Arabani, M., Mirabdolazimi, S. M., & Sasani, A. R. (2010). The effect of waste tire thread mesh on the dynamic behaviour of asphalt mixtures. *Construction and Building Materials*, *24*(6), 1060–1068. https://doi.org/10.1016/j.conbuildmat.2009.11.011

Ariyadejwanich, P., Tanthapanichakoon, W., Nakagawa, K., Mukai, S. ., & Tamon, H. (2003). Preparation and characterization of mesoporous activated carbons from waste tyre. *Carbon*, *7*(3), 474–478. https://doi.org/10.1002/apj.544

Avcı, A., İnci, İ., & Baylan, N. (2019). A Comparative Adsorption Study with Various Adsorbents for the Removal of Ciprofloxacin Hydrochloride from Water. *Water, Air, and Soil Pollution*, *230*(10). https://doi.org/10.1007/s11270-019-4315-6

Azman, A., Ngadi, N., Khairunnisa, D., Zaini, A., Jusoh, M., & Arsad, A. (2019). Effect of Adsorption Parameter on the Removal of Aspirin Using Tyre Waste Adsorbent, *7*(August 2018), 157–162. https://doi.org/10.3303/CET1972027

Bagheri, H., Roostaie, A., & Baktash, M. Y. (2014). A chitosan-polypyrrole magnetic nanocomposite as μ-sorbent for isolation of naproxen. *Analytica Chimica Acta*. https://doi.org/10.1016/j.aca.2014.01.028

Baral, S. S., Das, N., Ramulu, T. S., Sahoo, S. K., Das, S. N., & Chaudhury, G. R. (2009). Removal of Cr(VI) by thermally activated weed Salvinia cucullata in a fixed-bed column. *Journal of Hazardous Materials*, *161*(2–3), 1427–1435. https://doi.org/10.1016/j.jhazmat.2008.04.127

Barlaz, M. A., Eleazer, W. E., & Whittle, D. J. (1993). Potential To Use Waste Tires as Supplemental Fuel in Pulp and Paper Mill Boilers, Cement Kilns and in Road Pavement. *Waste Management Research*, *11*(6), 463–480.

Baskaran, S., Bolan, N. S., Rahman, A., & Tillman, R. W. (1996). Non-equilibrium sorption during the movement of pesticides in soils. *Pesticide Science*, *46*(4), 333–343. https://doi.org/10.1002/(SICI)1096-9063(199604)46:4<333::AID-PS361>3.0.CO;2-A

Basta, A. H., Fierro, V., El-Saied, H., & Celzard, A. (2009). 2-Steps KOH activation of rice

straw: An efficient method for preparing high-performance activated carbons. *Bioresource Technology*, *100*(17), 3941–3947. https://doi.org/10.1016/j.biortech.2009.02.028

Beesley, L., & Marmiroli, M. (2011). The immobilisation and retention of soluble arsenic, cadmium and zinc by biochar. *Environmental Pollution*, *159*(2), 474–480. https://doi.org/10.1016/j.envpol.2010.10.016

Briones, R. M., & Sarmah, A. K. (2019). Sorption and mobility of metformin and guanylurea in soils as affected by biosolid amendment: Batch and column tests. *Environmental Pollution*, *244*, 19–27. https://doi.org/10.1016/j.envpol.2018.10.025

Brown, R. (2012). Biochar production technology. In *Biochar for Environmental Management: Science and Technology* (pp. 127–146). https://doi.org/10.4324/9781849770552

Buchner, G. A., Stepputat, K. J., Zimmermann, A. W., & Schomäcker, R. (2019). Specifying Technology Readiness Levels for the Chemical Industry. *Industrial and Engineering Chemistry Research*, *58*(17), 6957–6969. https://doi.org/10.1021/acs.iecr.8b05693

Caceres-Jensen, L., Rodríguez-Becerra, J., Sierra-Rosales, P., Escudey, M., Valdebenito, J., Neira-Albornoz, A., … Villagra, C. A. (2019). Electrochemical method to study the environmental behavior of Glyphosate on volcanic soils: Proposal of adsorption-desorption and transport mechanisms. *Journal of Hazardous Materials*, *379*(April), 120746. https://doi.org/10.1016/j.jhazmat.2019.120746

Cagnetta, G., Robertson, J., Huang, J., Zhang, K., & Yu, G. (2016). Mechanochemical destruction of halogenated organic pollutants: A critical review. *Journal of Hazardous Materials*, *313*, 85–102. https://doi.org/10.1016/j.jhazmat.2016.03.076

Cagnetta, G., Zhang, Q., Huang, J., Lu, M., Wang, B., Wang, Y., … Yu, G. (2017). Mechanochemical destruction of perfluorinated pollutants and mechanosynthesis of lanthanum oxyfluoride: A Waste-to-Materials process. *Chemical Engineering Journal*, *316*, 1078–1090. https://doi.org/10.1016/j.cej.2017.02.050

Calisto, V., Ferreira, C. I. A., Santos, S. M., Gil, M. V., Otero, M., & Esteves, V. I. (2014). Production of adsorbents by pyrolysis of paper mill sludge and application on the removal of citalopram from water. *Bioresource Technology*, *166*, 335–344. https://doi.org/10.1016/j.biortech.2014.05.047

Carabineiro, S. A. C., Thavorn-Amornsri, T., Pereira, M. F. R., & Figueiredo, J. L. (2011). Adsorption of ciprofloxacin on surface-modified carbon materials. *Water Research*, *45*(15), 4583–4591. https://doi.org/10.1016/j.watres.2011.06.008

Carmosini, N., & Lee, L. S. (2009). Ciprofloxacin sorption by dissolved organic carbon from reference and bio-waste materials. *Chemosphere*, *77*(6), 813–820. https://doi.org/10.1016/j.chemosphere.2009.08.003

Chen, B., Chen, Z., & Lv, S. (2011). A novel magnetic biochar efficiently sorbs organic pollutants and phosphate. *Bioresource Technology*, *102*(2), 716–723. https://doi.org/10.1016/j.biortech.2010.08.067

https://doi.org/10.1016/j.biortech.2010.08.067

Cheng, W., Dastgheib, S. A., & Karanfil, T. (2005). Adsorption of dissolved natural organic

matter by modified activated carbons. *Water Research*, *39*(11), 2281–2290. https://doi.org/10.1016/j.watres.2005.01.031

Chia, C.H., Downie, A., Munroe, P. (2015). Characteristics of Biochar: Physical and Structural Properties. In: Biochar for Environmental Management: Science. Technology Technology and Implementation, p. 89.

Choi, J. W., Zhao, Y., Bediako, J. K., Cho, C. W., & Yun, Y. S. (2018). Estimating environmental fate of tricyclic antidepressants in wastewater treatment plant. *Science of the Total Environment*, *634*, 52–58. https://doi.org/10.1016/j.scitotenv.2018.03.278

Choy, K. K. H., Barford, J. P., & McKay, G. (2005). Production of activated carbon from bamboo scaffolding waste - Process design, evaluation and sensitivity analysis. *Chemical Engineering Journal*, *109*(1), 147–165. https://doi.org/10.1016/j.cej.2005.02.030

Chu, K. H. (2010). Fixed bed sorption: Setting the record straight on the Bohart-Adams and Thomas models. *Journal of Hazardous Materials*, *177*(1–3), 1006–1012. https://doi.org/10.1016/j.jhazmat.2010.01.019

Danalıoğlu, S. T., Bayazit, Ş. S., Kerkez Kuyumcu, Ö., & Salam, M. A. (2017). Efficient removal of antibiotics by a novel magnetic adsorbent: Magnetic activated carbon/chitosan (MACC) nanocomposite. *Journal of Molecular Liquids*, *240*, 589–596. https://doi.org/10.1016/j.molliq.2017.05.131

Darweesh, T. M., & Ahmed, M. J. (2017a). Adsorption of ciprofloxacin and norfloxacin from aqueous solution onto granular activated carbon in fixed bed column. *Ecotoxicology and Environmental Safety*, *138*(November 2016), 139–145. https://doi.org/10.1016/j.ecoenv.2016.12.032

Darweesh, T. M., & Ahmed, M. J. (2017b). Batch and fixed bed adsorption of levofloxacin on granular activated carbon from date (Phoenix dactylifera L.) stones by KOH chemical activation. *Environmental Toxicology and Pharmacology*, *50*, 159–166. https://doi.org/10.1016/j.etap.2017.02.005

Das, O., Sarmah, A. K., & Bhattacharyya, D. (2015). A novel approach in organic waste utilization through biochar addition in wood/polypropylene composites. *Waste Management*, *38*(1), 132–140. https://doi.org/10.1016/j.wasman.2015.01.015

Davidson, J. M., & McDougal, J. R. (1973). Experimental and Predicted Movement of Three Herbicides in a Water-Saturated Soil. *Journal of Environmental Quality*. https://doi.org/10.2134/jeq1973.00472425000200040003x

De Andrade, J. R., Oliveira, M. F., Da Silva, M. G. C., & Vieira, M. G. A. (2018). Adsorption of Pharmaceuticals from Water and Wastewater Using Nonconventional Low-Cost Materials: A Review. *Industrial and Engineering Chemistry Research*, *57*(9), 3103–3127. https://doi.org/10.1021/acs.iecr.7b05137

de Franco, M. A. E., de Carvalho, C. B., Bonetto, M. M., de Pelegrini Soares, R., & Féris, L. A. (2018). Diclofenac removal from water by adsorption using activated carbon in batch mode and fixed-bed column: Isotherms, thermodynamic study and breakthrough curves modeling. *Journal of Cleaner Production*, *181*, 145–154. https://doi.org/10.1016/j.jclepro.2018.01.138

de Franco, M. A. E., de Carvalho, C. B., Bonetto, M. M., Soares, R. de P., & Féris, L. A. (2017). Removal of amoxicillin from water by adsorption onto activated carbon in batch process and fixed bed column: Kinetics, isotherms, experimental design and breakthrough curves modelling. *Journal of Cleaner Production*, *161*, 947–956. https://doi.org/10.1016/j.jclepro.2017.05.197

De Gisi, S., Lofrano, G., Grassi, M., & Notarnicola, M. (2016). Characteristics and adsorption capacities of low-cost sorbents for wastewater treatment: A review. *Sustainable Materials and Technologies*, *9*, 10–40. https://doi.org/10.1016/j.susmat.2016.06.002

de Toledo, R. A., Hin Chao, U., Shen, T., Lu, Q., Li, X., & Shim, H. (2018). Development of hybrid processes for the removal of volatile organic compounds, plasticizer, and pharmaceutically active compound using sewage sludge, waste scrap tires, and wood chips as sorbents and microbial immobilization matrices. *Environmental Science and Pollution Research*. https://doi.org/10.1007/s11356-018-2877-2

Delgado, L. F., Charles, P., Glucina, K., & Morlay, C. (2012). The removal of endocrine disrupting compounds, pharmaceutically activated compounds and cyanobacterial toxins during drinking water preparation using activated carbon-A review. *Science of the Total Environment*, *435–436*, 509–525. https://doi.org/10.1016/j.scitotenv.2012.07.046

Deng, Y., Li, Y., Nie, W., Gao, X., Zhang, L., Yang, P., & Tan, X. (2019). Fast removal of propranolol from water by attapulgite/graphene oxide magnetic ternary composites. *Materials*, *16*(6). https://doi.org/10.3390/ma12060924

Deng, Y., Wu, F., Liu, B., Hu, X., & Sun, C. (2011). Sorptive removal of β-blocker propranolol from aqueous solution by modified attapulgite: Effect factors and sorption mechanisms. *Chemical Engineering Journal*. https://doi.org/10.1016/j.cej.2011.09.057

Devi, P., & Saroha, A. K. (2014). Synthesis of the magnetic biochar composites for use as an adsorbent for the removal of pentachlorophenol from the effluent. *Bioresource Technology*, *169*, 525–531. https://doi.org/10.1016/j.biortech.2014.07.062

Dieter, H. H., & Mückter, H. (2007). Assessment of so called organic trace compounds in drinking water from the regulatory, health and aesthetic-quality points of view, with special consideration given to pharmaceuticals. *Bundesgesundheitsblatt - Gesundheitsforschung - Gesundheitsschutz*, *50*(3), 322–331. https://doi.org/10.1007/s00103-007-0158-1

Dittmar, S., Zietzschmann, F., Mai, M., Worch, E., Jekel, M., & Ruhl, A. S. (2018). Simulating Effluent Organic Matter Competition in Micropollutant Adsorption onto Activated Carbon Using a Surrogate Competitor. *Environmental Science and Technology*, *52*(14), 7859–7866. https://doi.org/10.1021/acs.est.8b01503

Ebele, A. J., Abou-Elwafa Abdallah, M., & Harrad, S. (2017). Pharmaceuticals and personal care products (PPCPs) in the freshwater aquatic environment. *Emerging Contaminants*, *3*(1), 1–16. https://doi.org/10.1016/j.emcon.2016.12.004

El-Shafey, E. S. I., Al-Lawati, H., & Al-Sumri, A. S. (2012). Ciprofloxacin adsorption from aqueous solution onto chemically prepared carbon from date palm leaflets. *Journal of Environmental Sciences (China)*, *24*(9), 1579–1586. https://doi.org/10.1016/S1001-0742(11)60949-2

Emma Giltrowa, Paul D. Ecclesa, b, Matthew J. Winterc, P. J. M., & Mariann Rand-Weaverb, Thomas H. Hutchinsond, J. P. S. (2010). Chronic effects assessment and plasma concentrations of the _-blocker. https://doi.org/10.1016/j.aquatox.2009.09.002

Engelhardt, I., Sittig, S., Šimůnek, J., Groeneweg, J., Pütz, T., & Vereecken, H. (2015). Fate of the antibiotic sulfadiazine in natural soils: Experimental and numerical investigations. *Journal of Contaminant Hydrology*, *177–178*, 30–42. https://doi.org/10.1016/j.jconhyd.2015.02.006

Erdem, C. U., Ateia, M., Liu, C., & Karanfil, T. (2020). Activated carbon and organic matter characteristics impact the adsorption of DBP precursors when chlorine is added prior to GAC contactors. *Water Research*, *184*. https://doi.org/10.1016/j.watres.2020.116146

Estrada-Arriaga, E. B., Cortés-Muñoz, J. E., González-Herrera, A., Calderón-Mólgora, C. G., de Lourdes Rivera-Huerta, M., Ramírez-Camperos, E., … García-Sánchez, L. (2016). Assessment of full-scale biological nutrient removal systems upgraded with physico-chemical processes for the removal of emerging pollutants present in wastewaters from Mexico. *Science of the Total Environment*, *571*, 1172–1182. https://doi.org/10.1016/j.scitotenv.2016.07.118

European Environment Agency. (2009). Diverting waste from landfill: Effectiveness of waste management policies in the European Union, (7), 1–68.

Fan, Y., Wang, B., Yuan, S., Wu, X., Chen, J., & Wang, L. (2010). Adsorptive removal of chloramphenicol from wastewater by NaOH modified bamboo charcoal. *Bioresource Technology*, *101*(19), 7661–7664. https://doi.org/10.1016/j.biortech.2010.04.046

Fels, M., Pegg,M. (2008). A techno-economic and environmental assessment of a tire pyrolysis plant. Reported from the Dalhousie University, Halifax, NS, Canada.

Fernández-González, R., Martín-Lara, M. A., Moreno, J. A., Blázquez, G., & Calero, M. (2019). Effective removal of zinc from industrial plating wastewater using hydrolyzed olive cake: Scale-up and preparation of zinc-Based biochar. *Journal of Cleaner Production*, *227*, 634–644. https://doi.org/10.1016/j.jclepro.2019.04.195

Ferrari, B., Mons, R., Vollat, B., Fraysse, B., Pax??us, N., Lo Giudice, R., … Garric, J. (2004). Environmental risk assessment of six human pharmaceuticals: Are the current environmental risk assessment procedures sufficient for the protection of the aquatic environment? *Environmental Toxicology and Chemistry*, *23*(5), 1344–1354. https://doi.org/10.1897/03-246

Filloux, E., Gallard, H., & Croue, J. P. (2012). Identification of effluent organic matter fractions responsible for low-pressure membrane fouling. *Water Research*, *46*(17), 5531–5540. https://doi.org/10.1016/j.watres.2012.07.034

Fong, P. P., & Ford, A. T. (2014). The biological effects of antidepressants on the molluscs and crustaceans: A review. *Aquatic Toxicology*, *151*, 4–13. https://doi.org/10.1016/j.aquatox.2013.12.003

Fu, H., Ding, D., Sui, Y., Zhang, H., Hu, N., Li, F., … Wang, Y. (2019). Transport of uranium(VI) in red soil in South China: influence of initial pH and carbonate concentration. *Environmental Science and Pollution Research*, *26*(36), 37125–37136. https://doi.org/10.1007/s11356-019-06644-3

G. Nałe$cz-Jawecki, K. Wadhia, B. Adomas,A.I. Piotrowicz-Cies´lak, J. S. (2010). Application of Microbial Assay for Risk Assessment Biotest in Evaluation of Toxicity of Human and Veterinary Antibiotics. *Environmental Toxicology*, *165*(April), 16. https://doi.org/10.1002/tox

Gao, H., Lv, S., Dou, J., Kong, M., Dai, D., Si, C., & Liu, G. (2015). The efficient adsorption removal of Cr(vi) by using Fe3O4 nanoparticles hybridized with carbonaceous materials. *RSC Advances*, *5*(74), 60033–60040. https://doi.org/10.1039/c5ra10236g

Gao, X., Song, J., Zhang, D., Rong, Y., & Sui, H. (2021). Design of horizontal ball mills for

improving the rate of mechanochemical degradation of DDTs. *Powder Technology*, *380*, 246–255. https://doi.org/10.1016/j.powtec.2020.11.069

Giebułtowicz, J., & Nałecz-Jawecki, G. (2014). Occurrence of antidepressant residues in the sewage-impacted Vistula and Utrata rivers and in tap water in Warsaw (Poland). *Ecotoxicology and Environmental Safety*, *104*(1), 103–109. https://doi.org/10.1016/j.ecoenv.2014.02.020

Godoy, A. A., Kummrow, F., & Pamplin, P. A. Z. (2015). Occurrence, ecotoxicological effects and risk assessment of antihypertensive pharmaceutical residues in the aquatic environment - A review. *Chemosphere*, *138*, 281–291. https://doi.org/10.1016/j.chemosphere.2015.06.024

González, O., Justo, A., Bacardit, J., Ferrero, E., Malfeito, J. J., & Sans, C. (2013). Characterization and fate of effluent organic matter treated with UV/H2O2 and ozonation. *Chemical Engineering Journal*, *226*, 402–408. https://doi.org/10.1016/j.cej.2013.04.066

Grover, D. P., Zhou, J. L., Frickers, P. E., & Readman, J. W. (2011). Improved removal of estrogenic and pharmaceutical compounds in sewage effluent by full scale granular activated carbon: Impact on receiving river water. *Journal of Hazardous Materials*, *185*(2–3), 1005–1011. https://doi.org/10.1016/j.jhazmat.2010.10.005

Gupta, A., & Garg, A. (2019). Adsorption and oxidation of ciprofloxacin in a fixed bed column using activated sludge derived activated carbon. *Journal of Environmental Management*, *250*(August), 109474. https://doi.org/10.1016/j.jenvman.2019.109474

Gupta, H. (2018). Anthracene removal from water onto activated carbon derived from vehicular tyre. *Separation Science and Technology (Philadelphia)*, *53*(4), 613–625. https://doi.org/10.1080/01496395.2017.1405038

Gupta, V. K., Gupta, B., Rastogi, A., Agarwal, S., & Nayak, A. (2011a). A comparative investigation on adsorption performances of mesoporous activated carbon prepared from waste rubber tire and activated carbon for a hazardous azo dye-Acid Blue 113. *Journal of Hazardous Materials*, *186*(1), 891–901. https://doi.org/10.1016/j.jhazmat.2010.11.091

Gupta, V. K., Gupta, B., Rastogi, A., Agarwal, S., & Nayak, A. (2011b). Pesticides removal from waste water by activated carbon prepared from waste rubber tire. *Water Research*, *45*(13), 4047–4055. https://doi.org/10.1016/j.watres.2011.05.016

Gupta, Vinod Kumar, Nayak, A., Agarwal, S., & Tyagi, I. (2014). Potential of activated carbon from waste rubber tire for the adsorption of phenolics: Effect of pre-treatment conditions. *Journal of Colloid and Interface Science*, *417*, 420–430. https://doi.org/10.1016/j.jcis.2013.11.067

Gwenzi, W., & Chaukura, N. (2018). Organic contaminants in African aquatic systems: Current knowledge, health risks, and future research directions. *Science of the Total Environment*, *619–620*, 1493–1514. https://doi.org/10.1016/j.scitotenv.2017.11.121

Gwenzi, W., Chaukura, N., Noubactep, C., & Mukome, F. N. D. (2017). Biochar-based water treatment systems as a potential low-cost and sustainable technology for clean water provision. *Journal of Environmental Management*, *197*, 732–749. https://doi.org/10.1016/j.jenvman.2017.03.087

Hadi, P., Yeung, K. Y., Guo, J., Wang, H., & McKay, G. (2016). Sustainable development of tyre char-based activated carbons with different textural properties for value-added

applications. *Journal of Environmental Management*, *170*, 1–7. https://doi.org/10.1016/j.jenvman.2016.01.005

Hakimi Mohd Shaid, M. S., Zaini, M. A. A., & Nasri, N. S. (2019). Evaluation of methylene blue dye and phenol removal onto modified CO2-activated pyrolysis tyre powder. *Journal of Cleaner Production*, *223*. https://doi.org/10.1016/j.jclepro.2019.03.097

Hanna, K., Rusch, B., Lassabatere, L., Hofmann, A., & Humbert, B. (2010). Reactive transport of gentisic acid in a hematite-coated sand column: Experimental study and modeling. *Geochimica et Cosmochimica Acta*, *74*(12), 3351–3366. https://doi.org/10.1016/j.gca.2010.03.022

Heo, J., Yoon, Y., Lee, G., Kim, Y., Han, J., & Park, C. M. (2019). Enhanced adsorption of bisphenol A and sulfamethoxazole by a novel magnetic CuZnFe2O4–biochar composite. *Bioresource Technology*, *281*(December 2018), 179–187. https://doi.org/10.1016/j.biortech.2019.02.091

Hu, Y., Zhu, Y., Zhang, Y., Lin, T., Zeng, G., Zhang, S., … Long, H. (2019). An efficient adsorbent: Simultaneous activated and magnetic ZnO doped biochar derived from camphor leaves for ciprofloxacin adsorption. *Bioresource Technology*, *288*(May), 1–8. https://doi.org/10.1016/j.biortech.2019.121511

Huber, S. A., Balz, A., Abert, M., & Pronk, W. (2011). Characterisation of aquatic humic and non-humic matter with size-exclusion chromatography - organic carbon detection - organic nitrogen detection (LC-OCD-OND). *Water Research*, *45*(2), 879–885. https://doi.org/10.1016/j.watres.2010.09.023

Huggett, D. B., Brooks, B. W., Peterson, B., Foran, C. M., & Schlenk, D. (2002). Toxicity of select beta adrenergic receptor-blocking pharmaceuticals (B-blockers) on aquatic organisms. *Archives of Environmental Contamination and Toxicology*, *43*(2), 229–235. https://doi.org/10.1007/s00244-002-1182-7

Iraola-Arregui, I., Van Der Gryp, P., & Görgens, J. F. (2018). A review on the demineralisation of pre- and post-pyrolysis biomass and tyre wastes. *Waste Management*, *79*, 667–688. https://doi.org/10.1016/j.wasman.2018.08.034

Islam, M. A., Ahmed, M. J., Khanday, W. A., Asif, M., & Hameed, B. H. (2017). Mesoporous activated coconut shell-derived hydrochar prepared via hydrothermal carbonization-NaOH activation for methylene blue adsorption. *Journal of Environmental Management*, *203*, 237–244. https://doi.org/10.1016/j.jenvman.2017.07.029

Islam, M. R., Joardder, M. U. H., Hasan, S. M., Takai, K., & Haniu, H. (2011). Feasibility study for thermal treatment of solid tire wastes in Bangladesh by using pyrolysis technology. *Waste Management*, *31*(9–10), 2142–2149. https://doi.org/10.1016/j.wasman.2011.04.017

Jaria, G., Calisto, V., Silva, C. P., Gil, M. V., Otero, M., & Esteves, V. I. (2019). Fixed-bed performance of a waste-derived granular activated carbon for the removal of micropollutants from municipal wastewater. *Science of the Total Environment*, *683*, 699–708. https://doi.org/10.1016/j.scitotenv.2019.05.198

Jellali, S., Diamantopoulos, E., Kallali, H., Bennaceur, S., Anane, M., & Jedidi, N. (2010). Dynamic sorption of ammonium by sandy soil in fixed bed columns: Evaluation of equilibrium and non-equilibrium transport processes. *Journal of Environmental Management*, *91*(4), 897–905. https://doi.org/10.1016/j.jenvman.2009.11.006

Jellali, Salah, Diamantopoulos, E., Haddad, K., Anane, M., Durner, W., & Mlayah, A. (2016). Lead removal from aqueous solutions by raw sawdust and magnesium pretreated biochar: Experimental investigations and numerical modelling. *Journal of Environmental Management*, *180*, 439–449. https://doi.org/10.1016/j.jenvman.2016.05.055

Jiang, L., Liu, Y., Liu, S., Hu, X., Zeng, G., Hu, X., … Li, M. (2017). Fabrication of β-cyclodextrin/poly (L-glutamic acid) supported magnetic graphene oxide and its adsorption behavior for 17β-estradiol. *Chemical Engineering Journal*. https://doi.org/10.1016/j.cej.2016.09.067

Jing, X. R., Wang, Y. Y., Liu, W. J., Wang, Y. K., & Jiang, H. (2014). Enhanced adsorption performance of tetracycline in aqueous solutions by methanol-modified biochar. *Chemical Engineering Journal*, *248*, 168–174. https://doi.org/10.1016/j.cej.2014.03.006

Jung, C., Park, J., Lim, K. H., Park, S., Heo, J., Her, N., … Yoon, Y. (2013). Adsorption of selected endocrine disrupting compounds and pharmaceuticals on activated biochars. *Journal of Hazardous Materials*, *263*, 702–710. https://doi.org/10.1016/j.jhazmat.2013.10.033

Karakoyun, N., Kubilay, S., Aktas, N., Turhan, O., Kasimoglu, M., Yilmaz, S., & Sahiner, N. (2011). Hydrogel-Biochar composites for effective organic contaminant removal from aqueous media. *Desalination*, *280*(1–3), 319–325. https://doi.org/10.1016/j.desal.2011.07.014

Karanfil, T., Kilduff, J.E. (1999). Role of granular activated carbon surface chemistry on the adsorption of organic compounds. 1. Priority pollutants. Environmental Science and Technology 33 (18), 3217e3224.

Karthikeyan, K. G., & Meyer, M. T. (2006). Occurrence of antibiotics in wastewater treatment facilities in Wisconsin, USA. *Science of the Total Environment*, *361*(1–3), 196–207. https://doi.org/10.1016/j.scitotenv.2005.06.030

Kasparbauer, R. D. (2009). The Effects of Biomass Pretreatments on the Products of Fast Pyrolysis, 1–294.

Kasprzyk-Hordern, B., Dinsdale, R. M., & Guwy, A. J. (2008). The occurrence of pharmaceuticals, personal care products, endocrine disruptors and illicit drugs in surface water in South Wales, UK. *Water Research*, *42*(13), 3498–3518. https://doi.org/10.1016/j.watres.2008.04.026

Kim, D., Kim, Y., Choi, J. H., Hong, Y. P., & Ryoo, K. S. (2018). Adsorptive Removal of Cd(II) Ions on a Pyrolyzed Tire Carbon (PTC) Derived from Waste Automotive Tires. *Bulletin of the Korean Chemical Society*, *39*(10), 1206–1211. https://doi.org/10.1002/bkcs.11578

Ko, D. C. K., Mui, E. L. K., Lau, K. S. T., & McKay, G. (2004). Production of activated carbons from waste tire - Process design and economical analysis. *Waste Management*, *24*(9), 875–888. https://doi.org/10.1016/j.wasman.2004.03.006

Köhne, J. M., Köhne, S., & Šimůnek, J. (2009). A review of model applications for structured soils: b) Pesticide transport. *Journal of Contaminant Hydrology*, *104*(1–4), 36–60. https://doi.org/10.1016/j.jconhyd.2008.10.003

Kołodyńska, D., Wnetrzak, R., Leahy, J. J., Hayes, M. H. B., Kwapiński, W., & Hubicki, Z. (2012). Kinetic and adsorptive characterization of biochar in metal ions removal.

Chemical Engineering Journal, *197*, 295–305. https://doi.org/10.1016/j.cej.2012.05.025

Kolpin, D. W., Furlong, E. T., Meyer, M. T., Thurman, E. M., Zaugg, S. D., Barber, L. B., & Buxton, H. T. (2002). Pharmaceuticals, hormones, and other organic wastewater contaminants in U.S. streams, 1999-2000: A national reconnaissance. *Environmental Science and Technology*. https://doi.org/10.1021/es011055j

Kong, X., Liu, Y., Pi, J., Li, W., Liao, Q. J., & Shang, J. (2017a). Low-cost magnetic herbal biochar: characterization and application for antibiotic removal. *Environmental Science and Pollution Research*, *24*(7), 6679–6687. https://doi.org/10.1007/s11356-017-8376-z

Kong, X., Liu, Y., Pi, J., Li, W., Liao, Q. J., & Shang, J. (2017b). Low-cost magnetic herbal biochar: characterization and application for antibiotic removal. *Environmental Science and Pollution Research*, *24*(7), 6679–6687. https://doi.org/10.1007/s11356-017-8376-z

Kumar, A., & Jena, H. M. (2016). Removal of methylene blue and phenol onto prepared activated carbon from Fox nutshell by chemical activation in batch and fixed-bed column. *Journal of Cleaner Production*, *137*, 1246–1259. https://doi.org/10.1016/j.jclepro.2016.07.177

Kuśmierek, K., Świątkowski, A., Kotkowski, T., Cherbański, R., & Molga, E. (2020). Adsorption Properties of Activated Tire Pyrolysis Chars for Phenol and Chlorophenols. *Chemical Engineering and Technology*, *43*(4), 770–780. https://doi.org/10.1002/ceat.201900574

Labaki, M., & Jeguirim, M. (2017). Thermochemical conversion of waste tyres—a review. *Environmental Science and Pollution Research*, *24*(11), 9962–9992. https://doi.org/10.1007/s11356-016-7780-0

Lah, B., Klinar, D., & Likozar, B. (2013). Pyrolysis of natural, butadiene, styrene-butadiene rubber and tyre components: Modelling kinetics and transport phenomena at different heating rates and formulations. *Chemical Engineering Science*, *87*, 1–13. https://doi.org/10.1016/j.ces.2012.10.003

Lai, J. Y., & Ngu, L. H. (2020). The production cost analysis of oil palm waste activated carbon: a pilot-scale evaluation. *Greenhouse Gases: Science and Technology*. https://doi.org/10.1002/ghg.2020

Largitte, L., & Pasquier, R. (2016). A review of the kinetics adsorption models and their application to the adsorption of lead by an activated carbon. *Chemical Engineering Research and Design*, *109*, 495–504. https://doi.org/10.1016/j.cherd.2016.02.006

León, M., Silva, J., Carrasco, S., & Barrientos, N. (2020). Design, cost estimation and sensitivity analysis for a production process of activated carbon fromwaste nutshells by physical activation. *Processes*, *8*(8). https://doi.org/10.3390/PR8080945

Li, H., Zhang, D., Han, X., & Xing, B. (2014a). Adsorption of antibiotic ciprofloxacin on carbon nanotubes: PH dependence and thermodynamics. *Chemosphere*, *95*, 150–155. https://doi.org/10.1016/j.chemosphere.2013.08.053

Li, J., Yu, G., Pan, L., Li, C., You, F., Xie, S., … Shang, X. (2018a). Study of ciprofloxacin removal by biochar obtained from used tea leaves. *Journal of Environmental Sciences (China)*, *73*, 20–30. https://doi.org/10.1016/j.jes.2017.12.024

Li, L., Liu, S., & Zhu, T. (2010a). Application of activated carbon derived from scrap tires for adsorption of Rhodamine B. *Journal of Environmental Sciences*, *22*(8), 1273–1280.

https://doi.org/10.1016/S1001-0742(09)60250-3

Li, M. fang, Liu, Y. guo, Liu, S. bo, Zeng, G. ming, Hu, X. jiang, Tan, X. fei, … Liu, X. hui. (2018b). Performance of magnetic graphene oxide/diethylenetriaminepentaacetic acid nanocomposite for the tetracycline and ciprofloxacin adsorption in single and binary systems. *Journal of Colloid and Interface Science*, *521*, 150–159. https://doi.org/10.1016/j.jcis.2018.03.003

Li, Q., Snoeyink, V. L., Mariñas, B. J., & Campos, C. (2003). Pore blockage effect of NOM on atrazine adsorption kinetics of PAC: The roles of PAC pore size distribution and NOM molecular weight. *Water Research*, *37*(20), 4863–4872. https://doi.org/10.1016/j.watres.2003.08.018

Li, Ruining, Wang, Z., Guo, J., Li, Y., Zhang, H., Zhu, J., & Xie, X. (2018c). Enhanced adsorption of ciprofloxacin by KOH modified biochar derived from potato stems and leaves. *Water Science and Technology*, *77*(4), 1127–1136. https://doi.org/10.2166/wst.2017.636

Li, Ruining, Wang, Z., Zhao, X., Li, X., & Xie, X. (2018d). Magnetic biochar-based manganese oxide composite for enhanced fluoroquinolone antibiotic removal from water. *Environmental Science and Pollution Research*, *25*(31), 31136–31148. https://doi.org/10.1007/s11356-018-3064-1

Li, Ruobai, Cai, M., Xie, Z., Zhang, Q., Zeng, Y., Liu, H., … Lv, W. (2019). Construction of heterostructured CuFe2O4/g-C3N4 nanocomposite as an efficient visible light photocatalyst with peroxydisulfate for the organic oxidation. *Applied Catalysis B: Environmental*, *244*(December 2018), 974–982. https://doi.org/10.1016/j.apcatb.2018.12.043

Li, W. C. (2014b). Occurrence, sources, and fate of pharmaceuticals in aquatic environment and soil. *Environmental Pollution*, *187*, 193–201. https://doi.org/10.1016/j.envpol.2014.01.015

Li, Xiangping, Wang, C., Zhang, J., Liu, J., Liu, B., & Chen, G. (2020). Preparation and application of magnetic biochar in water treatment: A critical review. *Science of the Total Environment*, *711*, 134847. https://doi.org/10.1016/j.scitotenv.2019.134847

Li, Xiaona, Wang, W., Dou, J., Gao, J., Chen, S., Quan, X., & Zhao, H. (2016). Dynamic adsorption of ciprofloxacin on carbon nanofibers: Quantitative measurement by in situ fluorescence. *Journal of Water Process Engineering*, *9*, e14–e20. https://doi.org/10.1016/j.jwpe.2014.12.006

Li, Xingfu, Xu, H., Gao, Y., & Tao, Y. (2010b). Comparison of end-of-life tire treatment technologies: A Chinese case study. *Waste Management*, *30*(11), 2235–2246. https://doi.org/10.1016/j.wasman.2010.06.006

Liang, J., Fang, Y., Luo, Y., Zeng, G., Deng, J., Tan, X., … Ye, S. (2019). Magnetic nanoferromanganese oxides modified biochar derived from pine sawdust for adsorption of tetracycline hydrochloride. *Environmental Science and Pollution Research*, *26*(6), 5892–5903. https://doi.org/10.1007/s11356-018-4033-4

Liao, P., Zhan, Z., Dai, J., Wu, X., Zhang, W., Wang, K., & Yuan, S. (2013). Adsorption of tetracycline and chloramphenicol in aqueous solutions by bamboo charcoal: A batch and fixed-bed column study. *Chemical Engineering Journal*, *228*, 496–505. https://doi.org/10.1016/j.cej.2013.04.118

Lin, X., Huang, Q., Qi, G., Shi, S., Xiong, L., Huang, C., … Chen, X. (2017). Estimation of fixed-bed column parameters and mathematical modeling of breakthrough behaviors for adsorption of levulinic acid from aqueous solution using SY-01 resin. *Separation and Purification Technology*, *174*, 222–231. https://doi.org/10.1016/j.seppur.2016.10.016

Lin, Y. R., & Teng, H. (2002). Mesoporous carbons from waste tire char and their application in wastewater discoloration. *Microporous and Mesoporous Materials*, *54*(1–2), 167–174. https://doi.org/10.1016/S1387-1811(02)00380-3

Liu, L., Chen, X., Wang, Z., & Lin, S. (2019). Removal of aqueous fluoroquinolones with multi-functional activated carbon (MFAC) derived from recycled long-root Eichhornia crassipes : batch and column studies, 34345–34356.

Liu, Q. S., Zheng, T., Wang, P., Jiang, J. P., & Li, N. (2010). Adsorption isotherm, kinetic and mechanism studies of some substituted phenols on activated carbon fibers. *Chemical Engineering Journal*, *157*(2–3), 348–356. https://doi.org/10.1016/j.cej.2009.11.013

Liu, S., Xu, W. hua, Liu, Y. guo, Tan, X. fei, Zeng, G. ming, Li, X., … Cai, X. xi. (2017). Facile synthesis of Cu(II) impregnated biochar with enhanced adsorption activity for the removal of doxycycline hydrochloride from water. *Science of the Total Environment*, *592*, 546–553. https://doi.org/10.1016/j.scitotenv.2017.03.087

Loloie, Z., Mozaffarian, M., Soleimani, M., & Asassian, N. (2017). Carbonization and CO2activation of scrap tires: Optimization of specific surface area by the Taguchi method. *Korean Journal of Chemical Engineering*, *34*(2), 366–375. https://doi.org/10.1007/s11814-016-0266-4

Lu, J., Sun, J., Chen, X., Tian, S., Chen, D., He, C., & Xiong, Y. (2019). Efficient mineralization of aqueous antibiotics by simultaneous catalytic ozonation and photocatalysis using MgMnO3as a bifunctional catalyst. *Chemical Engineering Journal*, *358*(August 2018), 48–57. https://doi.org/10.1016/j.cej.2018.08.198

Lyu, H., Gao, B., He, F., Ding, C., Tang, J., & Crittenden, J. C. (2017). Ball-Milled Carbon Nanomaterials for Energy and Environmental Applications. *ACS Sustainable Chemistry and Engineering*, *5*(11), 9568–9585. https://doi.org/10.1021/acssuschemeng.7b02170

Lyu, H., Gao, B., He, F., Zimmerman, A. R., Ding, C., Huang, H., & Tang, J. (2018a). Effects of ball milling on the physicochemical and sorptive properties of biochar: Experimental observations and governing mechanisms. *Environmental Pollution*, *233*, 54–63. https://doi.org/10.1016/j.envpol.2017.10.037

Lyu, H., Gao, B., He, F., Zimmerman, A. R., Ding, C., Tang, J., & Crittenden, J. C. (2018b). Experimental and modeling investigations of ball-milled biochar for the removal of aqueous methylene blue. *Chemical Engineering Journal*, *335*(October 2017), 110–119. https://doi.org/10.1016/j.cej.2017.10.130

Ma, J., Yang, M., Yu, F., & Zheng, J. (2015). Water-enhanced Removal of Ciprofloxacin from Water by Porous Graphene Hydrogel. *Scientific Reports*, *5*, 1–10. https://doi.org/10.1038/srep13578

Makrigianni, Vasiliki, Giannakas, A., Deligiannakis, Y., & Konstantinou, I. (2015). Adsorption of phenol and methylene blue from aqueous solutions by pyrolytic tire char: Equilibrium and kinetic studies. *Journal of Environmental Chemical Engineering*, *3*(1), 574–582. https://doi.org/10.1016/j.jece.2015.01.006

Makrigianni, Vassiliki, Giannakas, A., Bairamis, F., Papadaki, M., & Konstaninou, I. (2017). Adsorption of Cr(VI) from aqueous solutions by HNO 3 -purified and chemically activated pyrolytic tire char. *Journal of Dispersion Science and Technology*, *38*(7), 992–1002. https://doi.org/10.1080/01932691.2016.1216862

Malkoc, E., Nuhoglu, Y., & Abali, Y. (2006). Cr(VI) adsorption by waste acorn of Quercus ithaburensis in fixed beds: Prediction of breakthrough curves. *Chemical Engineering Journal*, *119*(1), 61–68. https://doi.org/10.1016/j.cej.2006.01.019

Manaia, C. M., Vaz-Moreira, I., & Nunes, O. C. (2012). Antibiotic Resistance in Waste Water and Surface Water and Human Health Implications. In D. Barceló (Ed.), *Emerging Organic Contaminants and Human Health* (pp. 173–212). Berlin, Heidelberg: Springer Berlin Heidelberg. https://doi.org/10.1007/698_2011_118

Manirajah, K., Sukumaran, S. V., Abdullah, N., Razak, H. A., & Ainirazali, N. (2019). Evaluation of low cost-activated carbon produced from waste tyres pyrolysis for removal of 2-chlorophenol. *Bulletin of Chemical Reaction Engineering &Amp; Catalysis*, *14*(2), 443–449. https://doi.org/10.9767/bcrec.14.2.3617.443-449

Mansouri, H., Carmona, R. J., Gomis-Berenguer, A., Souissi-Najar, S., Ouederni, A., & Ania, C. O. (2015). Competitive adsorption of ibuprofen and amoxicillin mixtures from aqueous solution on activated carbons. *Journal of Colloid and Interface Science*, *449*, 252–260. https://doi.org/10.1016/j.jcis.2014.12.020

Manyà, J. J. (2012). Pyrolysis for biochar purposes: A review to establish current knowledge gaps and research needs. *Environmental Science and Technology*, *46*(15), 7939–7954. https://doi.org/10.1021/es301029g

Martínez-Hernández, V., Meffe, R., Kohfahl, C., & de Bustamante, I. (2017). Investigating natural attenuation of pharmaceuticals through unsaturated column tests. *Chemosphere*, *177*, 292–302. https://doi.org/10.1016/j.chemosphere.2017.03.021

Martínez, J. D., Puy, N., Murillo, R., García, T., Navarro, M. V., & Mastral, A. M. (2013). Waste tyre pyrolysis - A review. *Renewable and Sustainable Energy Reviews*, *23*, 179–213. https://doi.org/10.1016/j.rser.2013.02.038

Mashile, P. P., Dimpe, M. K., & Nomngongo, P. N. (2019). Application of waste tyre-based powdered activated carbon for the adsorptive removal of cylindrospermopsin toxins from environmental matrices: Optimization using response surface methodology and desirability function. *Journal of Environmental Science and Health - Part A Toxic/Hazardous Substances and Environmental Engineering*. https://doi.org/10.1080/10934529.2019.1579538

Mashile, P. P., Mpupa, A., & Nomngongo, P. N. (2018). Adsorptive removal of microcystin-LR from surface and wastewater using tyre-based powdered activated carbon: Kinetics and isotherms. *Toxicon*, *145*, 25–31. https://doi.org/10.1016/j.toxicon.2018.02.044

Maszkowska, J., Stolte, S., Kumirska, J., Łukaszewicz, P., Mioduszewska, K., Puckowski, A., … Białk-Bielin´ska, A. (2014a). Beta-blockers in the environment: Part I. Mobility and hydrolysis study. *Science of the Total Environment*, *493*, 1112–1121. https://doi.org/10.1016/j.scitotenv.2014.06.023

Maszkowska, J., Stolte, S., Kumirska, J., Łukaszewicz, P., Mioduszewska, K., Puckowski, A., … Białk-Bielin´ska, A. (2014b). Beta-blockers in the environment: Part II. Ecotoxicity study. *Science of the Total Environment*, *493*, 1122–1126.

https://doi.org/10.1016/j.scitotenv.2014.06.039

Matsui, Y., Fukuda, Y., Inoue, T., & Matsushita, T. (2003). Effect of natural organic matter on powdered activated carbon adsorption of trace contaminants: Characteristics and mechanism of competitive adsorption. *Water Research*, *37*(18), 4413–4424. https://doi.org/10.1016/S0043-1354(03)00423-8

McKay, G. (1982). Adsorption of Dyestuffs From Aqueous Solutions With Activated Carbon - 1. Equilibrium and Batch Contact-Time Studies. *Journal of Chemical Technology and Biotechnology*. https://doi.org/10.1002/jctb.5030320712

Meng, P., Fang, X., Maimaiti, A., Yu, G., & Deng, S. (2019). Efficient removal of perfluorinated compounds from water using a regenerable magnetic activated carbon. *Chemosphere*, *224*, 187–194. https://doi.org/10.1016/j.chemosphere.2019.02.132

Merchant, A. A., & Petrich, M. A. (1993). Pyrolysis of scrap tires and conversion of chars to activated carbon. *AIChE Journal*, *39*(8), 1370–1376. https://doi.org/10.1002/aic.690390814

Miguel, G. S., Fowler, G. D., & Sollars, C. J. (1998). Pyrolysis of tire rubber: Porosity and adsorption characteristics of the pyrolytic chars. *Industrial and Engineering Chemistry Research*, *37*(6), 2430–2435. https://doi.org/10.1021/ie970728x

Minguez, L., Farcy, E., Ballandonne, C., Lepailleur, A., Serpentini, A., Lebel, J. M., … Halm-Lemeille, M. P. (2014). Acute toxicity of 8 antidepressants: What are their modes of action? *Chemosphere*, *108*, 314–319. https://doi.org/10.1016/j.chemosphere.2014.01.057

Minguez, L., Pedelucq, J., Farcy, E., Ballandonne, C., Budzinski, H., & Halm-Lemeille, M. P. (2016). Toxicities of 48 pharmaceuticals and their freshwater and marine environmental assessment in northwestern France. *Environmental Science and Pollution Research*, *23*(6), 4992–5001. https://doi.org/10.1007/s11356-014-3662-5

Mohan, D., Sarswat, A., Ok, Y. S., & Pittman, C. U. (2014). Organic and inorganic contaminants removal from water with biochar, a renewable, low cost and sustainable adsorbent - A critical review. *Bioresource Technology*, *160*, 191–202. https://doi.org/10.1016/j.biortech.2014.01.120

Mohan, D., Sarswat, A., Singh, V. K., Alexandre-Franco, M., & Pittman, C. U. (2011). Development of magnetic activated carbon from almond shells for trinitrophenol removal from water. *Chemical Engineering Journal*, *172*(2–3), 1111–1125. https://doi.org/10.1016/j.cej.2011.06.054

Mondal, S., Aikat, K., & Halder, G. (2016). Ranitidine hydrochloride sorption onto superheated steam activated biochar derived from mung bean husk in fixed bed column. *Journal of Environmental Chemical Engineering*, *4*(1), 488–497. https://doi.org/10.1016/j.jece.2015.12.005

Moreno-Castilla, C. (2004). Adsorption of organic molecules from aqueous solutions on carbon materials. *Carbon*, *42*(1), 83–94. https://doi.org/10.1016/j.carbon.2003.09.022

Mui, E. L. K., Cheung, W. H., & McKay, G. (2010). Tyre char preparation from waste tyre rubber for dye removal from effluents. *Journal of Hazardous Materials*, *175*(1–3), 151–158. https://doi.org/10.1016/j.jhazmat.2009.09.142

Mukherjee, T., Rahaman, M., Ghosh, A., & Bose, S. (2019). Optimization of adsorbent derived from non-biodegradable waste employing response surface methodology toward the

removal of dye solutions. *International Journal of Environmental Science and Technology*, (2009). https://doi.org/10.1007/s13762-018-02184-4

Munagapati, V. S., & Kim, D. S. (2016). Adsorption of anionic azo dye Congo Red from aqueous solution by Cationic Modified Orange Peel Powder. *Journal of Molecular Liquids*, *220*, 540–548. https://doi.org/10.1016/j.molliq.2016.04.119

Muranaka, C. T., Julcour, C., Wilhelm, A. M., Delmas, H., & Nascimento, C. A. O. (2010). Regeneration of activated carbon by (Photo)-Fenton oxidation. *Industrial and Engineering Chemistry Research*, *49*(3), 989–995. https://doi.org/10.1021/ie900675d

Naghdi, M., Taheran, M., Brar, S. K., Rouissi, T., Verma, M., Surampalli, R. Y., & Valero, J. R. (2017). A green method for production of nanobiochar by ball milling- optimization and characterization. *Journal of Cleaner Production*, *164*, 1394–1405. https://doi.org/10.1016/j.jclepro.2017.07.084

Nassar, R., Trivella, A., Mokh, S., Al-Iskandarani, M., Budzinski, H., & Mazellier, P. (2017). Photodegradation of sulfamethazine, sulfamethoxypiridazine, amitriptyline, and clomipramine drugs in aqueous media. *Journal of Photochemistry and Photobiology A: Chemistry*, *336*, 176–182. https://doi.org/10.1016/j.jphotochem.2016.12.008

Navarro, F. J., Partal, P., Martínez-Boza, F. J., & Gallegos, C. (2010). Novel recycled polyethylene/ground tire rubber/bitumen blends for use in roofing applications: Thermo-mechanical properties. *Polymer Testing*, *29*(5), 588–595. https://doi.org/10.1016/j.polymertesting.2010.03.010

Nazari, G., Abolghasemi, H., Esmaieli, M., & Sadeghi Pouya, E. (2016). Aqueous phase adsorption of cephalexin by walnut shell-based activated carbon: A fixed-bed column study. *Applied Surface Science*, *375*, 144–153. https://doi.org/10.1016/j.apsusc.2016.03.096

Newcombe, G., Drikas, M., Hayes, R. (1997). Influence of characterised natural organic material on activated carbon adsorption: II. Effect on pore volume distribution and adsorption of 2-methylisoborneol. Water Res. 31, 1065e1073. https://doi.org/10.1016/S0043-1354(96)00325-9.

Nguyen, L. N., Hai, F. I., Kang, J., Price, W. E., & Nghiem, L. D. (2012). Removal of trace organic contaminants by a membrane bioreactor-granular activated carbon (MBR-GAC) system. *Bioresource Technology*, *113*, 169–173. https://doi.org/10.1016/j.biortech.2011.10.051

Nguyen, L. N., Hai, F. I., Kang, J., Price, W. E., & Nghiem, L. D. (2013). Coupling granular activated carbon adsorption with membrane bioreactor treatment for trace organic contaminant removal: Breakthrough behaviour of persistent and hydrophilic compounds. *Journal of Environmental Management*, *119*, 173–181. https://doi.org/10.1016/j.jenvman.2013.01.037

Nielsen, L., & Bandosz, T. J. (2016). Analysis of the competitive adsorption of pharmaceuticals on waste derived materials. *Chemical Engineering Journal*, *287*, 139–147. https://doi.org/10.1016/j.cej.2015.11.016

Norqay, K. (2004). End-of-Life Tyre Management : Storage Options. *Review Literature And Arts Of The Americas*, (July).

Obinson, A. P. A. R., Elden, J. A. B. B., & Ydy, M. I. J. L. (2005). Toxicity of Fluoroquinolone

Antibiotics To Aquatic Organisms, *24*(2), 423–430. https://doi.org/10.1897/04-210R.1

Oh, G. H., & Park, C. R. (2002). Preparation and characteristics of rice-straw-based porous carbons with high adsorption capacity. *Fuel*, *81*(3), 327–336. https://doi.org/10.1016/S0016-2361(01)00171-5

Oladipo, A. A., & Ifebajo, A. O. (2018). Highly efficient magnetic chicken bone biochar for removal of tetracycline and fluorescent dye from wastewater: Two-stage adsorber analysis. *Journal of Environmental Management*, *209*, 9–16. https://doi.org/10.1016/j.jenvman.2017.12.030

Owen, S. F., Giltrow, E., Huggett, D. B., Hutchinson, T. H., Saye, J. A., Winter, M. J., & Sumpter, J. P. (2007). Comparative physiology, pharmacology and toxicology of β-blockers: Mammals versus fish. *Aquatic Toxicology*. https://doi.org/10.1016/j.aquatox.2007.02.007

Pal, A., Gin, K. Y. H., Lin, A. Y. C., & Reinhard, M. (2010). Impacts of emerging organic contaminants on freshwater resources: Review of recent occurrences, sources, fate and effects. *Science of the Total Environment*, *408*(24), 6062–6069. https://doi.org/10.1016/j.scitotenv.2010.09.026

Pan, L., Takagi, Y., Matsui, Y., Matsushita, T., & Shirasaki, N. (2017). Micro-milling of spent granular activated carbon for its possible reuse as an adsorbent: Remaining capacity and characteristics. *Water Research*, *114*, 50–58. https://doi.org/10.1016/j.watres.2017.02.028

Parker, J. C., & Jardine, P. M. (1986). Effects of Heterogeneous Adsorption Behavior on Ion Transport. *Water Resources Research*, *22*(8), 1334–1340. https://doi.org/10.1029/WR022i008p01334

Parshetti, G. K., Chowdhury, S., & Balasubramanian, R. (2014). Hydrothermal conversion of urban food waste to chars for removal of textile dyes from contaminated waters. *Bioresource Technology*, *161*, 310–319. https://doi.org/10.1016/j.biortech.2014.03.087

Patel, H. (2019). Fixed-bed column adsorption study: a comprehensive review. *Applied Water Science*, *9*(3). https://doi.org/10.1007/s13201-019-0927-7

Pei, Z., Kong, J., Shan, X. quan, & Wen, B. (2012). Sorption of aromatic hydrocarbons onto montmorillonite as affected by norfloxacin. *Journal of Hazardous Materials*, *203–204*, 137–144. https://doi.org/10.1016/j.jhazmat.2011.11.087

Peng, H., Pan, B., Wu, M., Liu, Y., Zhang, D., & Xing, B. (2012). Adsorption of ofloxacin and norfloxacin on carbon nanotubes: Hydrophobicity- and structure-controlled process. *Journal of Hazardous Materials*, *233–234*, 89–96. https://doi.org/10.1016/j.jhazmat.2012.06.058

Peng, X., Hu, F., Huang, J., Wang, Y., Dai, H., & Liu, Z. (2016). Preparation of a graphitic ordered mesoporous carbon and its application in sorption of ciprofloxacin: Kinetics, isotherm, adsorption mechanisms studies. *Microporous and Mesoporous Materials*, *228*, 196–206. https://doi.org/10.1016/j.micromeso.2016.03.047

Perdue, E.M., Lytle, C.R., (1983). Distribution model for binding of protons and metal-ions by humic substances. Environmental Science & Technology 17, 654e660.

Perini, J. A. L., Tonetti, A. L., Vidal, C., Montagner, C. C., & Nogueira, R. F. P. (2018). Simultaneous degradation of ciprofloxacin, amoxicillin, sulfathiazole and sulfamethazine,

and disinfection of hospital effluent after biological treatment via photo-Fenton process under ultraviolet germicidal irradiation. *Applied Catalysis B: Environmental*, *224*(November 2017), 761–771. https://doi.org/10.1016/j.apcatb.2017.11.021

Praneeth, S., Guo, R., Wang, T., Dubey, B. K., & Sarmah, A. K. (2020). Accelerated carbonation of biochar reinforced cement-fly ash composites: Enhancing and sequestering CO_2 in building materials. *Construction and Building Materials*, *244*, 118363. https://doi.org/10.1016/j.conbuildmat.2020.118363

Quek, A., & Balasubramanian, R. (2009). Low-energy and chemical-free activation of pyrolytic tire char and its adsorption characteristics. *Journal of the Air and Waste Management Association*, *59*(6), 747–756. https://doi.org/10.3155/1047-3289.59.6.747

Quek, A., & Balasubramanian, R. (2011). Removal of copper by oxygenated pyrolytic tire char: Kinetics and mechanistic insights. *Journal of Colloid and Interface Science*, *356*(1), 203–210. https://doi.org/10.1016/j.jcis.2010.12.025

Radhika, R., Jayalatha, T., G., R. K., Jacob, S., Rajeev, R., & George, B. K. (2018). Adsorption performance of packed bed column for the removal of perchlorate using modified activated carbon. *Process Safety and Environmental Protection*, *117*, 350–362. https://doi.org/10.1016/j.psep.2018.04.026

Radjenović, J., Petrović, M., & Barceló, D. (2009). Fate and distribution of pharmaceuticals in wastewater and sewage sludge of the conventional activated sludge (CAS) and advanced membrane bioreactor (MBR) treatment. *Water Research*, *43*(3), 831–841. https://doi.org/10.1016/j.watres.2008.11.043

Rajapaksha, A. U., Chen, S. S., Tsang, D. C. W., Zhang, M., Vithanage, M., Mandal, S., … Ok, Y. S. (2016). Engineered/designer biochar for contaminant removal/immobilization from soil and water: Potential and implication of biochar modification. *Chemosphere*, *148*, 276–291. https://doi.org/10.1016/j.chemosphere.2016.01.043

Rakshit, S., Sarkar, D., Elzinga, E. J., Punamiya, P., & Datta, R. (2013). Mechanisms of ciprofloxacin removal by nano-sized magnetite. *Journal of Hazardous Materials*, *246–247*, 221–226. https://doi.org/10.1016/j.jhazmat.2012.12.032

Ramil, M., El Aref, T., Fink, G., Scheurer, M., & Ternes, T. A. (2010). Fate of beta blockers in aquatic-sediment systems: Sorption and biotransformation. *Environmental Science and Technology*, *44*(3), 962–970. https://doi.org/10.1021/es9027452

Ray. (2002). *New Zealand Municipal Wastewater Monitoring Guidelines* (Vol. 53). New Zealand Water Environment Research Foundation.

Reguyal, F., & Sarmah, A. K. (2018). Adsorption of sulfamethoxazole by magnetic biochar: Effects of pH, ionic strength, natural organic matter and 17α-ethinylestradiol. *Science of the Total Environment*. https://doi.org/10.1016/j.scitotenv.2018.01.323

Reguyal, F., Sarmah, A. K., & Gao, W. (2017). Synthesis of magnetic biochar from pine sawdust via oxidative hydrolysis of FeCl2 for the removal sulfamethoxazole from aqueous solution. *Journal of Hazardous Materials*, *321*, 868–878. https://doi.org/10.1016/j.jhazmat.2016.10.006

Reynel-Avila, H. E., Mendoza-Castillo, D. I., Bonilla-Petriciolet, A., & Silvestre-Albero, J. (2015). Assessment of naproxen adsorption on bone char in aqueous solutions using batch and fixed-bed processes. *Journal of Molecular Liquids*, *209*, 187–195.

https://doi.org/10.1016/j.molliq.2015.05.013

Rocha, L. S., Pereira, D., Sousa, É., Otero, M., Esteves, V. I., & Calisto, V. (2020). Recent advances on the development and application of magnetic activated carbon and char for the removal of pharmaceutical compounds from waters: A review. *Science of the Total Environment*, *718*, 137272. https://doi.org/10.1016/j.scitotenv.2020.137272

Rozada, F., Otero, M., García, A. I., & Morán, A. (2007). Application in fixed-bed systems of adsorbents obtained from sewage sludge and discarded tyres. *Dyes and Pigments*, *72*(1), 47–56. https://doi.org/10.1016/j.dyepig.2005.07.016

Rozada, F., Otero, M., Morán, A., & García, A. I. (2005a). Activated carbons from sewage sludge and discarded tyres: Production and optimization. *Journal of Hazardous Materials*, *124*(1–3), 181–191. https://doi.org/10.1016/j.jhazmat.2005.05.002

Rozada, F., Otero, M., Parra, J. B., Morán, A., & García, A. I. (2005b). Producing adsorbents from sewage sludge and discarded tyres: Characterization and utilization for the removal of pollutants from water. *Chemical Engineering Journal*, *114*(1–3), 161–169. https://doi.org/10.1016/j.cej.2005.08.019

Saleh, T. A., Al-Saadi, A. A., & Gupta, V. K. (2014a). Carbonaceous adsorbent prepared from waste tires: Experimental and computational evaluations of organic dye methyl orange. *Journal of Molecular Liquids*, *191*, 85–91. https://doi.org/10.1016/j.molliq.2013.11.028

Saleh, T. A., & Gupta, V. K. (2014b). Processing methods, characteristics and adsorption behavior of tire derived carbons: A review. *Advances in Colloid and Interface Science*, *211*, 93–101. https://doi.org/10.1016/j.cis.2014.06.006

Samara, M., Nasser, A., & Mingelgrin, U. (2016). Mechanochemical removal of carbamazepine. *Chemosphere*, *160*, 266–272. https://doi.org/10.1016/j.chemosphere.2016.06.082

San Miguel, G., Fowler, G. D., & Sollars, C. J. (2003). A study of the characteristics of activated carbons produced by steam and carbon dioxide activation of waste tyre rubber. *Carbon*, *41*(5), 1009–1016. https://doi.org/10.1016/S0008-6223(02)00449-9

Šandrk Nukic, I., & Milicevic, I. (2019). Fostering Eco-Innovation: Waste Tyre Rubber and Circular Economy in Croatia. *Interdisciplinary Description of Complex Systems*, *17*(2), 326–344. https://doi.org/10.7906/indecs.17.2.9

Sarmah, A. K., Meyer, M. T., & Boxall, A. B. A. (2006). A global perspective on the use, sales, exposure pathways, occurrence, fate and effects of veterinary antibiotics (VAs) in the environment. *Chemosphere*, *65*(5), 725–759. https://doi.org/10.1016/j.chemosphere.2006.03.026

Saucier, C., Karthickeyan, P., Ranjithkumar, V., Lima, E. C., dos Reis, G. S., & de Brum, I. A. S. (2017). Efficient removal of amoxicillin and paracetamol from aqueous solutions using magnetic activated carbon. *Environmental Science and Pollution Research*, *24*(6), 5918–5932. https://doi.org/10.1007/s11356-016-8304-7

Sellaoui, L., Lima, E. C., Dotto, G. L., & Lamine, A. Ben. (2017). Adsorption of amoxicillin and paracetamol on modified activated carbons: Equilibrium and positional entropy studies. *Journal of Molecular Liquids*, *234*, 375–381. https://doi.org/10.1016/j.molliq.2017.03.111

Shan, D., Deng, S., Zhao, T., Wang, B., Wang, Y., Huang, J., … Wiesner, M. R. (2016).

Preparation of ultrafine magnetic biochar and activated carbon for pharmaceutical adsorption and subsequent degradation by ball milling. *Journal of Hazardous Materials*, *305*, 156–163. https://doi.org/10.1016/j.jhazmat.2015.11.047

Šandrk Nukic, I., & Milicevic, I. (2019). Fostering Eco-Innovation: Waste Tyre Rubber and Circular Economy in Croatia. *Interdisciplinary Description of Complex Systems*, *17*(2), 326–344. https://doi.org/10.7906/indecs.17.2.9

Shang, J. G., Kong, X. R., He, L. L., Li, W. H., & Liao, Q. J. H. (2016). Low-cost biochar derived from herbal residue: characterization and application for ciprofloxacin adsorption. *International Journal of Environmental Science and Technology*, *13*(10), 2449–2458. https://doi.org/10.1007/s13762-016-1075-3

Shanmuganathan, S., Loganathan, P., Kazner, C., Johir, M. A. H., & Vigneswaran, S. (2017). Submerged membrane filtration adsorption hybrid system for the removal of organic micropollutants from a water reclamation plant reverse osmosis concentrate. *Desalination*, *401*, 134–141. https://doi.org/10.1016/j.desal.2016.07.048

Shanmuganathan, S., Nguyen, T. V., Jeong, S., Kandasamy, J., & Vigneswaran, S. (2015). Submerged membrane - (GAC) adsorption hybrid system in reverse osmosis concentrate treatment. *Separation and Purification Technology*, *146*, 8–14. https://doi.org/10.1016/j.seppur.2015.03.017

Shon, H. K., Vigneswaran, S., & Snyder, S. A. (2006). Effluent organic matter (EfOM) in wastewater: Constituents, effects, and treatment. *Critical Reviews in Environmental Science and Technology*, *36*(4), 327–374. https://doi.org/10.1080/10643380600580011

Siddique, R., & Naik, T. R. (2004). Properties of concrete containing scrap-tire rubber - An overview. *Waste Management*, *24*(6), 563–569. https://doi.org/10.1016/j.wasman.2004.01.006

Šimůnek, J., & van Genuchten, M. T. (2008). Modeling Nonequilibrium Flow and Transport Processes Using HYDRUS. *Vadose Zone Journal*, *7*(2), 782–797. https://doi.org/10.2136/vzj2007.0074

Song, Z., Lian, F., Yu, Z., Zhu, L., Xing, B., & Qiu, W. (2014). Synthesis and characterization of a novel MnOx-loaded biochar and its adsorption properties for Cu2+ in aqueous solution. *Chemical Engineering Journal*, *242*, 36–42. https://doi.org/10.1016/j.cej.2013.12.061

Sophia A., C., & Lima, E. C. (2018). Removal of emerging contaminants from the environment by adsorption. *Ecotoxicology and Environmental Safety*, *150*(December 2017), 1–17. https://doi.org/10.1016/j.ecoenv.2017.12.026

Styszko, K., Baran, P., Sekuła, M., & Zarębska, K. (2017). Sorption of pharmaceuticals residues from water to char (scrap tires) impregnated with amines. *E3S Web of Conferences*, *14*, 02029. https://doi.org/10.1051/e3sconf/20171402029

Suárez, F., Bachmann, J., Muñoz, J. F., Ortiz, C., Tyler, S. W., Alister, C., & Kogan, M. (2007). Transport of simazine in unsaturated sandy soil and predictions of its leaching under hypothetical field conditions. *Journal of Contaminant Hydrology*, *94*(3–4), 166–177. https://doi.org/10.1016/j.jconhyd.2007.05.009

Suárez, F., Guzmán, E., Muñoz, J. F., Bachmann, J., Ortiz, C., Alister, C., & Kogan, M. (2013). Simazine transport in undisturbed soils from a vineyard at the Casablanca valley, Chile.

Journal of Environmental Management, *117*, 32–41. https://doi.org/10.1016/j.jenvman.2012.12.026

Summers, R.S., Roberts, P.V. (1988). Activated carbon adsorption of humic substances. II. Size

exclusion and electrostatic interactions. J. Colloid Interface Sci. 122, 382e397.

Sun, Y., Yue, Q., Gao, B., Gao, Y., Xu, X., Li, Q., & Wang, Y. (2014). Adsorption and cosorption of ciprofloxacin and Ni(II) on activated carbon-mechanism study. *Journal of the Taiwan Institute of Chemical Engineers*, *45*(2), 681–688. https://doi.org/10.1016/j.jtice.2013.05.013

Tahir, S. S., & Rauf, N. (2006). Removal of a cationic dye from aqueous solutions by adsorption onto bentonite clay. *Chemosphere*, *63*(11), 1842–1848. https://doi.org/10.1016/j.chemosphere.2005.10.033

Tan, X., Liu, Y., Zeng, G., Wang, X., Hu, X., Gu, Y., & Yang, Z. (2015). Application of biochar for the removal of pollutants from aqueous solutions. *Chemosphere*. https://doi.org/10.1016/j.chemosphere.2014.12.058

Tan, Z., Qiu, J., Zeng, H., Liu, H., & Xiang, J. (2011). Removal of elemental mercury by bamboo charcoal impregnated with H $2O2$. *Fuel*, *90*(4), 1471–1475. https://doi.org/10.1016/j.fuel.2010.12.004

Tang, L., Yu, J., Pang, Y., Zeng, G., Deng, Y., Wang, J., … Feng, H. (2018). Sustainable efficient adsorbent: Alkali-acid modified magnetic biochar derived from sewage sludge for aqueous organic contaminant removal. *Chemical Engineering Journal*, *336*(November 2017), 160–169. https://doi.org/10.1016/j.cej.2017.11.048

Tasalloti, A., Chiaro, G., Palermo, A., & Banasiak, L. (2020). Effect of Rubber Crumbs Volumetric Content on the Shear Strength of Gravelly Soil in Direct Shear Apparatus. *American Society of Civil Engineers*, 612–621.

Thines, K. R., Abdullah, E. C., Mubarak, N. M., & Ruthiraan, M. (2017). Synthesis of magnetic biochar from agricultural waste biomass to enhancing route for waste water and polymer application: A review. *Renewable and Sustainable Energy Reviews*, *67*, 257–276. https://doi.org/10.1016/j.rser.2016.09.057

Thompson, K. A., Shimabuku, K. K., Kearns, J. P., Knappe, D. R. U., Summers, R. S., & Cook, S. M. (2016). Environmental Comparison of Biochar and Activated Carbon for Tertiary Wastewater Treatment. *Environmental Science and Technology*, *50*(20), 11253–11262. https://doi.org/10.1021/acs.est.6b03239

Tiek Wong, K., Yoon, Y., & Jang, M. (2015). Enhanced recyclable magnetized palm shell waste-based powdered activated carbon for the removal of ibuprofen: Insights for kinetics and mechanisms. *PLoS ONE*, *10*(10), 1–18. https://doi.org/10.1371/journal.pone.0141013

Toles, C. A., Marshall, W. E., Wartelle, L. H., & McAloon, A. (2000). Steam- or carbon dioxide-activated carbons from almond shells: Physical, chemical and adsorptive properties and estimated cost of production. *Bioresource Technology*, *75*(3), 197–203. https://doi.org/10.1016/S0960-8524(00)00058-4

Tong, D. S., Zhou, C. H., Lu, Y., Yu, H., Zhang, G. F., & Yu, W. H. (2010). Adsorption of Acid Red G dye on octadecyl trimethylammonium montmorillonite. *Applied Clay Science*, *50*(3), 427–431. https://doi.org/10.1016/j.clay.2010.08.018

Tuzen, M., Sarı, A., & Saleh, T. A. (2018). Response surface optimization, kinetic and thermodynamic studies for effective removal of rhodamine B by magnetic AC/CeO2 nanocomposite. *Journal of Environmental Management*, *206*, 170–177. https://doi.org/10.1016/j.jenvman.2017.10.016

Velten, S., Knappe, D. R. U., Traber, J., Kaiser, H. P., von Gunten, U., Boller, M., & Meylan, S. (2011). Characterization of natural organic matter adsorption in granular activated carbon adsorbers. *Water Research*, *45*(13), 3951–3959. https://doi.org/10.1016/j.watres.2011.04.047

Vilardi, G., Rodriguez-Rodriguez, J., Miguel Ochando-Pulido, J., Di Palma, L., & Verdone, N. (2019). Fixed-bed reactor scale-up and modelling for Cr(VI) removal using nano iron-based coated biomass as packing material. *Chemical Engineering Journal*, *361*(November 2018), 990–998. https://doi.org/10.1016/j.cej.2018.12.166

vom Eyser, C., Palmu, K., Schmidt, T. C., & Tuerk, J. (2015). Pharmaceutical load in sewage sludge and biochar produced by hydrothermal carbonization. *Science of the Total Environment*, *537*, 180–186. https://doi.org/10.1016/j.scitotenv.2015.08.021

Wan, J., Deng, H. P., Shi, J., Zhou, L., & Su, T. (2014). Synthesized magnetic manganese ferrite nanoparticles on activated carbon for sulfamethoxazole removal. *Clean - Soil, Air, Water*, *42*(9), 1199–1207. https://doi.org/10.1002/clen.201300432

Wang, B., Jiang, Y. song, Li, F. yun, & Yang, D. yue. (2017a). Preparation of biochar by simultaneous carbonization, magnetization and activation for norfloxacin removal in water. *Bioresource Technology*, *233*, 159–165. https://doi.org/10.1016/j.biortech.2017.02.103

Wang, F., Ren, X., Sun, H., Ma, L., Zhu, H., & Xu, J. (2016). Sorption of polychlorinated biphenyls onto biochars derived from corn straw and the effect of propranolol. *Bioresource Technology*, *219*, 458–465. https://doi.org/10.1016/j.biortech.2016.08.006

Wang, F., Sun, H., Ren, X., Liu, Y., Zhu, H., Zhang, P., & Ren, C. (2017b). Effects of humic acid and heavy metals on the sorption of polar and apolar organic pollutants onto biochars. *Environmental Pollution*, *231*, 229–236. https://doi.org/10.1016/j.envpol.2017.08.023

Wang, M., Zhang, L., Li, A., Irfan, M., Du, Y., & Di, W. (2019). Comparative pyrolysis behaviors of tire tread and side wall from waste tire and characterization of the resulting chars. *Journal of Environmental Management*, *232*(November 2018), 364–371. https://doi.org/10.1016/j.jenvman.2018.10.091

Wang, S., Gao, B., Zimmerman, A. R., Li, Y., Ma, L., Harris, W. G., & Migliaccio, K. W. (2015). Removal of arsenic by magnetic biochar prepared from pinewood and natural hematite. *Bioresource Technology*, *175*, 391–395. https://doi.org/10.1016/j.biortech.2014.10.104

Wang, S. Y., Tang, Y. K., Li, K., Mo, Y. Y., Li, H. F., & Gu, Z. Q. (2014). Combined performance of biochar sorption and magnetic separation processes for treatment of chromium-contained electroplating wastewater. *Bioresource Technology*, *174*, 67–73. https://doi.org/10.1016/j.biortech.2014.10.007

Westerhoff, P., Yoon, Y., Snyder, S., & Wert, E. (2005). Fate of endocrine-disruptor, pharmaceutical, and personal care product chemicals during simulated drinking water treatment processes. *Environmental Science and Technology*, *39*(17), 6649–6663. https://doi.org/10.1021/es0484799

Wick, A., Fink, G., Joss, A., Siegrist, H., & Ternes, T. A. (2009). Fate of beta blockers and psycho-active drugs in conventional wastewater treatment. *Water Research*, *43*(4), 1060–1074. https://doi.org/10.1016/j.watres.2008.11.031

Winter, J., Wray, H. E., Schulz, M., Vortisch, R., Barbeau, B., & Bérubé, P. R. (2018). The impact of loading approach and biological activity on NOM removal by ion exchange resins. *Water Research*, *134*, 301–310. https://doi.org/10.1016/j.watres.2018.01.052

Wu, H., Feng, Q., Yang, H., Alam, E., Gao, B., & Gu, D. (2017). Modified biochar supported Ag/Fe nanoparticles used for removal of cephalexin in solution: Characterization, kinetics and mechanisms. *Colloids and Surfaces A: Physicochemical and Engineering Aspects*, *517*, 63–71. https://doi.org/10.1016/j.colsurfa.2017.01.005

Xin-hui, D., Srinivasakannan, C., Qu, W. W., Xin, W., Jin-hui, P., & Li-bo, Z. (2012). Regeneration of microwave assisted spent activated carbon: Process optimization, adsorption isotherms and kinetics. *Chemical Engineering and Processing: Process Intensification*, *53*, 53–62. https://doi.org/10.1016/j.cep.2011.12.011

Xiong, Z., Shihong, Z., Haiping, Y., Tao, S., Yingquan, C., & Hanping, C. (2013). Influence of NH3/CO2 Modification on the Characteristic of Biochar and the CO2 Capture. *Bioenergy Research*, *6*(4), 1147–1153. https://doi.org/10.1007/s12155-013-9304-9

Xue, Y., Gao, B., Yao, Y., Inyang, M., Zhang, M., Zimmerman, A. R., & Ro, K. S. (2012). Hydrogen peroxide modification enhances the ability of biochar (hydrochar) produced from hydrothermal carbonization of peanut hull to remove aqueous heavy metals: Batch and column tests. *Chemical Engineering Journal*, *200–202*, 673–680. https://doi.org/10.1016/j.cej.2012.06.116

Yaghmaeian, K., Moussavi, G., & Alahabadi, A. (2014). Removal of amoxicillin from contaminated water using NH4Cl-activated carbon: CONTINUOUS flow fixed-bed adsorption and catalytic ozonation regeneration. *Chemical Engineering Journal*, *236*, 538–544. https://doi.org/10.1016/j.cej.2013.08.118

Yan, X., Liu, X., Qi, C., Lin, C., Li, P., & Wang, H. (2017). Disposal of hexabromocyclododecane (HBCD) by grinding assisted with sodium persulfate. *RSC Advances*, *7*(38), 23313–23318. https://doi.org/10.1039/c7ra02689g

Yang, Y., Wei, Z., Zhang, X., Chen, X., Yue, D., Yin, Q., … Yang, L. (2014). Biochar from Alternanthera philoxeroides could remove Pb(II) efficiently. *Bioresource Technology*, *171*(1), 227–232. https://doi.org/10.1016/j.biortech.2014.08.015

Yanyan, L., Kurniawan, T. A., Zhu, M., Ouyang, T., Avtar, R., Dzarfan Othman, M. H., … Albadarin, A. B. (2018). Removal of acetaminophen from synthetic wastewater in a fixed-bed column adsorption using low-cost coconut shell waste pretreated with NaOH, HNO 3 , ozone, and/or chitosan. *Journal of Environmental Management*, *226*(April), 365–376. https://doi.org/10.1016/j.jenvman.2018.08.032

Yao, Y., Gao, B., Chen, H., Jiang, L., Inyang, M., Zimmerman, A. R., … Li, H. (2012). Adsorption of sulfamethoxazole on biochar and its impact on reclaimed water irrigation. *Journal of Hazardous Materials*, *209–210*, 408–413. https://doi.org/10.1016/j.jhazmat.2012.01.046

Yao, Y., Gao, B., Fang, J., Zhang, M., Chen, H., Zhou, Y., … Yang, L. (2014). Characterization and environmental applications of clay-biochar composites. *Chemical Engineering Journal*, *242*, 136–143. https://doi.org/10.1016/j.cej.2013.12.062

Yazdani, M. R., Duimovich, N., Tiraferri, A., Laurell, P., Borghei, M., Zimmerman, J. B., & Vahala, R. (2019). Tailored mesoporous biochar sorbents from pinecone biomass for the adsorption of natural organic matter from lake water. *Journal of Molecular Liquids*, *291*,

111248. https://doi.org/10.1016/j.molliq.2019.111248

Yu, X.Q., Zipp, G.L., Davidson, G. W. R. (1994). The Effect of Temperature and pH on the Solubility of Quinolone Compounds: Estimation of Heat of Fusion.

Yu, F., Sun, S., Han, S., Zheng, J., & Ma, J. (2016). Adsorption removal of ciprofloxacin by multi-walled carbon nanotubes with different oxygen contents from aqueous solutions. *Chemical Engineering Journal*, *285*, 588–595. https://doi.org/10.1016/j.cej.2015.10.039

Yu, J., Lv, L., Lan, P., Zhang, S., Pan, B., & Zhang, W. (2012). Effect of effluent organic matter on the adsorption of perfluorinated compounds onto activated carbon. *Journal of Hazardous Materials*, *225–226*, 99–106. https://doi.org/10.1016/j.jhazmat.2012.04.073

Yu, Y., Huang, J., Zhang, W., Zhang, K., Deng, S., & Yu, G. (2013). Mechanochemical destruction of mirex co-ground with iron and quartz in a planetary ball mill. *Chemosphere*, *90*(5), 1729–1735. https://doi.org/10.1016/j.chemosphere.2012.10.020

Yuan, S., Jiang, X., Xia, X., Zhang, H., & Zheng, S. (2013). Detection, occurrence and fate of 22 psychiatric pharmaceuticals in psychiatric hospital and municipal wastewater treatment plants in Beijing, China. *Chemosphere*, *90*(10), 2520–2525. https://doi.org/10.1016/j.chemosphere.2012.10.089

Yoon, Y.H., Nelson, J.H. (1984). Application of gas adsorption kinetics I. A theoretical model for respirator cartridge service life. Am. Ind. Hyg. Assoc. J. 45, 509–516.

Zabaniotou, A., Antoniou, N., & Bruton, G. (2014). Analysis of good practices, barriers and drivers for ELTs pyrolysis industrial application. *Waste Management*, *34*(11), 2335–2346. https://doi.org/10.1016/j.wasman.2014.08.002

Załeska-Radziwiłł, M., Affek, K., & Rybak, J. (2014). Ecotoxicity of chosen pharmaceuticals in relation to micro-organisms-risk assessment. *Desalination and Water Treatment*, *52*(19–21), 3908–3917. https://doi.org/10.1080/19443994.2014.887503

Zeng, Z. W., Tian, S. R., Liu, Y. G., Tan, X. F., Zeng, G. M., Jiang, L. H., … Li, J. (2018). Comparative study of rice husk biochars for aqueous antibiotics removal. *Journal of Chemical Technology and Biotechnology*, *93*(4), 1075–1084. https://doi.org/10.1002/jctb.5464

Zhang, Z. Bin, Cao, X. H., Liang, P., & Liu, Y. H. (2013a). Adsorption of uranium from aqueous solution using biochar produced by hydrothermal carbonization. *Journal of Radioanalytical and Nuclear Chemistry*, *295*(2), 1201–1208. https://doi.org/10.1007/s10967-012-2017-2

Zhang, H. (2002). Regeneration of exhausted activated carbon by electrochemical method. *Chemical Engineering Journal*, *85*(1), 81–85. https://doi.org/10.1016/S1385-8947(01)00176-0

Zhang, M., Gao, B., Varnoosfaderani, S., Hebard, A., Yao, Y., & Inyang, M. (2013b). Preparation and characterization of a novel magnetic biochar for arsenic removal. *Bioresource Technology*, *130*, 457–462. https://doi.org/10.1016/j.biortech.2012.11.132

Zhang, M. M., Liu, Y. G., Li, T. T., Xu, W. H., Zheng, B. H., Tan, X. F., … Wang, S. F. (2015).

Chitosan modification of magnetic biochar produced from Eichhornia crassipes for enhanced sorption of Cr(vi) from aqueous solution. *RSC Advances*, *5*(58), 46955–46964. https://doi.org/10.1039/c5ra02388b

Zhang, Q., Saito, F., Ikoma, T., Tero-Kubota, S., & Hatakeda, K. (2001). Effects of quartz addition on the mechanochemical dechlorination of chlorobiphenyl by using CaO. *Environmental Science and Technology*, *35*(24), 4933–4935. https://doi.org/10.1021/es010638q

Zhang, S., Dong, Y., Yang, Z., Yang, W., Wu, J., & Dong, C. (2016). Adsorption of pharmaceuticals on chitosan-based magnetic composite particles with core-brush topology. *Chemical Engineering Journal*, *304*, 325–334. https://doi.org/10.1016/j.cej.2016.06.087

Zhao, J., Liang, G., Zhang, X., Cai, X., Li, R., Xie, X., & Wang, Z. (2019). Coating magnetic biochar with humic acid for high efficient removal of fluoroquinolone antibiotics in water. *Science of the Total Environment*, *688*, 1205–1215. https://doi.org/10.1016/j.scitotenv.2019.06.287

Zhao, Y., Choi, J. W., Bediako, J. K., Song, M. H., Lin, S., Cho, C. W., & Yun, Y. S. (2018). Adsorptive interaction of cationic pharmaceuticals on activated charcoal: Experimental determination and QSAR modelling. *Journal of Hazardous Materials*, *360*(February), 529–535. https://doi.org/10.1016/j.jhazmat.2018.08.039

Zhou, J. L., Zhang, Z. L., Banks, E., Grover, D., & Jiang, J. Q. (2009). Pharmaceutical residues in wastewater treatment works effluents and their impact on receiving river water. *Journal of Hazardous Materials*, *166*(2–3), 655–661. https://doi.org/10.1016/j.jhazmat.2008.11.070

Zhou, Y., Cao, S., Xi, C., Li, X., Zhang, L., Wang, G., & Chen, Z. (2019). A novel Fe3O4/graphene oxide/citrus peel-derived bio-char based nanocomposite with enhanced adsorption affinity and sensitivity of ciprofloxacin and sparfloxacin. *Bioresource Technology*, *292*(July), 121951. https://doi.org/10.1016/j.biortech.2019.121951

Zhu, D., Hyun, S., Pignatello, J. J., & Lee, L. S. (2004). Evidence for π-π electron donor-acceptor interactions between π-donor aromatic compounds and π-acceptor sites in soil organic matter through pH effects on sorption. *Environmental Science and Technology*. https://doi.org/10.1021/es035379e

Zhu, X., Liu, Y., Qian, F., Zhou, C., Zhang, S., & Chen, J. (2014). Preparation of magnetic porous carbon from waste hydrochar by simultaneous activation and magnetization for tetracycline removal. *Bioresource Technology*, *154*, 209–214. https://doi.org/10.1016/j.biortech.2013.12.019

Ziarrusta, H., Mijangos, L., Prieto, A., Etxebarria, N., Zuloaga, O., & Olivares, M. (2016). Determination of tricyclic antidepressants in biota tissue and environmental waters by liquid chromatography-tandem mass spectrometry. *Analytical and Bioanalytical Chemistry*, *408*(4), 1205–1216. https://doi.org/10.1007/s00216-015-9224-y

Zietzschmann, F., Mitchell, R. L., & Jekel, M. (2015). Impacts of ozonation on the competition between organic micro-pollutants and effluent organic matter in powdered activated carbon adsorption. *Water Research*, *84*, 153–160. https://doi.org/10.1016/j.watres.2015.07.031

Zietzschmann, Frederik, Worch, E., Altmann, J., Ruhl, A. S., Sperlich, A., Meinel, F., & Jekel,

M. (2014). Impact of EfOM size on competition in activated carbon adsorption of organic micro-pollutants from treated wastewater. *Water Research*, *65*, 297–306. https://doi.org/10.1016/j.watres.2014.07.043

Žukauskaitė, Z., Lukšienė, B., Filistovič, V., Tarasiuk, N., Maceika, E., & Kazakevičiūtė-Jakučiūnienė, L. (2019). Experimental and modelling studies of radiocesium sorption/desorption processes in the fixed-bed moss column. *Journal of Environmental Radioactivity*, *203*(October 2018), 1–7. https://doi.org/10.1016/j.jenvrad.2019.02.007

Zusman, O. B., Kummel, M. L., De la Rosa, J. M., & Mishael, Y. G. (2020). Dissolved organic matter adsorption from surface waters by granular composites versus granular activated carbon columns: An applicable approach. *Water Research*, *181*. https://doi.org/10.1016/j.watres.2020.115920